Surface Modification of Synthetic Fibers for Antibacterial Applications

Dissertation

zur Erlangung des akademischen Grades eines

Doktors der Naturwissenschaften

Doctor rerum naturalium

(Dr. rer. nat.)

vorgelegt von

Nasser Hassan Abdella Mohamed

Kairo, Ägypten

1974

Deutsches Textilforschungszentrum Nord-West e.V.,

Institut an der Universität Duisburg-Essen

2013

Surface Modification of Synthetic Fibers for Antibacterial Applications

By

Nasser Hassan Abdella Mohamed

04. February 1974

Cairo – Egypt

Dissertation submitted to the

Department of Chemistry of University Duisburg-Essen, in partial fulfillment of the requirements of the degree of

Doctor rerum naturalium (Dr. rer. nat.)

First referee: Prof. Dr. Jochen Gutmann

Second referee: Prof. Dr. Mathias Ulbricht

Day of promotion: 10. January 2013

Essen, 2013

Deutsches Textilforschungszentrum Nord-West e.V.

Institut an der Universität Duisburg-Essen

UNIVERSITÄT DUISBURG ESSEN

Die vorliegende Arbeit wurde im Zeitraum von October 2008 bis October 2012 im Arbeitskreis von Prof. Dr. Jochen Gutmann und Prof. Dr. Mathias Ulbricht am Deutsches Textilforschungszentrum Nord-West e.V., (DTNW) Institut an derUniversität Duisburg-Essen durchgeführt.

Tag der Disputation: 10.01.2013

Erstgutachter: Prof. Dr. Jochen Gutmann
Zweitgutachter: Prof. Dr. Mathias Ulbricht

Vorsitzender: Prof. Dr. Gebhard Haberhauer

Declaration

This work was performed during the period from October 2008 to October 2012 at the Deutsches Textilforschungszentrum Nord-West e.V., (DTNW) Institut an der Universität Duisburg-Essen, under the supervision of Prof. Dr. Jochen Gutmann and Prof. Dr. Mathias Ulbricht.

I declare that this dissertation represents my own work, except where due acknowledgement is made.

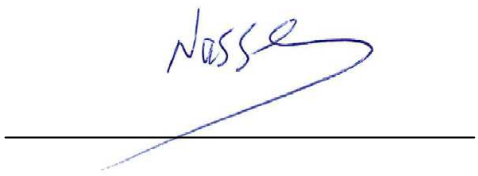

Nasser Hassan Abdella Mohamed

Acknowledgement

I would like to express my gratitude to those who gave me the possibility to complete this dissertation.

First of all, I am grateful to ***Prof. Dr. Eckhard. Schollmeyer*** *and* ***Prof. Dr. Jochen Gutmann*** *for giving me the great opportunity, to work in DTNW.*

I would like to express my appreciation to my advisor, ***Prof. Dr. Mathias Ulbricht****. I want to thank him for always having an open door for me, for his understanding, always positive attitude and many valuable advices.*

I am grateful to ***Dr. Thomas Bahners*** *for giving me the great opportunity to work in his research group. He always supported me through the difficulties of my research work and encouraged me. I would like to pay my gratitude to* ***Dr. A. Wego*** *for his understanding, always-positive attitude and many valuable advices. Furthermore, I would like to thank to* ***Dr. D. Knittel****,* ***Dr. T. Textor and Dr. K. Opwis*** *for many valuable discussions throughout my research. I am very thankful to* ***Dr. Eva Berndt*** *for her help for NMR and GPC measurements. I want to thank* ***Dr. Robert Kaufmann*** *of DWI, Aachen, for XPS analyses and* ***Dr. Meyer-Zaika*** *university of Duisburg-Essen, for TEM measurement. I wish to thank all staff members of DTNW, special thanks to* ***Ms Artz, Ms Simone*** *for their help me in biological lab,* ***Mrs. Leonie, Ms Wallmeier, Ms Fischer, Mr Molkenthin and Ms Core*** *for their concern and kindly support, and special thanks to* ***Ms Gebert*** *for SEM-EDX measurements, all staff members in Oeko-Tex Prüflabor for ICP-OES measurement and* ***Ms Roskothen*** *for secretarial work.*

Special thanks to the Egyptian Missions Department for giving me the opportunity and the financial support to pursue my Ph.D degree in Germany. And I would like also to extend my gratitude to the Egyptian Cultural Counselor and all members of the Egyptian Culture Office in Berlin.

I would like to extend special appreciation to ***my parents****,* ***my wife*** *and* ***my children*** *for their endless support and love. Finally, I would like to acknowledge all* ***my friends*** *who have not been mentioned here. Thank you very much.*

Nasser Hassan Abdella Mohamed

To my parents, my wife and my children

Abstract

Photo-chemical reactions and surface modifications of poly(ethylene terephthalate) 100% (PET) fabrics with active monomer dimethylaminopropyl methacrylamide (DMAPMA) and benzophenone (BP) as photo-initiator using a broad-band UV lamp source were investigated. The quaternization reactions were initially optimized for homo PDMAPMA, prior to reaction on the PET grafted PDMAPMA chains. The quaternization reaction of homo PDMAPMA was confirmed by one and two dimensional NMR spectroscopy (1D and 2D ^{1}HNMR), and attenuated total reflection- Fourier transform infrared spectroscopy (ATR-FTIR) The molecular weights (M_n and M_w) and molecular weight distributions (M_w/M_n; poly dispersity index, PDI) of homo PDMAPMA and quaternized homo PDMAPMA with $C_8H_{17}Br$ (C_8) were analyzed by gel permeation chromatograph (GPC). The tertiary amino groups of the grafted polyDMAPMA chains on the surface of PET fabrics were subsequently quaternized with alkyl bromides of different chain lengths to establish antibacterial activity. The surface composition, structure and morphology of modified PET fabrics were characterized by ATR-FTIR spectroscopy, X-ray photoelectron spectroscopy (XPS) and scanning electron microscopy (SEM). To evaluate the amount of quaternary and tertiary ammonium groups on the modified surface, PET was dyed with an acid dye (Telon Red AFG) which binds to the ammonium groups. Therefore, the color depth is a direct indicator of the amount of ammonium groups. The amount of positive charges on the surface PET was measured by polyelectrolyte titration and the nitrogen content of the PET-g-PDMAPMA and quaternized PET-g-PDMAPMA was determined. The resulting antibacterial activity of the modified PET fabrics was tested with *Escherichia coli.* The results of all experiments show that a photochemical modification of PET is possible using DMAPMA, benzophenone and UV light. Also, the quaternization of tertiary amino groups as well as the increase of antibacterial activity of the modified PET by the established quaternary ammonium groups were successful.

Silver nanoparticles (NPs) were prepared by a simple and inexpensive single step synthesis based on UV activation of mixture solution of silver nitrate

and poly(methacrylic acid) which acts as stabilizer agent at pH 8. Transmission electron microscopy (TEM) and dynamic light scattering (DLS) were used to prove the occurrence of nanoparticles and the size distribution of the Ag nanoparticle was measured. The UV-VIS spectroscopy revealed the formation of silver NPs by exciting the typical surface plasmon absorption from the UV–Vis spectrum. The mechanism of formation of those silver nanoparticles was also discussed. The streaming potential versus pH curve was negative. Ag NPs colloid was stable at pH values more than 6 (sufficient negative charge is present). The isoelectric point has been observed at pH values of 3.5 - 4. Silver NPs colloid showed high antimicrobial and bactericidal activity against bacteria such as *Micrococcus luteus* (*M. luteus*) and *Escherichia coli (E. coli).*

Deposition of silver NPs on the fabrics made from polyester 100% (PET) and polyamide-6 100% (PA) surface was studied by the exhaustion method using a dyeing machine at temperature 80°C. In order to enhance wettability, the fabrics were plasma pre-treated in air. Energy dispersive X-ray spectroscopy (EDX) confirmed presence of elemental silver on the surface of PET fibers, and silver NPs were well dispersed on the surface as indicated by SEM. The amount of silver particles loaded on the PET and PA 6 samples before and after laundering was determined using inductively coupled plasma optical emission spectrometry (ICP-OES). Additionally, the antibacterial activity of the modified fabrics was measured by quantitative and qualitative methods. After the deposition of silver nanoparticles, the fabrics showed high antimicrobial and bactericidal activity with regard to *M. luteus* and *E. coli*. The samples which had been pre-treated by plasma exhibited antibacterial efficacy of the impregnated fabrics with Ag NPs was maintained also after laundering. Moreover, antibacterial efficacy of the impregnated fabrics with Ag NPs was maintained also after many times laundering.

Content

List of Figures

List of Tables

List of Schemes

List of abbreviations and symbols

2D-NMR	Two-Dimensional Nuclear Magnetic Resonance
AA	Acrylic Acid
Aam	Acrylamide
ADMH	3-allyl-5,5-dimethylhydantoin
AFM	Atomic Forces Microscopy
Ag NPs	Silver Nanoparticles
AIBN	Azobisisobutyronitrile
ASTM	American Society for Testing and Materials
ATCC	American Type Culture Collection
ATR-FTIR	Attenuated Total Reflection Fourier Transform Infrared pectroscopy
BP	Benzophenone
CF4	Tetrafluoromethane
CFU	Colony Forming Units
CPC	Cetylpyridium Chloride
DADMAC	Diallyl Dimethyl Ammonium Chloride
DCDMS	Dichlorodimethyl Silane
DLS	Dynamic Light Scattering
DMAEMA	2-(dimethylamino) ethyl methacrylate
DMAPMA	Dimethylaminopropyl Methacrylamide
DNA	Deoxyribonucleic acid
DSC	Differential Scanning Calorimetry
E. Coli	*Escherichia coli*
EDA	Ethylene Diamine
EDX	Energy-Dispersive X-ray spectroscopy
GE	Grafting efficiency
GPC	Gel Permeation Chromatograph
GTA	Glutaraldehyde
GY	Graft yield
HEMA	2-Hydroxy ethyl Methacrylate
HTCC	N-(2-Hydroxy) propyl-3-Trimethyl ammonium Chitosan Chloride
ICP-OES	Inductively Coupled Plasma -Optical Emission Spectrometry
IEP	Isoelectric point

ISC	Inter-system Crossing
K/S	Color strength
KES	Kwabata Evaluation System
LSPR	localized surface plasmon resonance
M.Lutues	*Micrococcus lutues*
MBC	Minimum Biocidal Concentration
MIC	Minimum Inhibitory Concentration
Mn	Number average molecular weigh
Mw	Weight average molecular weight
Na PMAA	Sodium salt of poly (methacrylic acid)
NMR	Nuclear Magnetic Resonance
NPs	Nanoparticles
PA 6	Polyamide-6
PCD	Particle charge detector
PDADMAC	Polydiallylmethyl ammonium chloride
PDI	Poly dispersity index
PE	polyethylene
PES-Na	Poly ethylene sulfonic acid, sodium salt
PET	Poly (ethylene terephthalate)
PETA	Pentaerythritol Tetraacrylate
PHMB	Poly (Hexamethylene Biguanide)
PMAA	Poly (methacrylic acid)
PP	polypropylene
PVA	Polyvinalyalcohol
QA	8-Quinolinyl Acrylate
QACs	Quaternary Ammonium Compounds,
QAGs	Quaternary Ammonium Groups
QASs	Quaternary Ammonium Salts
QY	Quaternization yield
RAFT	Fragmentation Chain Transfer Polymerization
RF	Radio Frequency
RNA	Ribonucleic acid
SEM	Scanning Electron Microscopy
SF6	Sulfur hexafluoride

TATAT	Triallyl-1, 3, 5-triazine-2, 4, 6(1H, 3H, 5H)-trione
TEM	Transmission Electron Microscopy
TMS	Tetramethylsilane
TTC	2,3,5- Triphenyltetrazolium chloride
UV	Ultraviolet
VPA	vinyl phosphonic acid
XPS	X-ray Photoelectron Spectroscopy

1. Chapter 1: Introduction

1.1 Motivation

It is well know that more than hundreds of thousands of microorganisms such as bacteria, fungi, yeast, algae and other germs, live with human on the earth all time. Bacteria, are unicellular organisms, and can be separated into two categories: gram negative and gram positive. Gram-negative is identified by absorption and retention of the Gram stain (Gram's Iodine, a kind of mordant dye). Gram-positive bacteria remain colorless after immersed to the Gram stain followed by washing with alcohols. Due to the outer membrane of Gram negative bacteria (Figure 1-1), they are normally less sensitive to antibacterial agent [1].

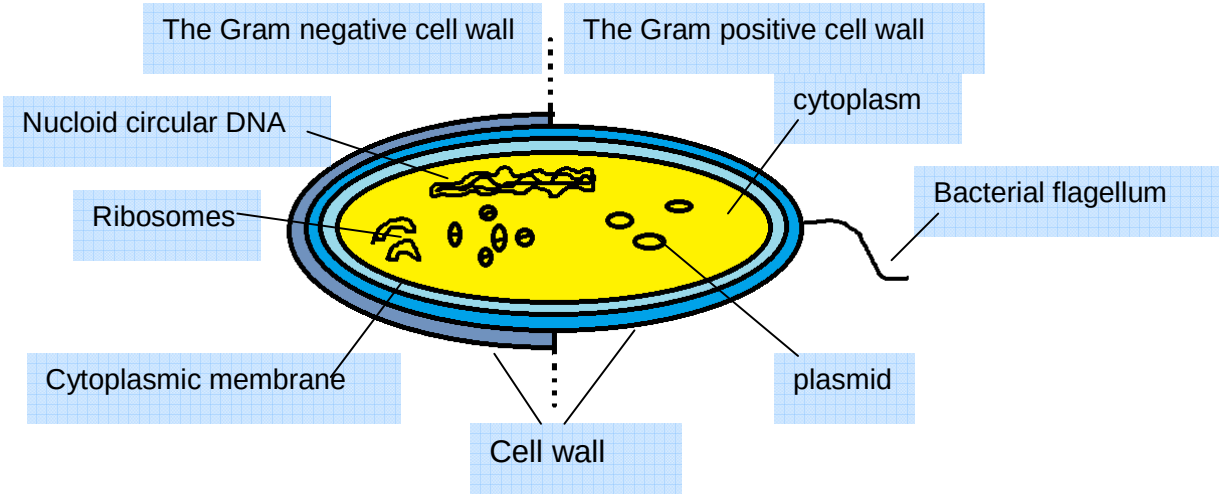

Figure 1-1: Basic structure the two types of bacteria [2]

Poly (ethylene terephthalate) (PET) and polyamide-6 (PA 6) products are the most polymers produced, consumed worldwide and widely used in hospitals and health care places. They consist of bulk fibers, yarns, woven cloth or other textile products due to good mechanical properties, durability, thermal stability, ease of processing and low production cost [3]. The main problem in the hospitals and health care places is contamination of surfaces with microorganisms; these microorganisms can grow on textile materials, and caused some problems for human life, such as odor generation or transmission of disease or infection, especially the types of harmful [4].

Therefore, the research trend was urgent and necessary to treat the textiles and their products with antibacterial agents to have ability to resist and control growth of these microorganisms or eliminate them from the surface, this so-called antibacterial textile products or medical textile products. Many technologies have been attempted in the surface modification of synthetic fabrics. Impregnated, blending, coating and grafting are the most commonly used methods to add new functionalities to synthetic surface and production of high value- added products in field medical and antibacterial applications.

In the literatures [5], [6] there are several different classifications of antimicrobial agents according to efficiency, mechanism of antimicrobial activity and washing resistance. According to these studies, antibacterial agents can be divided into bactericides and bacteristats, leaching and bound antibacterial, controlled-release and barrier-forming agents, and poor and good washing resistance. In general, the activity of antimicrobial finishes can be bactericidal or bacteristatic. The bactericides include agents that kill bacteria, while the bacteriostats inhibit the microorganisms growth. The mode of action is directly related to the concentration of the active substance in the textile. The minimum inhibitory concentration (MIC) is required for bacteristatic activity, but the minimum biocidal concentration (MBC) should be exceeded for bactericidal activity. The majority of antibacterial agents in the textile industry utilize a controlled-release mechanism. These antibacterial agents, which are also called “leaching”, are not chemically bound to the textile fibers and their antibacterial activity is attributed to their gradual and persistent release from the textile into their surroundings in the presence of moisture, where they act as a poison to a wide spectrum of bacteria. The antibacterial efficiency depends directly on the concentration, which should not drop below the MIC. Owing to leaching of the agent into its surroundings, the concentration of the active substance in the textile decreases and gradually falls under the limit of effectiveness. This can induce resistance to these substances in microorganisms; in addition, leaching agents do not withstand repeated laundering [5].

The Second type is bound antibacterial agents, include finishes that are chemically bound to the surface of the textile fibers, where they act as a barrier and control microorganisms living, which are exposed to the fiber surface. Because these agents do not leach into the surroundings of the textile substrate, the probability of microorganisms developing resistance to them is small; we should mention that the surfaces that fixed with antibacterial agents, might the efficiency reduced due to dead bacteria covered and masked the activity sites on the surface over the course of time. Covalent binding of the antibacterial agent to the textile surface can be ensured if there are enough reactive groups in the antibacterial agents and on the fibers, if the application process is carried out under suitable conditions.

Accordingly, when using bound antimicrobial agents, the mechanism of chemical binding to the textile surface and the conditions that initiate or catalyze the reaction should be known. Bound antimicrobial agents are much more resistant to repeated laundering in comparison to leaching agents [6].

Quaternary ammonium compounds (QACs) are the most widely used as antibacterial agents due to their good antibacterial properties, their low toxicity for humans, their lack of skin irritation and good environmental stability. To improve and change synthetic fibers surface properties and therefore to extend its applications for antibacterial applications [7], it is necessary to introduce specific functional groups onto the surface, like quaternary ammonium groups, as antibacterial agents. One special modification method is using UV irradiation [8], which generates free radicals just within the surface regions of the polymer substrate. The generated radicals initiate then effectively the grafting and polymerization reactive substances on the surface. UV-initiated surface graft polymerization exhibits some advantages, such as fast reaction rate, low cost of processing, simple equipment, and easy handling.

Silver Nanoparticles (Ag NPs) have been found to exhibit interesting antibacterial activities due to the large surface to volume ratio. Many methods have been reported for the preparation of silver nanoparticles such as chemical reduction, electrochemical synthesis, photochemical reduction, by exposure to

UV or γ-radiation. Addition of water-soluble polymers may control particle growth and stabilize intermediates. One of the most frequently applied additives is the sodium salt of poly (methacrylic acid) (PMAA). Using Na PMAA offers numerous advantages due to its physical and chemical properties. Furthermore, it does not show any toxic chemical effect. Moreover, it fulfils the ever-increasing demand for safe, eco-friendly and low- cost processing of materials [9- 12] . The application of silver NPs in the antibacterial finishing of textiles special synthetic fibers such as PET and PA 6 is favourable due to their stability and high surface-to-volume ratio. Therefore, considerable amount of silver atoms on the surface of the NPs is exposed toward the surrounding medium, providing a significant bactericidal efficiency. To improve the wettability and adhesion Ag NPs onto the surface of the textile, a plasma treatment provides a solution and interesting to modify the surface of textile through interaction charged particles (ions, radicals and electrons) and photons are present in the plasma zone with surface of the substrates. Moreover, the plasma treatment has energy efficient, and it does not produce mostly waste. Most plasma treatments have involved low pressure. Recently, atmospheric pressure plasma can be applied in ambient air and in the production line without the need for vacuum[13].

1.2 Objective of the research

.An-interesting objective is to set up antibacterial properties on the synthetic fibers specially PET and PA 6 fabrics. There are lot of functional materials that can give antibacterial properties, we will choose two types of antibacterial agents, quaternary ammonium groups (QAGs) and silver nanoparticles.

To introduce QAGs onto PET surface we need certain surface chemistry, which provides by photografting reaction. The photo-grafting process is a bit complicated and needs to be studied in detail, for the reason we will applied photografting process onto PET surface only. In this study tertiary amino group, containing monomers such as dimethylaminopropyl methacrylamide (DMAPMA) will be grafted copolymerization onto PET surface via UV irradiation. The following quaternization process will be done using alkyl bromides to achieve

PET fabrics with surface antibacterial properties. To evaluate the photochemical reaction, detailed studies will be analyzed regarding reaction conditions of photochemical reaction such as monomer concentration photo-initiator concentration and the time of the reaction, surface analysis and surface characterization. To establish the antibacterial activity on the surface, will be perform antibacterial test against Gram-negative bacterium *Escherichia coli*.

Second type of antibacterial agents is Ag NPs, which can be prepared by a simple and inexpensive single step synthesis based on UV activation of a solution of silver nitrate ($AgNO_3$) and sodium salt poly methacrylic acid (Na PMAA). To improve wettability of the synthetic fibers (PET and PA 6) and adhesion of the Ag NPs colloid onto the surface of the textile, for this reason we decide to use an atmospheric pressure plasma treatment. The achieved bactericidal effect on both Gram-positive bacterium *Micrococcus luteus* and Gram-negative bacterium *Escherichia coli* will be examined. Additionally, the laundering durability of the bactericidal effects will be studied.

1.3 Scope of the thesis

This thesis comprises seven chapters and abstract.

In chapter, one introduced the background information stating the objectives.

Chapter, two provided comprehensive literature reviews on most of antibacterial agents are used to get antibacterial textiles, also surface modification of synthetic fibers, especially PET and PA 6 fabrics by UV irradiation and plasma treatment.

Chapter, three described the experimental section of this thesis including samples preparation, treatment of the textiles, methods of the analysis and antibacterial activity. The characterization techniques and instruments are also included.

Chapter, four can be divided into two parts; first part investigated the synthesized homo PDMAPMA and quaternized homo PDMAPMA by ^1H NMR, GPC and ATR-FTIR analysis. Second part studied the surface modification of PET fabric via photochemical reaction of DMAPMA and surface properties such

as dyeability, amount of positive charges on the surface, hydrphilic properties, mechanicals prperties and antibactrial properties. The parameters influence on the photochemical reaction such as monomer and photoinitiator , also surface analysis and the mechanism of photochemical reaction , are included.

Chapter, five can be divied into four parts , first part studied the synthesis of Ag NPs by photochemical reduction, properties of Ag NPs formation and antibacterial activity are included . second part investicated the antibacterial properties of PET impregnated with Ag NPs colloid , third part investigated antibacterial properties of plasma pre-treatment PET fabrics impregnated with Ag NPs. Fourth part part investigated antibacterial properties of plasma pre-treatment PA 6 fabrics impregnated with Ag NPs. Surface analysis , mechanichal properties and Laundering durability of the samples are included.

Chapter, six summarized the most of the results and showed some conclusion. The recommendations for this work and possible future research work are suggested.

Finally, chapter, seven provided all references.

2. Chapter 2: Literature Review

2.1. Antibacterial agents and antibacterial textiles

There are lot of functional materials that can give antimicrobial properties, such as Quaternary Ammonium Compounds, Nanoparticles of Noble Metals and Metal Oxides, N-halamines, Chitosan, Polybiguanides, Halogenated Phenols, and antibiotics, and others. These antibacterial agents differ in their chemical structure, effectiveness, methods of application, and influence on people and the environment as well as cost[14].

2.1.1. Quaternary ammonium compounds

Quaternary ammonium compounds (QACs) are the most widely used agents due to their good antibacterial properties, their low toxicity for humans, their lack of skin irritation, good environmental stability and excellent cell membrane penetration properties. The antibacterial activity of QACs is strongly dependent on their overall molecular structure and the length of their alkyl chain [15-19]. For antibacterial activity, at least one of the alkyl groups must have a chain length in the range C_8- C_{18}. This long alkyl chain provides a hydrophobic segment that is compatible with the lipid bilayer of the bacterial cytoplasmic membrane [20, 21]. The generally accepted mechanism for the antimicrobial action of such QACs [22] can be described as shown in figure 2-1.

(i) Electrostatic interaction leading to the adsorption of positively charged QACs on the negatively charged cell surface of the microorganisms,

(ii) Diffusion through the cell wall, promoted by the long lipophilic alkyl chain,

(iii) Binding to the cytoplasmic membrane,

(iv) Disruption of the cytoplasmic membrane, and

(v) Loss of cytoplasmic constituents.

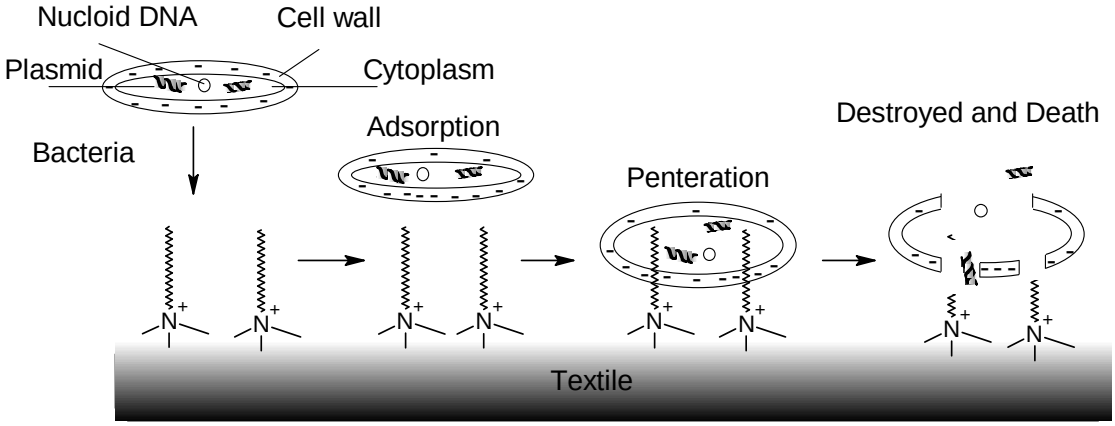

Figure 2-1: Mechanisms of quaternary ammonium groups with the bacteria

Cationic surface active agents (cationic surfactants), including particular QACs, have been known as antiseptic and antibacterial agents for many years, and are used as antimicrobial agents for textiles [23,,24], such as mono-ammonium and “gemini’’ or “dimeric’’ ammonium surfactants (Figure 2-2) with an alkyl, and aryl groups are used [25].

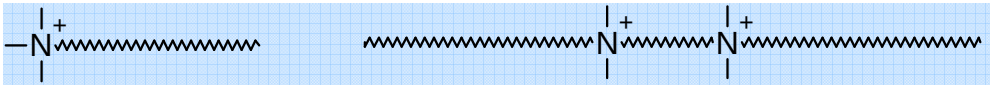

Figure 2-2: Mono-quaternary and di-quaternary ammonium salts

Carboxylic acid end groups of nylon were converted to carboxylate anions with base to allow ionic interaction with cationic antimicrobial QACs. This interaction provided durable antimicrobial functions. Bulky QACs showed low exhaustion ratio and poor durability [26]. With regard to antimicrobial agent functionalization, durability is a key factor. Despite many positive properties, QACs have an inherent weakness: leaching from the textile. There are no reactive functional groups in the structure of the QACs to allow its chemical bonding to the fibers. Owing to the lack of physical bonding, leaching of the QACs occurs, resulting in a fast decrease in concentration to below the MIC. In addition, QACs have poor wash durability. To develop new, permanently bonded, non-leaching QACs

biocidal groups for textile fibers, contemporary studies have synthesized polymerizable QACs [27, 28] with acrylate or methacrylate groups for incorporation in the structure (Figure 2-3). Such QACs monomers have been named surfactant monomers or “surfmers”. Under appropriate conditions, “surfmers” polymerize into a bulk polymer network with a polycationic structure, including side QACs groups chemically bonded to the main polyacrylate chain. The merit of fixed bonding to the textile surface is that the QACs groups can act as a bio-barrier and kill microorganisms by contact. Furthermore, the formation of a polymer network on the surface of the fibers strongly increases the durability and wash resistance of the antimicrobial agent.

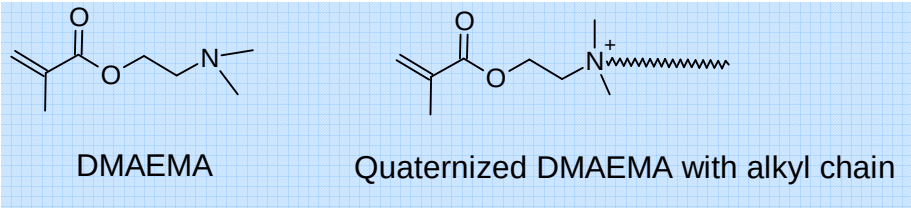

Figure 2-3: Chemicals structures of monomer DMAEMA and quaternized DMAEMA with alkyl chain (surfmers)

A number of different approaches have been described to establish QACs or quaternary ammonium groups (QAGs) on fiber surfaces. Tertiary amino groups can be established on the surface by grafting of monomer content these groups, after that functionalization these groups by quaternization in a second step.

Roy et al.[29] grafted a cellulose filter paper with 2-(dimethylamino) ethyl methacrylate (DMAEMA) by means of reversible addition fragmentation chain transfer polymerization (RAFT). The tertiary amino groups of the grafted PDMAEMA chains were subsequently quaternized with alkyl bromides of different chain lengths (C_8, C_{12}, and C_{16}). Tests using *Escherichia coli* showed that the antibacterial activity of these quaternized cellulose-g-PDMAEMA samples depended on alkyl chain length, degree of quaternization and the over all hydrophobicity of the treated surfaces. Roy et al. report that quaternization with a shorter alkyl chain (C_8) bromide leads to higher effect against *E. coli* than quaternization with a longer alkyl chain (C_{12} and C_{16}) bromides. This indicates

the hydrophobicity as the governing factor for the interaction between the microbial cells and the cellulose-g-PDMAEMA surfaces.

As above mention, some graft copolymerization reaction of functional monomer on the surface does not lead to active antimicrobial surface, because modified surface have hydrophobic properties with long chain alkyl network polymer results through crosslinking formation between the polymers chains, which is caused the biocidal functions, do not reach to bacteria cell and antibacterial activity decreased.

Sol–gel technology has also been used in antibacterial textiles. Using this technology can be formed polymer network with an organic– inorganic hybrid structure containing quaternary ammonium groups[30] as shown in figure 2-4 [30].

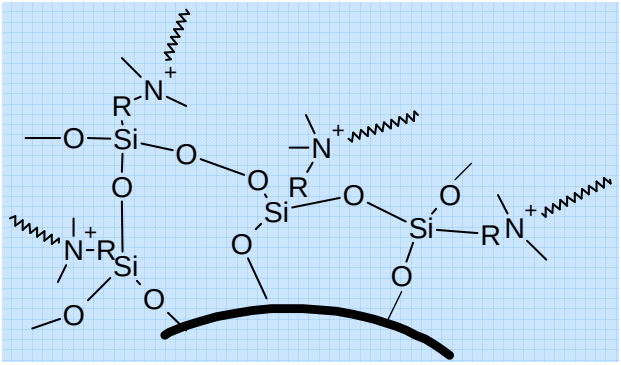

Figure 2-4: Composite bonding model of organic-inorganic hybrid structure

Colloidal solutions (sols) have been prepared in sol-gel method, consisting of mixtures of tetraalkoxysilane (Si (OR) $_4$) and QACs with different structures or organic–inorganic hybrids, including alkyltrialkoxysilanes (Rx-Si $(OR)_3$), with incorporated QAGs (Figure 5) [31-33]. Alkoxysilanes are sol– gel precursors with alkoxy groups that can hydrolyze in the presence of a catalyst to form silanol (–SiOH) groups, which further condense among each other or with the hydroxyl (–OH) groups of the fibers. The formation of covalent bonds between –SiOH groups of the precursor and –OH groups of the fibers provides increased durability and wash resistance for the nanocomposite network on the finished fibers.

Cationic dyes, which include QACs, were connected to QACs to make antimicrobial cationic dyes such as *N, N*-dimethylbutylamine, *N, N*-dimethyloctylamine, or *N, N*-dimethyldodecylamine was applied as QACs parts.

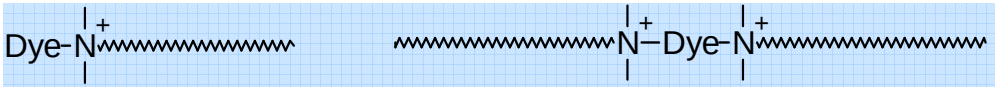

Figure2-5: Mono and di-substituted with dyes

One or even two QACs groups of differing structure have already been introduced into molecules of mono- and diazo dyes (Figure 2-5) with the aim of obtaining cationic antimicrobial dyes [34-36]. Most acid azo dyes have sulfonate groups; thus, acid dyed nylon 66 and nylon 6 fabrics were readily treated with QACs and durable antibacterial nylon fabrics were prepared [37, 38]. The presence of a chemically bonded QACs group enables the biostatic activity of the dyes.

2.1.2. Nanoparticles of noble metals and metal oxides.

Heavy metals such as Ag, Zn, As, Cu, Sb and their salts, compounds have toxicity to living organisms. The mechanism of metal or metal salts to inactivate microorganisms is because most metal ions can combine with electron donor groups such as sulfur, oxygen, or nitrogen. Thus, thiols, carboxylates, phosphates, hydroxyl, amines, imidazoles and indoles in biological systems can combine with the metal ions as shown in figure 2-6.

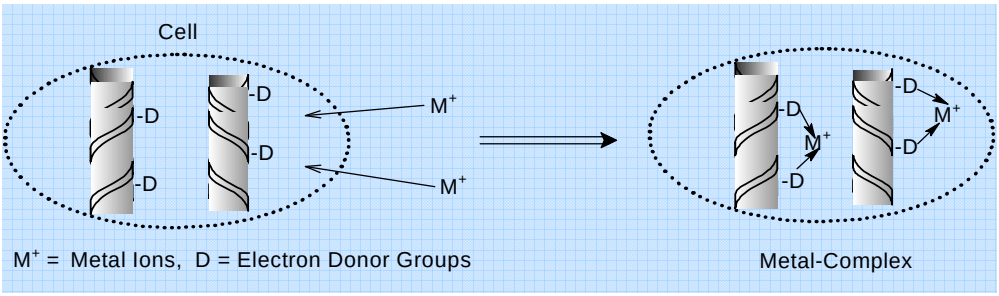

Figure 2-6: Antimicrobial mechanism of metal ions [39]

In addition to the direct antimicrobial activity of the metal nanoparticles, their large specific surface area enables a large increase in the concentration of metal

cations released from the particle surface, which results in increased in biocidal activity. The efficiency of metal nanoparticles strongly increases with reduced size, because smaller particles have a larger specific surface area with which they can interact with microorganism [40].

Preparation of nano-sized metals and metal oxides, mainly silver (Ag) [41, 42] titanium dioxide (TiO_2), zinc oxide (ZnO) and cooper II oxide (CuO) [43, 44], has enabled the development of a new generation of biocides. The method of synthesis of metal nanoparticles has a major influence on their size, shape and morphology. As conventional nanomaterial synthesis involves the use of hazardous chemicals, low material conversions, high energy requirements and wasteful purification, most novel production methods are focused on “green synthesis,” including the use of non-toxic chemicals, environmentally benign solvents and renewable materials [45–48].

In recent years, Ag NPs have been found to exhibit interesting antibacterial activities due to the large surface to volume ratio. Many methods have been reported for the preparation of Ag NPs. In general, Ag NPs synthesized stabilized by using chemical method such as chemical reduction[49, 50]. First synthesis of Ag NPs colloids have been reported by reducing Ag NO_3 with citrate in aqueous solution in 1982 by Lee and Meisel [51]. The mechanistic study of the citrate reduction reaction carried out through oxidation and decomposition of citrate, where the citrate molecules is oxidized into acetonedicarboxylate, a transitory intermediate, which then decomposes rapidly into acetoacetate. Formate and/ or CO_2 are released as byproducts during the reactions[52]. The popular reaction for chemical deposition and mass production of Ag NPs is Tollen’s reaction. In this reaction, Ag^+ ions are reduced by sugar or an aldehyde –containing compounds to produce elemental Ag^0. A polyol process is important method to generate Ag NPs with wide verity of size and shapes. In this method a polyol substances such as polyvinalyalcohol (PVA), ethylene glycol and so on, react as a solvent, reducing agent as well as stabilizing agent with high degree of control over both nucleation and growth, and thus the final products by varying reaction conditions[53]. In thermal chemical reduction

methods, the use of reducing agents such as sodium borohydride is common[54]. Photochemical reactions could be used to produce Ag NPs. In general photochemical depends on the generation of reducing species in the photodecomposition of used chemicals substances. It was found that nanocomposites could be rapidly produced at ambient temperature by photo-initiated cross-linking polymerization of oligomers [55]. Recently, polyelectrolytes give interesting substances in Ag NPs formation and act as reducing agents and stabilizing agents at the same time. In addition, water-soluble polymers may control particle growth and stabilize intermediates. One of the most frequently applied additives is the sodium salt of poly (methacrylic acid) (Na PMAA). Using low molecular weight Na PMAA offers numerous advantages due to its physical and chemical properties. Furthermore, it does not show any toxic chemical effect. Moreover, it fulfils the ever-increasing demand for safe, eco-friendly and low- cost processing of materials [8-12].

The application of Ag NPs in the antibacterial finishing of textiles is favorable due to their stability and high surface-to-volume ratio. Therefore, considerable amount of silver atoms on the surface of the NPs is exposed toward the surrounding medium, providing a significant bactericidal efficiency. Polyester (PET) and polyamide-6 (PA 6) fabric surfaces were functionalized by RF-plasma or vacuum-UV the fabrics are immersed in solutions with different concentrations of $AgNO_3$ solution. Ag clusters were deposited on the two polymer components of the fabric but having widely different sizes. The antimicrobial activity of the fabrics was effective against *E. coli* [56]. Deposition of colloidal silver nanoparticles onto synthetic fabrics such as PA 6 and PET fabrics provides excellent antibacterial effect and antifungal effect. Plasma treatment positively affected the loading of silver nanoparticles as well as antibacterial activity, antifungal activity and laundering durability of this textile nanocomposite materials [57-60].

Silver ion exhibits higher toxicity to microorganisms such as bacteria, while it exhibits lower toxicity to mammalian cells [61]. Also, the toxicity of silver ions and silver nanoparticles depend on its concentration, additives which are used in preparation of nanoparticles, size and shape of particles. The toxic

effects of silver ions on bacteria and the acting mechanism of silver has been known [62], where Ag^+ ions inhibit phosphate uptake and exchange as well as mannitol, succinate, glutamine, and proline in biological system inside bacteria cell of *E. coli* and causes destroyed the cell. Moreover, Ag^+ ions also form complexes with donor groups in DNA and causes destroyed the cell. In addition, Ag^+ can lead to enzyme inactivation via formatting silver complexes with electron donors groups containing sulfur, oxygen, or nitrogen (thiols, carboxylates, phosphates, hydroxyl, amines, imidazoles, indoles). Furthermore, silver ions inhibit oxidation of glucose, glycerol, fumarate, and succinate in *E. coli* cells [63].

The possible mechanism of antibacterial activity of Ag NPs in the bacterial *E. coli* cells has been suggested according to the morphological and structural changes in the bacterial cells. When *E. coli* cells exposure to Ag NPs, resulted in an accumulation of envelope protein precursors. This indicates that Ag NPs may target at the bacterial membrane, leading to a dissipation of the proton motive force [64]. When Ag NPs enter the bacterial cell, they form a low molecular weight region inside the bacteria. Thus, the bacteria conglomerate to protect the DNA from the Ag NPs. Consequently, the nanoparticles preferably attack the respiratory chain, cell division finally leading to cell death [62]. Moreover Ag^+ ions could be released from Ag NPs (Ag^o) can interact with phosphorous moieties in DNA resulting in inactivation of DNA replication, or can react with sulfur-containing proteins to inhibit enzyme functions [65].

The photocatalytic activity of metal oxides such as TiO_2 and ZnO, allows a thin layer coating of the material to exert self-cleaning and antimicrobial properties. Exposure to UV radiation results in the production of the ($^{\bullet}OH$) radical, which is a strong oxidizing agent. Photocatalytic activity of metal oxide has recently been tried for antimicrobial textiles. Nanoparticles of ZnO were added into polyamide-6 to give antimicrobial properties of polyamide-6 fibers when extruded through melt spinning [66.] To stabilize nanoparticle structure, control the concentration of released nanoparticles or metal ions, prolong the release time and therefore improve the durability and wash resistance of the finish, nanosized metals and metal oxides have been loaded into polymer

matrices such as zeolites [67,] a hydrogel network based on crosslinked poly(acrylamide) and carbohydrates [68, 69], or silica matrices [70-72]. Silver nanoparticle and metal oxide such as TiO_2 and ZnO loaded into silica sols for finishing textile, the chemical structure of nanocomposite polymer networks is shown physical bonded with Ag nanoparticle while TiO_2 or ZnO nanoparticles held by chemical bond with silica matrix[73] (figure 8). To increase antimicrobial properties of silica matrix loaded with metal or metal oxide nanoparticles, silica matrix was prepared with alkyltrialkoxysilanes with content quaternary ammonium groups[74], (Figure 2-7).

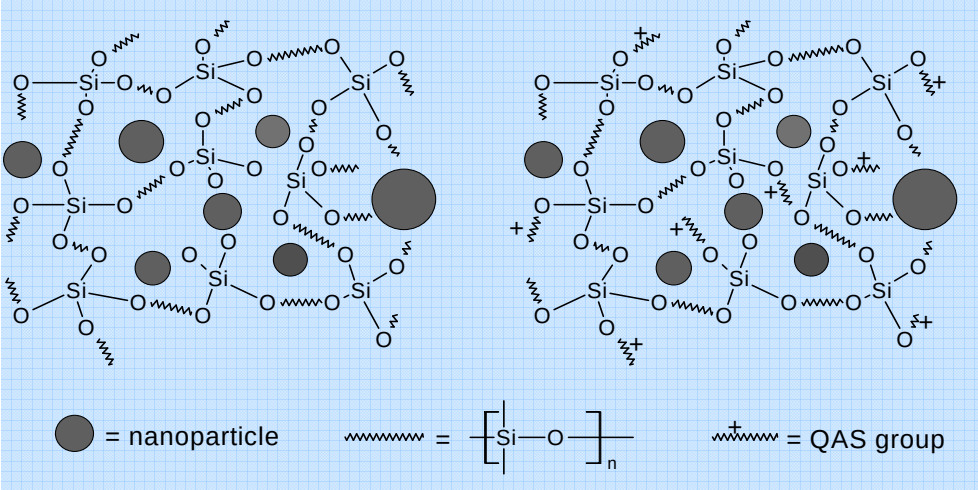

Figure 2-7: Chemical structure of metal nanoparticles loaded into non-functionalized and quaternary ammonium (QAS) group functionalized silica matrix.

TiO_2 nanoparticles have a relatively high-energy band gap (3.2 eV); TiO_2 nanoparticles can only be excited by high-energy UV irradiation with a wavelength shorter than 387.5 nm. Addition of noble metals such as gold and silver increases the photocatalytic activities of titanium dioxide. In addition, antibacterial activity could be enhancement because surface coating of silver on titanium dioxide maximizes the number of silver nanoparticle per unit area on the surface compared to using equal mass fraction of pure silver [75.] D. Mihailović et al [76] indicated that PET polyester fabrics modified with colloidal Ag and TiO_2 nanoparticles (NPs) can simultaneously provide antimicrobial, UV protective, and

photocatalytic properties. It was found that these effects depend on the order of Ag and TiO_2 NPs loading. Moreover, the antimicrobial activity after five washing cycles was active, it was recommended to treat the PET fabric with TiO_2 NPs prior to loading of Ag NPs, and all fabrics loaded with Ag and TiO_2 NPs exhibited considerably better photo-degradation ability compared to PET fabric loaded with TiO_2 NPs alone.

2.1.3. N-halamines

N-halamines are compounds, which have at least one nitrogen and halogen covalent bond within the structure. N-halamines are heterocyclic organic compounds containing one or two covalent bonds formed between nitrogen and a halogen (N–X), in which the latter is usually chlorine [77.] N–Cl bonds of different stability can be formed by the chlorination of amine; amide or imide groups in dilute sodium hypochlorite (figure 2-8). Thus, *N*-halamines are regenerable and are strong biocides against microorganisms. Their antimicrobial properties are based on the electrophilic substitution of Cl in the N-Cl bond with H this reaction can be carried out in the presence of water and results in the transfer of Cl^+ ions that can bind to acceptor regions on microorganisms. This hinders enzymatic and metabolic processes, leading to the destruction of the microorganisms. As an N–H bond, which does not have antimicrobial properties, is formed in the substitution reaction, further exposure of the agent to dilute sodium hypochlorite is needed for regeneration of its antimicrobial activity [78, 79].

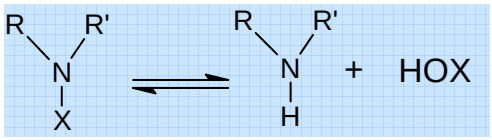

Figure 2-8: General rechargeable reaction of N-halamines

Various *N*-halamine compounds have been used as an effective antimicrobial compounds for treating polyester, nylon, etc [80] . N-halamines are biocides that are active for a broad spectrum of bacteria, fungi and viruses. N-halamines can be applied to various textile surfaces including, polyamide-6 [81] and PET [82] fibers. Synthetic fibers have been challenged to apply *N*-halamine

precursors. PET fabrics were modified with ammonium hydroxide solution to impart *N*-halamine moieties, and then the treated PET fabrics were chlorinated [83]. A cyclic-amine monomer, 3-allyl-5,5-dimethylhydantoin (ADMH) was grafted on polyethylene (PE), polypropylene (PP), acrylic, polyester/polyamide-6 (PET/PA 6) and polyamide 66 fabrics with triallyl-1,3,5-triazine-2,4,6(1H,3H,5H)-trione (TATAT). The treated fabrics exerted antimicrobial activity against *E. coli* [84]. Antimicrobial PA 6 fabrics were prepared. After attaching a hydroxymethyl functional group on polyamide 66, *N*-halamine precursors were imparted. The chlorinated fabrics showed 7 log reductions against Gram-positive and Gram negative bacteria in 30 min contact-time [85].

2.1.4. Chitosan

Chitosan is a deacetylated derivate of chitin, which is a natural polysaccharide mainly derived from the shells of shrimps and other sea crustaceans. Chitosan can be designated as poly-β-(1→4)-D-glucosamine or poly-(1,4)- 2-amido-deoxy-β-D-glucose (Figure 2-9) [86]

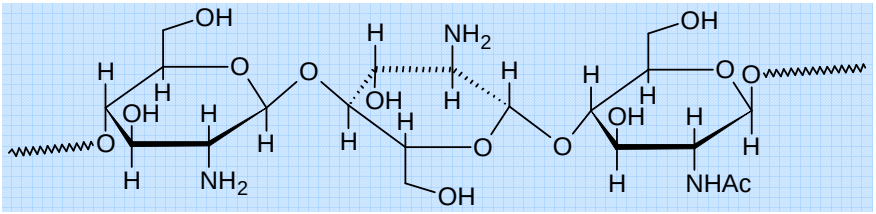

Figure 2-9: Chemical structure of chitosan

Because of non-toxicity to humans, ready degradation into the environment and abundance next to cellulose, chitosan is a wide-researched material for textile finishing. Chitosan is the derivative of chitin and is prepared through the deacetylation of chitin. It is assumed that positively charged chitosan interacts with the negatively charged components of microorganisms. This may cause inactivation of microorganisms. Considerable research of chitosan applications is on going for antimicrobial textiles. Chitosan is positively charged and soluble in acidic to neutral solutions because the amino groups in chitosan have a pKa of ~6.5. Its antimicrobial function arises from its polycationic nature,

which is caused by protonation of the amino groups at the C-2 atoms of the glucosamine units, thus, the antimicrobial activity is very similar to that determined for QACs. Positively charged amino groups can bind to the negatively charged bacterial surface, resulting in the disruption of the cell membrane and an increase in its permeability. Chitosan can also interact with the DNA of microorganisms to prevent protein synthesis. The antimicrobial efficiency of chitosan depends on its average molecular weight, degree of deacetylation and the ratio between protonated and unprotonated amino groups in the structure. Yu-Bin Chang et al. discusses various plasma treatment and grafting conditions on antibacterial effects of chitosan grafted PET fabrics. The fabrics, was grafted with chitosan, showed antibacterial activity after pre-activated 60 and 120 seconds with plasma [87]

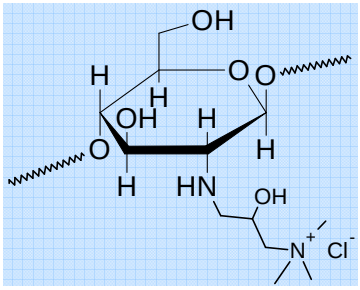

Figure 2-10: Chemical structure of *N*-(2-hydroxy) propyl-3-trimethylammonium chitosan chloride (HTCC)

Quaternized N-chitosan (Figure 2-10) [88] which is water-soluble and show antimicrobial activity over a wide pH range. An important disadvantage of chitosan is its weak adhesion to textile, resulting in a gradual leaching from the fiber surface with repetitive washing. To enable chitosan to bind strongly to textile, various crosslinking agents are used, including mostly polycarboxylic acids (1,2,3,4-butantetracarboxylic and citric acids) and derivates of imidazolidinone. In the presence of a crosslinking agent, hydroxyl groups of chitosan and surface of textile can form covalent bonds with carboxyl groups of polycarboxylic acid in an esterification reaction or with hydroxyl groups of imidazolidinone in an etherification reaction, thus leading to the formation of a

crosslink between chitosan and textile this greatly improves durability and wash resistance.

2.1.5. Polybiguanides

Polybiguanides are polymeric polycationic amines that include cationic biguanide repeat units separated by hydrocarbon chain linkers of identical or dissimilar length. One of the most important antimicrobial agents among them is poly (hexamethylenebiguanide) (PHMB) with an average of 11 biguanide units (Figure 2-11) [89] PHMB exhibits much greater antimicrobial activity than corresponding monomeric or dimeric biguanides.

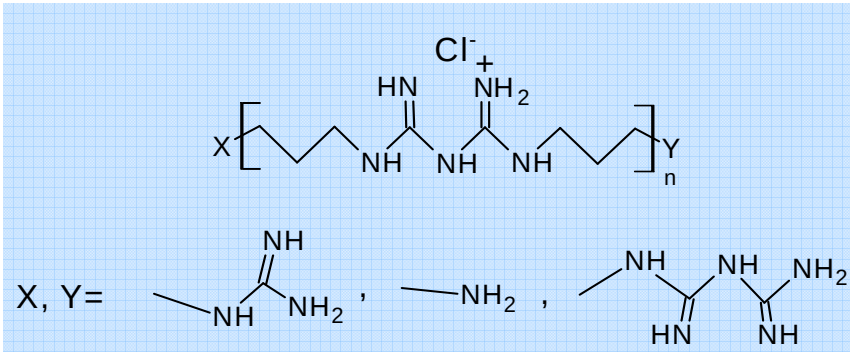

Figure 2-11: Basic structure of polybiguanides

PHMB is widely used in medicine as an antiseptic agent, especially for preventing wound infection by antibiotic- resistant bacteria [90]. Owing to its high biocidal activity and low toxicity, it has also attracted attention for the antimicrobial finishing of textiles.

2.1.6. Halogenated phenols

Among halogenated phenols, chloro-cresol and triclosan 5-chloro-2-(2.4-dichlorophenoxy) phenol (Figure 2-12) are the most widely used biocide; they are present in many contemporary consumer and personal health-care products, detergents and household objects, including textiles and plastics.

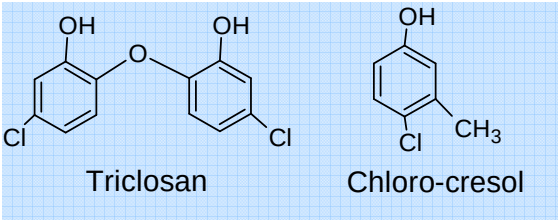

Figure 2-12: Chemical structure of halogenated phenols

PET was fully coated with triclosan after plasma and the antibacterial activity for *Staphylococcus aureus* and *Escherichia coli*, increased with increasing operating frequency and reaction time [91.]

2.1.7. Antibiotic

Ciprofloxacin (Cipro), and Doxycycline (Doxy) (figure 2-13) are considered important antibiotics used in resistance of growth the bacteria, can be directly incorporated into the polymer-using textile by dyeing technology [92, 93]

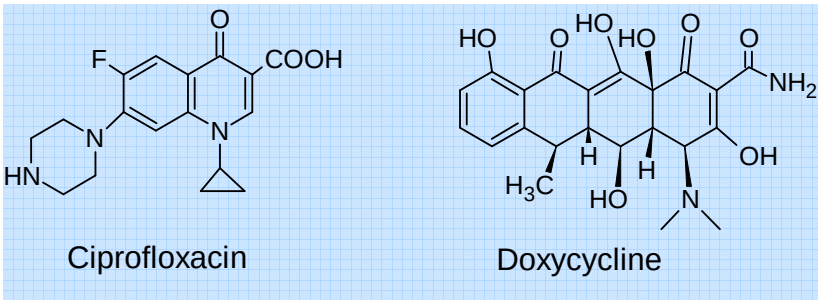

Figure 2-13: Chemical structure of ciprofloxacin and Doxycycline

Abo El-Ola [93] showed the ionic interaction between carboyxlate groups in polyamide and wool substrates and cationic reactive groups of antibiotic molecules (Doxycycline) is a promising means of providing infection resistant textile fabrics. A novel infection-resistant biomaterial was created by applying the antibiotic ciprofloxacin (figure 2-13) to the recently developed bi-functionalized PET fabrics using textile-dyeing technology. Dacron was modified *via* exposure to ethylene diamine (EDA) to create amine and carboxylic acid sites within the polymer backbone. Ciprofloxacin was applied to the bi-functionalized PET

construct under varied experimental conditions, with the resulting antimicrobial activity determined *via* the inhibition zone test [94].

2.1.8. Bioactive dyes and natural antimicrobial agents

A series of heterocyclic mono-azo dyes containing quinazoline moiety have been synthesized by conventional method and are applied to silk, wool, nylon, and polyester fabrics. The synthesized dyes showed good to excellent antibacterial activity at MIC against Gram-Positive bacteria and Gram-Negative bacteria, also showed good to excellent antifungal activity at MIC against *Candida Albicans* [95]. Dyeing PET fabric with fluoroquinolone dyes is first application process using pad-heat technique to improve antibacterial properties and sustained release and, thus prolonged infection resistance [96.]

Natural bioactive agents with antimicrobial properties have become increasingly important for bio-functionalization of textile fibers because they enable the production of safe, non-toxic, skin- and environment-friendly bioactive textile products. These antimicrobial compounds, which are mostly extracted from plants, include phenolics and polyphenols (simple phenols, phenolic acids, quinines, flavonoids, flavones, flavonols, tannins and coumarins), terpenoids, essential oils, alkaloids, lectins, polypeptides and polyacetylenes [97–99]. As many of the identified compounds from plants are colored, they are used as natural antimicrobial dyes and pigments for dyeing natural and synthetic fibers [100]. To improve wash fastness of the applied bioactive plant based antimicrobial agents on the textile fibers. Different methods are presented in the literature, including crosslinking the agent with a resin, e.g., glyoxal in combination with glycol [101], embedding liquid bioactive components such as essential oils into a sol–gel matrix [102], and micro-capsulation using phase separation / coacervation followed by the application of microcapsules using a pad–dry–cure method [103, 104]

2.1.9. Miscellaneous

Aldehyde such as Glutaraldehyde (GTA) acts as cross-linking agent on amino groups in bacteria proteins [105].

Alcohols usually have biocidal activity. They can make hydrogen bonds with proteins/ enzymes, denature them and render them inactive. These are widely used by hospitals, biological laboratories, in antiseptic gels and hand decontamination products. Due to volatility, they can only supply relatively short-period protection with no residue [106].

Peroxygens are strong biocides. The major peroxygens are hydrogen peroxide (H_2O_2), peracetic acid (CH_3COOOH) and ozone (O_3). They disrupt enzymes and proteins by oxidizing thiol groups. Moreover, they destroy bio-film with oxygen bubbles assisting the penetration of the active agent. Hydrogen peroxide is a straightforward oxidizing agent. The hydroxyl radical ($^{\bullet}OH$), which oxidizes thiol groups in target microorganisms, is the main feature of peroxy-biocides. Peracetic acid is the most powerful peroxygen.

Ozone is a powerful bactericidal, however, ozone does not remain in water long enough to supply a residual protection against latent contamination [107]. Halogen biocides such as Cl_2, Br_2, I_2, HOCl, HOBr, NaOCl, and ClO_2 are powerful antimicrobial agents. Halogen compounds readily halogenate amino groups in proteins. Since chlorine can oxidize the sulphyl group of triosephosphoric dehyrogenase, the enzyme that supports the oxidation of triosephosphoric acid to phosphoglyceric acid, enzymatic activity is destroyed [108].

Halogen compounds, especially hypochlorites, are inexpensive and broad spectrum biocides. They are widely used and powerful oxidizing agents having bactericidal activity[109]. In water systems and swimming pools, chlorine has been the predominant biocidal agent. Stabilized halogen biocides such as monochloroamine have been shown to more effectively penetrate and destroy bio-films than free halogen such as free chlorine [110].

2.2. Surface modification of synthetic fibers

PET and PA 6 fabrics are among the most of the synthetic fibers widely used in textile industries due to their good physical and chemical properties, can be found them everywhere in our life, such as clothes, carpets, car components, filter, hospital material and so on[3]. In general, the synthetic fibers such as PET and PA 6 are composited from polymeric materials, which are long chains of

carbon and hydrogen atoms with various oxygen and nitrogen groups as shown in figure 2-14.

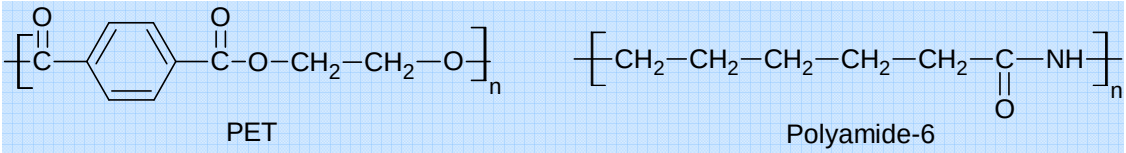

Figure 2-14: Chemical structure of PET and PA 6.

In addition, it already finds many applications for synthetic fibers in industry and research institutes, the nature of the fibers surface effect at its properties such as wettability, adhesion, antimicrobial properties, and dyeability. The requirement to improvement of the products and various application are continually increasing, this leads to a variety of ways to treatment surfaces for new products.

The treatment process, which is used to introduce functional groups is called finishing which is final step in fabric producing processes. Usually the finishing process can be classified as chemical (wet) methods and physical (dry) methods, the chemical methods use chemicals compounds such as active monomers, softening agent initiators, antimicrobial agents and so on to get desirable properties. The most important in chemical finish methods development is characterized by fewer chemicals usage and use new technologies to turn environmental problem related to water, and chemical use to outcome products by using environmentally friendly processes, in addition, the treatment methods have to be fast.

The photochemical treatment by UV irradiation and plasma treatment of synthetic textile fibers are considered an important way to modify fabric surface properties without changing the bulk properties of the polymer matrix, and offer practical solutions and rapid reduction of the environmental problems as well as save time and reduce the cost of treatment processes.

2.2.1. Photochemical treatment

Although UV irradiation is a by-product of plasma discharge, textile materials are often treated exclusively by UV radiation from UV lamps.

Photochemical treatment could be modifying the surface of the textile especially inert textile such as PET using UV irradiation. Photochemical treatment has become an accepted technology in textile finishing. It is already realized in industrial scale. UV irradiation is used in wastewater treatment and reduction of dyes instead of chemical in textile industries UV irradiation could be useful in high – added value textile finishing processes including hydrophobic/ oilphobic treatment, flame retardant finishing, dyeability, antibacterial properties etc.

Most of the photochemical reactions could be performed with UV lamps such as conventional UV source with broadband spectrum, (Hg lamps), monochromatic UV lamps (excimer UV lamps) or others. In general, the excimer lamps are expensive and provide only small area beams. On the other hand, broadband lamps are available from high current arc discharges in xenon and mercury / rare gas mixtures, which emit broadband radiation.

According to quantum mechanics equation the energy of the radiation or photon is $E = h\nu = hc/\lambda$, where c is the speed of light= 2.99×10^{10} cm/s, and h is planck′s constant= 6.626×10^{-34} J.s, or 4.135×10^{-15} eV.s, any way the energy of UV radiation in range 100-400 is 3 - 6 eV. The table 2-1 [111] shows the range of chemical bond energies, so that when the chemical bonds absorb the energy from the UV radiation they will break into radicals that participate in surface interaction. For textile material, UV radiation for chemical modification is restricted to the surface of a substrate without changing the bulk properties of the polymer matrix.

Table 2-1: Dissociation Energy of Typical Bonds

Bond type	***Bond Dissociation Energy (bond breakage energy in eV)***
C-C	3.47
C-H	4.12
C-O	3.5
C-N	2.91
O-H	4.61
N-N	3.9

Therefore, photochemical reaction is based on a bond cleavage initiated by the absorption of energetic photons and leading to the generation of radicals on the irradiated polymer surfaces, which allows subsequent reactions such as photo oxidation, grafting and cross-linking on the surface [112, 113].

A photo-initiator substances can be used to increase free radical production and increase initiation step for photochemical surface modification, Benzophenone and its derivatives are most chemical substances used as photochemical initiators , which absorb a energy of photon from UV radiation then excited to singlet state, then relaxes to a triplet state with long life time. Extraction of hydrogen atoms (from the polymer surface or from any substance) is common during this process, resulting in free radical on the polymer back bone or free radical substances on the polymer surface and photo-grafting onto polymer surface or homopolymerization when we used active monomer, this process can be expressed as the following figure 2-15. The molecular mechanism of photochemical reaction onto surface substance with reactive monomer and Benzophenone (BP) as photo-initiator has been illustrated in figure 2-15. BP molecules with triplet state can be abstracted Hydrogen atoms from the substrate surface and forms acetyl radical and surface radical on the substrate. The surface radicals can react with reactive monomer and form grafted chains on the surface substrate [114].

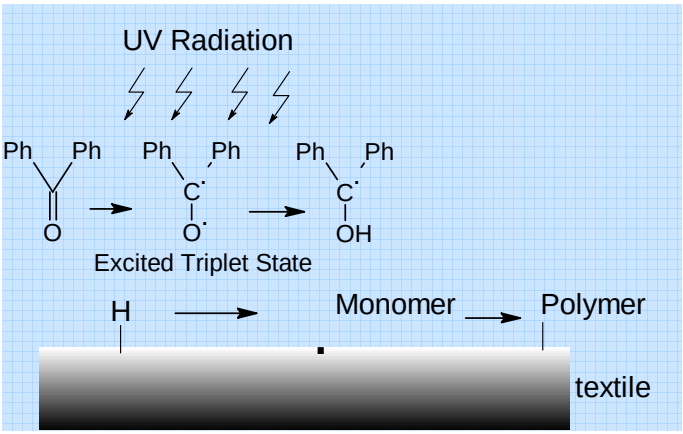

Figure 2-15: Schematic process for surface photochemical reaction of reactive monomer onto textile substrate with Benzophenone as photo-initiator.

2.2.1.1 Some UV irradiation applications on textiles

UV-initiated grafting or copolymerization is increasingly proposed for effective surface modification in recent years. A photochemical surface modification is based on bond breaking by absorbed photons and the generation of free radicals. These radicals initiate grafting and polymerization reaction of other reactive substances on the surface. UV-initiated graft polymerization exhibits some advantages and offers the unique ability to tune and manipulate surface properties without damaging the bulk material [112.] The most important characteristic of UV-initiated grafting or co-polymerization is the influence of the absorption properties of substrate and reactive compound for the chosen UV wavelengths. Depending on both, radical generation can be confined to the substrate surface yielding graft co-polymerization or be induced in the reactive compound as well [113].

Recently photochemical treatment was modified the surface of PET fibers without affecting the bulk properties by photografting reaction of acrylic acid (AA) and hydroxyethyl methacrylate (HEMA) to improve the hydrophilic properties [115] . Basic dyeability of PET fabrics was improved on exposure the excimer lamp, followed by grafting with acrylic acid AA [116]. Photochemical treatment by using a mercury UV lamp and vinyl phosphonic acid (VPA) for a permanent flame retardant finishing of textiles made of cotton (CO), polyamide (PA) and polyester (PET) was described[117]. UV excimer lamp with wavelength of 222 nm has also been carried out for surface modification of PET[118]. Photochemical reaction of the PET fabric in the presence of unsaturated compounds such as allylic compounds was carried to improve permanent hydrophilic properties on the PET surface [119]. In contrast, hydrophobic groups such as perfluorinated carbon groups, results in hydrophobic properties after the photochemical treatment of textile [120]. Protection the PET fabrics against alkaline hydrolysis can be achieved using photochemical treatment with diallylic compounds[121]. UV excimer lamp with 222-nm and a 172-nm, could be successfully grafted some specific chemical compounds on to surface PET [122]. We know UV radiation is range wavelength λ

=100-400, in UV irradiation with shorter than 200nm are accompanied ozone formation, which used in photochemical reaction [123].

Uchida and Ikada [124] introduced quaternary amines onto PET film surface by two different methods using UV-induced graft polymerization. A first concept is a two-step process consisting of graft polymerization of N, N-(dimethylamino) ethyl methacrylate (DMAEMA) onto the PET film and the subsequent quaternization of the tertiary N, N-dimethylamino groups of grafted chains with alkyl bromides. The second concept is based on a direct graft polymerization of DMAEMA having pendant quaternary amines. They used n-propyl, n-butyl, noctyl, n-lauryl, and n-cetyl bromide for quaternization of the monomers and grafted chains. Wirsén et al. [125] used photografting reaction onto PET surfece in a solvent-free vapor of acrylamide and benzophenone. The surface bound amide groups were then converted by the Hofmann reaction into amine groups. UV-induced photo-grafting of dimethylaminopropyl methacrylamide (DMAPMA) was studied with regard to reactive dyeing of fabrics made of meta-aramid fabrics (Kim et al. [126]) and of PET/wool (Dong et al. [127]), respectively. Both groups report improved dyeability after photografting.

2.2.2. Plasma treatment

The plasma was defined as the "4th state of matter" (solid, liquid, gas and plasma) by Crookes [128.] It is an ionized gas in a neutral state with an equal density of positive and negative charges (physical definition of plasma) and consists of free electrons, radicals, ions, UV-radiation, and various highly excited neutral and charged species independent of the gases used. Low-temperature plasma treatment is carried out under low pressure or atmospheric pressure, is suitable to apply to textile processing because most textile materials are heat sensitive polymers. Thus, plasma treatments are considered as a dry process, i.e., it does not require water or wet chemicals. In addition, plasma treatment is considered new technology for modification of textile and, an environmentally clean. By controlling plasma variables such as the nature of the gas, discharge power, pressure and exposure time, a great variety of surface effects can be generated without affecting bulk properties. Furthermore, Plasma surface

modifications (such as wettability enhancement, water/oil-repellency, dyeability, antibacterial properties etc.) can be achieved over large textile areas.

2.2.2.1 Effect of plasma on the surface properties

In plasma bulk, the reactive species are generated by ionization, fragmentation and excitation. They interact with surface of the substrate physically and chemically to create unstable intermediate depending on plasma conditions such as gas, power, pressure, frequency and exposure time.

In figure 2-16 is shown the effects of plasma on surface substances

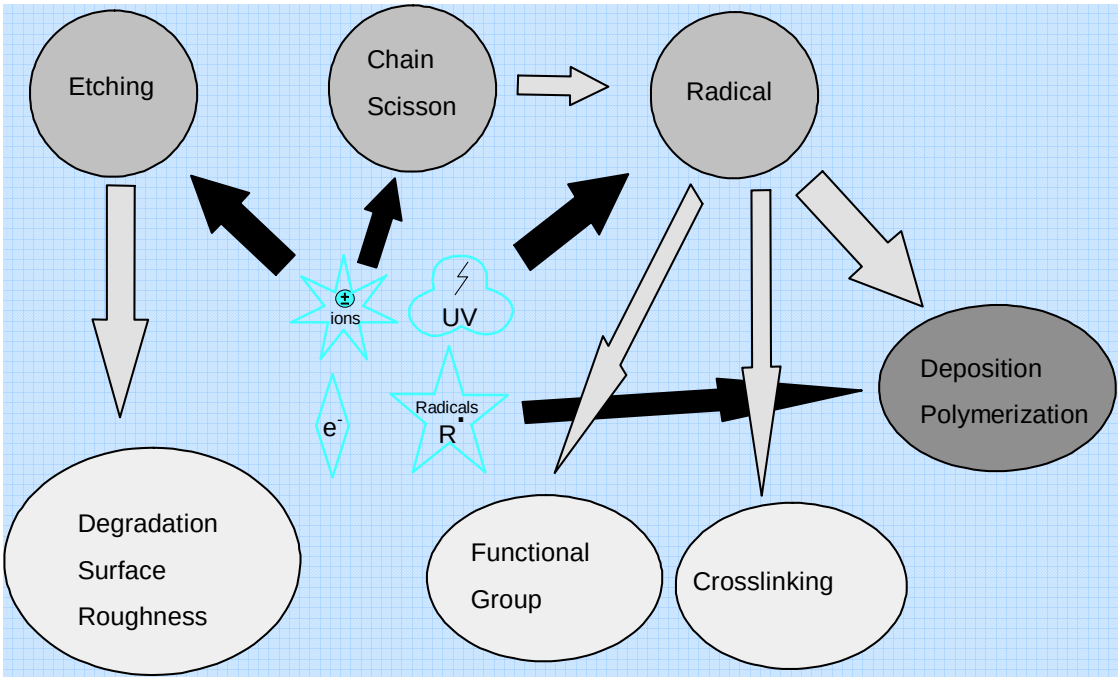

Figure 2-16: Mechanism of Plasma – substrate interaction

2.2.2.1.1 Etching effects and surface morphology change

Etching in plasma is a physical removing process of material on the surface substrate. Surface morphology is achieved by etching process, preferring to remove amorphous region [129]. Etching rate is related to the ion energy flux and etching species. The exposure of the PET film surfaces to the plasma led to the etching process on the surfaces and to change in the topography of the surfaces. Padhye et al. [130] studied the effect of etching on PET filaments and nylon 66 films in RF gas discharge. They expected that the etching effect would be stronger at

the amorphous region than crystalline because of the loose molecular structure; thus, the weight loss of plasma treated PET film would be lower in the films with higher crystallinity ratio. However, they did not find significant change of the crystallinity while the surface morphology was changed significantly.

2.2.2.1.2 Radical formation on substrate surface

The free radicals are formed when the substrate is exposed on gas plasma, initially; the gas molecules are dissociated into active species such as ions, electrons, and radicals in the plasma zone. The active species would collide with the molecules on substrate surface. UV radiation and the collisions lead to the radical formation by chain scission of molecules and abstraction of atoms from substrate surface [131]. Bond energy for the most common polymeric bonds is shown in the Table 2-1. Free radical intensity is a function of plasma gas and treated substrate. In plasma treatment, the free radicals generated on the polymeric surface plays an important in surface modification via interaction with the radicals on surface of substrate, so new functional groups are generated.

Unstable free radical would recombine rapidly with other active specie while stable free radical remains as living radical [132.] These phenomena would make graft polymerization on substrate surface by inducing monomer gas in vacuum chamber without generating plasma [133]. The free radical intensity of plasma treated fibers is related to plasma parameters (gas, pressure, and exposure time), fiber structures and chemical composition of fibers [134]. The active particles (ions and radicals) in plasma cannot penetrate the surface substrate and produce the radicals, which will, functionalized it, while UV photons have sufficient energy to penetrate much deeper into the polymer substrate, and then create radicals [135, 136], as shown in Figure 2-17.

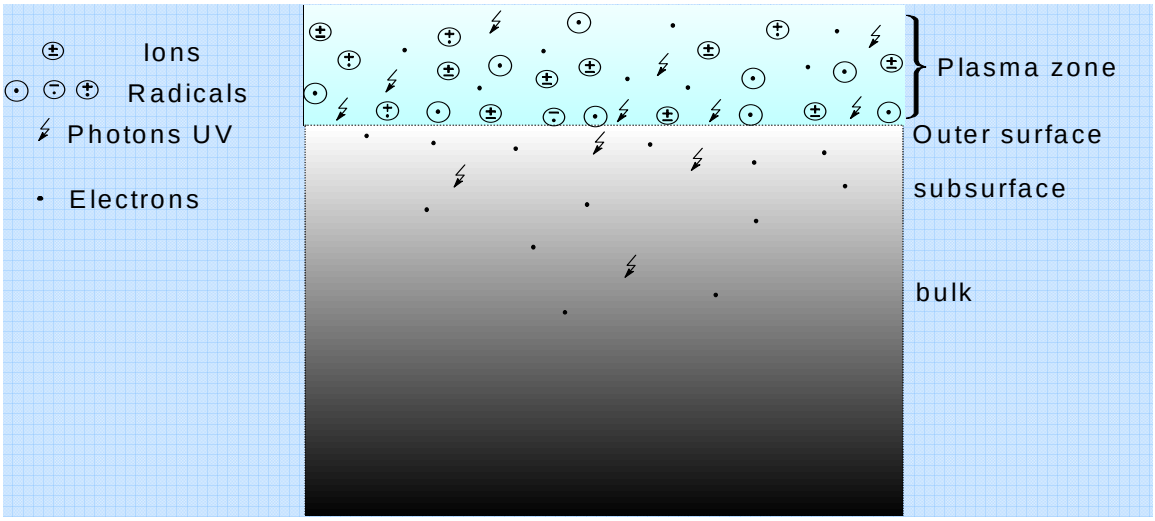

Figure 2-17: The scheme of penetration into substrate surface by plasma particles

Öteyaka et al.[137] investigated the effect of a polyethylene terephthalate (PET) forming process on radiofrequency ammonia plasma surface-treated PET flat films and fibers obtained by melt blowing. Ammonia plasma treatment allowed for the incorporation of amino functionalities on both the film and fibre surfaces, with higher values observed at very short treatment times. This plasma treatment also induced polymer chain scissions, which were observed as the formation of hydrophilic nodules that coalesced together and were loosely bound to the underlying polymeric materials

2.2.2.1.3 Physical properties of textiles

Cross-linking, chain scission and etching are strongly related to physical property changes of the polymer substrate such as morphology, tensile strength and friction force. In general, plasma treatment does not alter bulk properties of the substrate. However, in the extreme conditions of plasma, the bulk properties can be deteriorated. To overcome the defects of plasma, the optimum conditions should be considered to achieve advantages of plasma treatment.

PET fibers treated by microwave plasma with oxygen and a mixture of oxygen and tetrafluoromethane showed the reduction of tensile strength even at short exposure time (<200 sec.) [138].

2.2.2.2 Some plasma applications on textiles

2.2.2.2.1 Wettability and hydrophilicity enhancement

The inert gases used in plasma treatment are hydrogen, helium, neon and argon. Physical modification is a main effect on the surface by inert gas plasma treatment. Regardless, oxygen-related functional groups (-COH, -C=O and –COOH) were introduced by inert gas plasma treatment [139]. In oxygen plasma, the various active particles of oxygen molecules can be obtained by dissociation and combination reactions in oxygen plasma, while the inert gas plasma has ions and electrons. However, the radicals generated by plasma can interact with oxygen and H_2O in air after plasma exposure, and then hydrophilic functional groups can be introduced on substrate surface. The increase in the polar groups on the fabric surface was confirmed by the dyeing/staining procedure with a cationic dye, methylene blue. In addition, plasma treatment can lead to surface oxidation by forming oxygen containing hydrophilic group [140].

For the textile applications of wettability improvement, increased durability has been obtained using plasma graft polymerization techniques. The monomers used in plasma graft polymerization for wettability improvement are acrylic acid[141], nitro compounds [142], 2-hydroxyethyl methacrylate (HEMA)[143], acrylamide (AAm) and acrylonitrile [144].

2.2.2.2.2 Dyeability enhancement

Dyeing in textile industry requires the development of environmentally friendly and economic processes due to pollution and economic limitations. Plasma techniques have been studied to replace or aid the conventional wet dyeing process. Atmospheric pressure plasma treatment can be used as an effective technique for surface modification of PET fabrics to increase the surface roughness, wettability and dyeability. The color strength values of the oxygen plasma-treated fabric, dyed with disperse dyes at 100 °C, were slightly higher than those obtained using the untreated fabric at 130 °C[145.] Wakida's group[146] extensively investigated the effect of plasma treatment on dyeing properties of nylon 6 fibers. Compared to acid dyes, oxygen plasma treatment enhanced the dye uptake, dyeing rate and dye exhaustion for nylon fibers dyed with basic dyes.

Oxygen plasma treatment incorporated –OH and –COOH functional groups on the nylon fiber surface, leading to electronegativity on the fiber surface. Thus, the adsorption of basic dye can be higher than that of acid dye for oxygen plasma treated nylon fibers. Byrne et al.[147] showed that plasma-induced graft polymerization with acrylic acid improved dyeability of PET fabric using basic dye, as well as antisoiling and soil release. Park et al.[148] explained that generation of carboxylic acid groups (-COOH) on the PET surface could result in dyeability enhancement. When acrylic acid was grafted on PET fabric in plasma, the higher wettability resulted form the generation hydrophilic functional groups and the carboxylic acid groups can help to interact with basic dye, resulting in enhancement of dyeability. Carboxyl content of PET fabric after plasma treatment with monomer acrylic acid plays an important role in dyeability improvement due to the acid-base intermolecular interaction between acidic functional groups and basic dyes[149, 150 .]

2.2.2.2.3 Antimicrobial enhancement

The effect of plasma pre-treatment on wettability and on particle adhesion on the surface was studied. The treatment was effected by atmospheric air plasma, which can be applied in the production line without the need for vacuum.

Many studies examined the influence of dyeing on antibacterial efficiency of corona activated PA 6 and PET fabrics loaded with colloidal Ag nanoparticles as well as the influence of the presence of Ag nanoparticles on the color change of dyed fabrics [151]. Oxygen and argon RF plasmas successfully activated the surface of PET fabrics, inducing the enhanced deposition of colloidal TiO_2 nanoparticles. PET fabrics loaded with TiO_2 nanoparticles ensured excellent antibacterial activity against Gram-negative bacterium *E. coli.* In particular oxygen plasma pretreated PET fabrics loaded with TiO_2 nanoparticles exhibited good laundering durability of obtained effects[152]. PET texture was exposed to oxygen plasma glow discharge to produce peroxides on its surfaces. These peroxides were then used as catalysts for polymerization of acrylic acid in order to prepare a PET introduced by a carboxylic acid group. Chitosan and quaternized chitosan were then coupled with the carboxyl groups on PET-acrylic

acid to obtain chitosan grafted PET and quaternary chitosan grafted PET, that showed a high growth inhibition with range of 75–86% and still maintained a 48–58% bacterial growth inhibition after laundering [153]. Non-woven PET was activated by argon gas plasma, and subsequently water-soluble monomers (acrylamide and itaconic) were grafted onto PET by UV-induced surface graft polymerization. After the plasma activation and/or grafting, the hydrophobic surface of the non-woven fibers was modified into a hydrophilic surface to improve wound healing. The following three biocides have been studied $AgNO_3$ solution complexes, vinyl quaternary ammonium salt, and chitosan [154]. Deposition of the silver particles on the textiles surface increased with increasing silver ions concentration after pretreatment of RF-plasma and vacuum UV, and silver particles could be diffused to the inner layers of textiles [155].

Atmospheric pressure plasma is used to induce free radical chain polymerization of the diallyldimethylammonium chloride (DADMAC) monomer to introduce a graft-polymerized network on the nylon-cotton blend fabric with durable antimicrobial properties. Pentaerythritol tetraacrylate (PETA) was used as a cross-linking agent to obtain a highly cross-linked, durable polymer network[156]. Many studies suggested strong hydrophilicity of plasma treated PET surfaces. The samples were padded with triclosan as antibacterial agent with different concentrations. The results revealed that the antibacterial activity slightly increased after treating with triclosan[157]. PET film was exposed to oxygen plasma glow discharge to produce peroxides on its surface. These peroxides were then used as catalysts for the polymerization of 8-quinolinyl acrylate (QA) to prepare the PET grafted with QA (PET-Q). The antibacterial activity of the surface modified showed the inhibition (91%) of the growth of the gram-positive microorganism, S. aureus. Even after laundering ten times, an effectiveness of the inhibition was found [158].

3. Chapter 3: Experimental Section

3.1. Materials and preparation

3.1.1. Preparation of poly (DMAPMA)

In first step the monomer DMAPMA is weighted and dissolved in ethanol solvent in three necked flask equipped with a nitrogen inlet system and stirred continuously with a magnetic stirrer for 15 min. then azobisisobutyronitrile (AIBN) (Sigma-Aldrich, 98%) is slowly added drop-wise with stirring at 65 ^{o}C for 20 h. After expiry of the time, the excess ethanol is removed from the flask under reduced pressure after that the mixture is stirred into water to remove unreacted monomers, where the polymeric product precipitate after separation and filtration the product dried at 40 ^{o}C under vacuum for 48 h the weight of homopolymer is measured by gravimetry.

3.1.2. Quaternization of homo poly (DMAPMA)

Poly (DMAPMA) is placed in ethanol as solvent containing an excess amount of alkyl bromides (1-bromooctane or 1-bromohexadecane) the reaction mixture is stirred at 60 ^{o}C for 40 h, the excess ethanol is removed from the reaction mixture under reduced pressure. The quaternized polymer is precipitated in cold ethyl acetate after separation and filtration the product dried at 40 ^{o}C, under vacuum for 48 h. The weight of quaternized PDMAPMA due to the quaternization reaction is measured by gravimetry.

3.1.3. Preparation of silver nanoparticles

The Silver nitrate, $AgNO_3$ (99.9% - Carl Roth GmbH) was dissolved (3.5 – 28 x 10^{-5} mol/l), in distilled water with 5% of Polymethacralic acid sodium salt (40% solution in water- Aldrich). 10 ml of this solution was poured in a Petri dish then exposed a broad band UV lamp with a main emission band from 200 to 300 nm (UVACUBE 2000, Dr. Hönle, München, Germany) (figure 3-1) at a distance 10 cm.

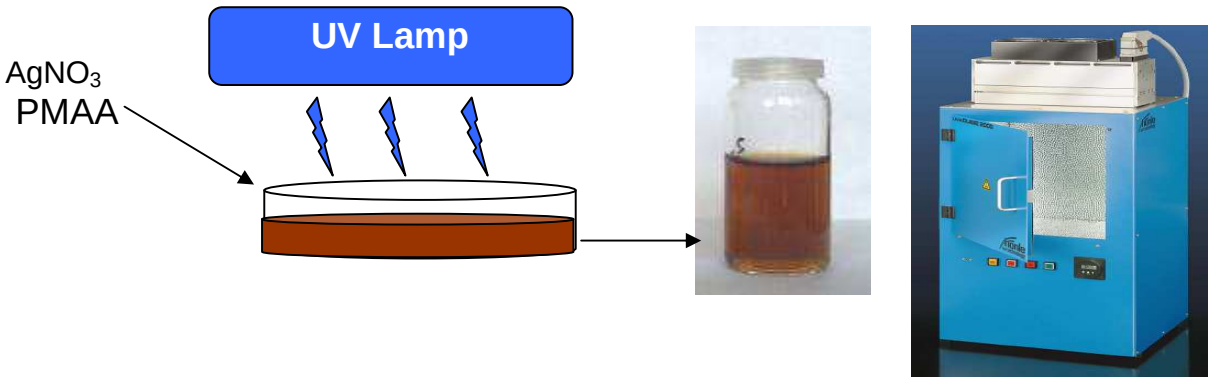

Figure 3-1: Preparation of silver nanoparticles with Broad Band lamp (Dr. Hönle UV Technology) as light source.

3.2. Textile treatments and finishes

3.2.1. Photo-grafting process

Commercially available textile fabrics made of PET fabrics served as samples. The PET fabric had a weight of 112 g/m^2, and the fabric thickness was 0.12 mm. The PET fabrics were cut into strips of 5 cm × 8 cm. The samples were washed with methanol and acetone to remove impurities, and then were died in an oven at 40 ^{o}C. Then PET fabrics finished with the grafting solution. Careful padding ensured a total add-on of 50 % weighting increased. The concentration of the functional monomer Dimethylaminopropyl methacrylamide (DMAPMA, Aldrich, 99%) was varied from 5 to 40 wt % in the solution, and the photo-initiator Benzophenone (BP, Aldrich chemical Co. 99%) from 0.25 to 2.5 wt. % in the solution. The wetted samples were exposed to UV light under inert gas (argon), Broad Band lamp (Dr. Hönle UV Technology) as light source, and the irradiation times varied from 2 - 15 min. After irradiation, the fabric samples were weighed. Then the samples were washed and were extracted with a Soxhlet extractor for 20 h to ensure that all un-reacted monomer, BP and homo-polymer have been removed, using acetone and subsequently with methanol. The samples were dried in oven at 40 ^{o}C about 4 h and were weighed again.

The graft yield (GY) and grafting efficiency (GE) to obtain PET-g-PDMAPMA were calculated using the following formulae:

$$GY\ \% = \frac{(W_3 - W_1)}{W_1} \times 100$$

$$GE\ \% = \frac{(W_3 - W_1)}{(W_2 - W_1)} \times 100$$

W_1 is the weight of original fabric, W_2 is the weight of fabric after UV irradiation, and W_3 is the weight of fabric after washing.

3.2.2. Quaternization of PET-g-PDMAPMA

Following a procedure was described by Ramadan et al[159], PET-g-PDMAPMA samples were quaternized using the four different substances alkyl bromide, 1-Bromohexane (Fluka, 98%), 1-bromoctane (Merck, 98%), 1-bromododecane (Janssen, 98%), and 1-bromohexadecane (Aldrich, 97%) were used as alkylation agents for the quaternization process of tertiary amine groups. Quaternization was achieved by immersing the grafted fabric samples in 30 ml of alkylation agents in ethanol. The amount of alkylation agents was three times higher than the available ammonium groups according to graft yield GY. The samples were stirred at reflux at 60^{o}C for 2 h, then were removed and were thoroughly washed with ethanol. Finally, the samples were dried in oven at 40 ^{o}C about 4 hours and were weighed.

The quaternization yield (QY) reaction was calculated as follows:

$$QY\ \% = \frac{W'_1}{W'_2}$$

Here, W'_1 is experimentally determined amount (weight) of the alkylating agents after quaternization. W'_2 is theoretical weight at complete quaternization of available ammonium groups.

3.2.3. Atmospheric air plasma treatments

The equipment used for plasma treatment was 3D Treater (Ahlbrandt Company), figure (3-2). The power connection 230 V(50/60 Hz), the distance of the spray head of the plasma to the material 2.5 cm , the speed of samples are controlled by the computer from 0.5- 6 sec. /cm. Atmospheric air was used as gas during the atmospheric plasma treatments.

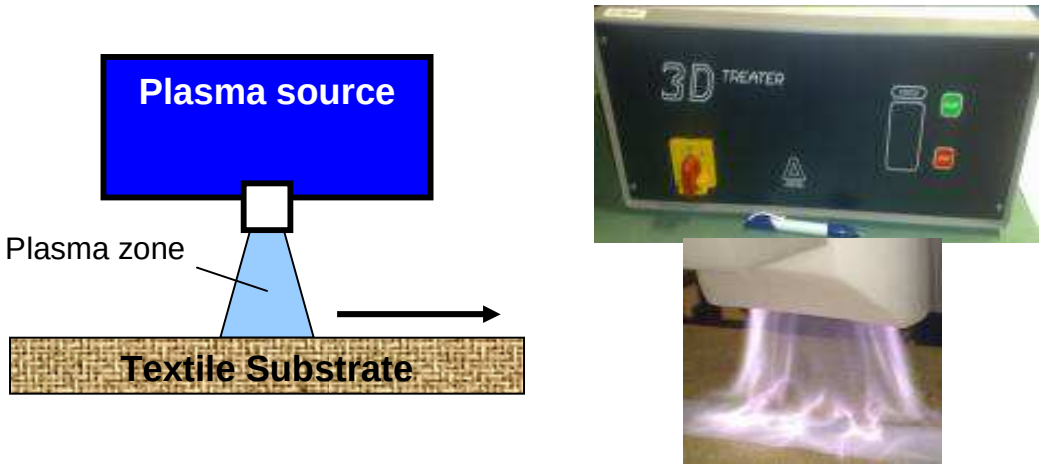

Figure 3-2: Activation of textile substrate with atmospheric plasma source

3.2.4. Treatment the fabrics with Ag nanoparticles

Textile fabrics were used are 100% PET (a weight of 112 g/m^2, and the fabric thickness was 0.12 mm) and 100% PA 6 (TEXPLORER GmbH- article No. 0700-006-001-B00-Dessin TLF 200 100% PA 6). The samples of fabrics were finished with the silver nanoparticle colloid by conventional exhaustion finishing in dyeing machine at 1:20 liquor ratio. The samples were immersed in a fresh silver nanoparticle colloid for 5 min at ambient temperature, after which the temperature of the bath was slowly increased to 80 ^{o}C during 30 min. Finally, the samples were taken out of the bath, were rinsed with water and were dried in an oven at 40 ^{o}C.

3.3. Analytical measurements and surface analysis

3.3.1. Carboxyl content

The effect of the plasma treatment was characterized by determining the carboxyl content on the surface with a method described by Klemm et al[160]. Approx. 1 g of the samples of known water content was suspended in 25 ml of aqueous methylene blue chloride solution (50 mg/l) and 25 ml of buffer solution of pH = 8.5 for 1h at 20 °C in an 100 ml Erlenmeyer flask and then filtered through a sintered-glass disk. 5 or 10 ml of the filtrate were transferred to a 100 ml calibrated flask. Then 10 ml of 0.1 N HCl and subsequently water, up to 100 ml, were added and the methylene blue content of the liquid was determined photometrically, employing a calibration plot (figure 3-3). The total amount of free, i.e. non-adsorbed, methylene blue (A) was calculated from experimental results. The number of mol of the dye is equivalent to number of mol of carboxyl groups. Hence, the carboxyl group content of the sample in mmol /kg fabric is obtained according to the equation.

$$COOH = \frac{(A_o - A)}{E} \times 0.00313 \quad \text{mmol / Kg Fabric}$$

Where A_0 and A is the total amount of free methylene blue before and after treatment with fabrics [mg], respectively, and E is the weight of oven-dry sample [g]. All presented values are the mean value of three parallel measurements.

$$Dye^+ Cl^- + PET\text{-}COOH \quad \leftrightarrow \quad PET\text{-}COO^- {}^+Dye + HCl$$

In the assuming, that the number of mole of dye is equivalent to number of mole of carboxyl groups.

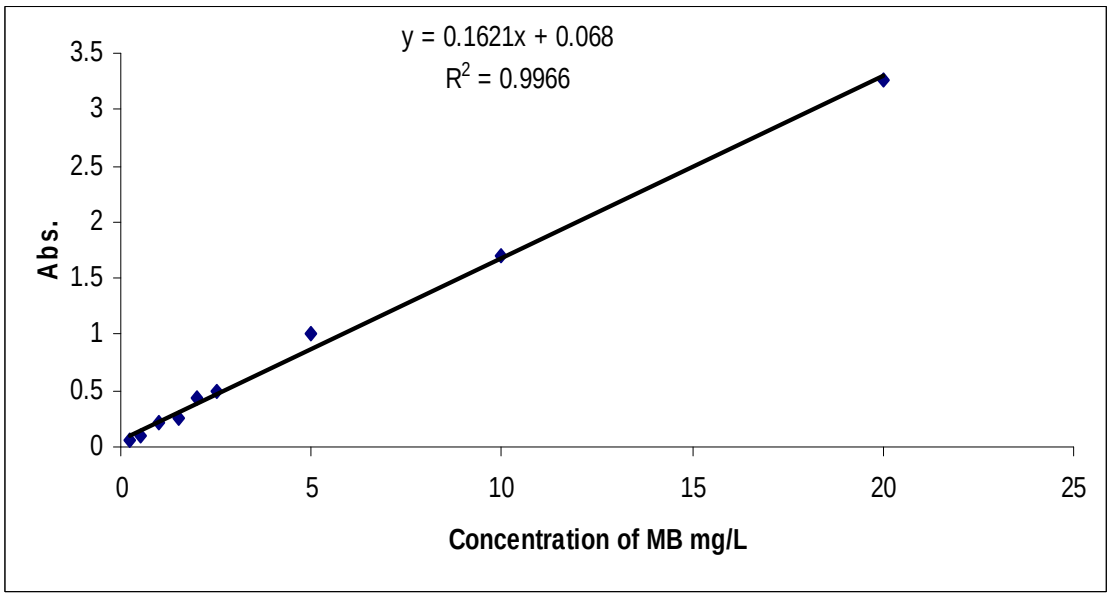

Figure 3-3: Calibration curve of absorbance against concentration of methylene blue.

3.3.2. Nitrogen content

Nitrogen content of the treated samples was determined according to Kjeldahl method [161]. In this test, 1 g of the tested fabric was immersed in 10 ml concentrated sulphuric acid with the addition of catalyst (5 g potassium sulphate, 0.15 g copper sulphate and 0.15 g titanium dioxide). Chemical decomposition of the sample is complete when the medium has become clear and colorless. Then the solution was distilled with sodium hydroxide, which converts the ammonium salt to ammonia. The amount of ammonia present (hence the amount of nitrogen present in the sample) is determined by back titration. The end of the condenser is dipped into a solution of HCl. The ammonia reacts with the acid and the remainder of the acid is then titrated with a sodium hydroxide solution using phenolphthalein as indicator.

The nitrogen percentage (N %) of the sample was calculated as follows:

$$N\ \% = \frac{0.014\ (N \times V)}{W} \times 100$$

Where: W= sample weight (gram).

N = normality of HCl.

V = volume of HCl (ml).

3.3.3. Infrared and ultraviolet-visible spectroscopy (IR-UV-Visible)

Absorption spectroscopy is employed as an analytical chemistry tool to determine the presence of a particular substance in a sample and, in many cases, to quantify the amount of the substance present. IR-UV-Visible spectroscopy is particularly common in analytical applications. Thus, Absorbance spectra of samples such as the silver nanoparticles colloid, solutions of dyes and chemicals substances were recorded using UV spectroscopy using a Cary 5E UV-VIS-NIR spectrometer.

3.3.4. Attenuated total reflectance fourier transform infrared spectroscopy (ATR-FT-IR) analysis

FTIR uses infrared radiation to determine and observe the chemical functional groups present in samples. When an infrared (IR) beam exposed to a sample, chemical bonds stretch, contract, and bend, causing it to absorb IR radiation in a defined wave number. In ATR-FTIR, the incident IR beam first passes through a diamond crystal. The resulting plot is of absorbance (or transmittance) versus wave number. Sampling depth is dependent on the infrared transmitting crystal used to internal reflecting the incident IR beam as well as the refractive index of the sample [162]. ATR-FTIR spectra of samples were obtained using an infrared spectrophotometer (IR Prestige-21, Shimadzu). Spectra were recorded from 600 to 4000 cm^{-1} wave number range with average scan at resolution of 4 cm^{-1}. In measurement of ATR-FTIR spectra, each sample was put down of the ATR crystal, and then a little was pressed on the sample. Baseline correction was applied for all spectra using shimadzu spectrum software.

3.3.5. Nuclear magnetic resonance spectroscopy (^{1}H NMR) analysis

The one-dimension (1D) and two-dimension (2D) ^{1}H-NMR analysis of PDMAPMA before and after quaternization with different alkyl chain (C_8 and C_{16}) were carried out at university of Duisburg- essen using Bruker nuclear magnetic resonance. $CDCl_3$ and MeOD were used as solvent for homo-PDMAPMA and quaternized homo-PDMAMA (C_8, C_{16}) and tetramethylsilane (TMS) as internal reference. By the introduction of additional spectral dimensions, these spectra are simplified and some extra information is obtained. The 2D ^{1}H-NMR spectrum, with two frequency axes, has a characteristic topology: A diagonal of signals divides the spectrum in two equal halves. Symmetrical to this diagonal, there are more signals, called cross signals. The diagonal results from contributions of the magnetization that has not been changed by the mixing sequence (equal frequency in both dimensions) i.e. from contributions, which remained on the same nucleus during both evolution times [163]. The cross signals originate from nuclei that exchanged magnetization during the mixing time (frequencies of the first and second nucleus in each dimension, respectively). They indicate an interaction of these two nuclei. Therefore, the cross signals contain the important information of 2D NMR spectra [164].

3.3.6. X-ray photoelectron spectroscopy (XPS) analysis

XPS is used to determine the atomic composition of the surfaces of substrates. Upon exposure to X-ray photons, a surface emits photoelectrons whose binding energies can be compared to known values to identify the element and its chemical structure. The spectra of XPS are obtained by irradiating a material with a beam of X-rays while simultaneously measuring the kinetic energy and number of electrons that escape from the top 1 to 10 nm of the material being analyzed. XPS spectrum is a plot the intensity count of electrons detected versus the binding energy of the electrons detected. The intensity of the ejected photoelectrons relates directly to the material surface atomic distribution and can therefore be used to quantify percent atomic composition and stoichiometric ratios. These characteristic peaks correspond to

the electron configuration of the electrons within the atoms, e.g., 1s, 2s, 2p, 3s, etc [165]. X-ray photoelectron spectroscopy spectra were carried out by Dr. R. Kaufmann at DWI, Aachen-Germany.

3.3.7. Gel permeation chromatograph (GPC) analysis

GPC is a type of size exclusion chromatography (SEC) and is often used for the analysis of polymers such as polydispersity index (PDI) and relative molecular weight of the polymers.

Relative molecular weights (M_n and M_w) and molecular distributions (M_w/ M_n) of homo-PDMAPMA and quaternized homo-PDMAPMA (C_8) were determined at university of Duisburg- essen by a gel permeation chromatograph (GPC, Jasco PU-2080) equipped with an ETA-2020 RI detector. A series of low-ploy dispersity poly (methyl methacrylate) PMMA-280510 standards were employed for the GPC calibration. The eluent was (DMF+ 0.01M LiBr) at a flow rate of 1.0 mL/ min at ambient temperature.

3.3.8. Inductively coupled plasma optical emission spectrometry (ICP-OES) to determine concentration of silver atoms

ICP-OES is an analytical technique used for the detection of trace metals. It is a type of emission spectroscopy that uses the inductively coupled plasma to produce excited atoms and ions that emit photons electromagnetic radiation at wavelengths characteristic of a particular element. The intensity of this emission is indicative of the concentration of the element within the sample.

The concentration of silver atoms deposited on the fabric was measured by inductively coupled plasma optical emission spectrometry (ICP-OES) (spectrometer Varian 720- ES). Where the samples were digested in a microwave digester (MarsXpress, CEM, Kamp-Lintfort) at 180 ^oC with conc. nitric acid (65%). After complete digestion of the samples, the residual clear solutions were diluted to 100 ml with deionised. Finally, the diluted solutions were measured using ICP/OES instrument to calculate silver atoms concentration

3.4. Surface characterization

3.4.1. Scanning electron microscopy (SEM)

SEM is a type of electron microscope that produces images of a sample by scanning over it with a focused beam of electrons. The electrons interact with electrons in the sample, producing various signals that can be detected and that contain information about the sample's surface morphology and elemental composition the surface samples. Thus, the morphology of the samples surfaces (textiles) were examined by SEM images using a Hitachi 3400 S-3400N.Typ II. To determine the elemental composition of the particles (Silver) studied during electron microscopy, an energy-dispersive X-ray (EDX) detector from EDAX was used with the SEM.

3.4.2. Transmission electron microscopy (TEM)

TEM is a microscopy technique whereby a beam of electrons is transmitted through an ultra thin specimen, interacting with the specimen as it passes through. An image is formed from the interaction of the electrons transmitted through the specimen; the image is magnified and focused onto an imaging device, such as on a layer of photographic film, or to be detected by a sensor such as a camera.

Morphological observations of shape, size and its distribution of silver nanoparticles were carried out with TEM images, in the University of Duisburg – Essen by Dr. Meyer- Zaika. The Instrument used is a FEI (former Philips) CM 200 FEG with a “Super-TWIN” Lens, Lens parameters: f = 1, 7 mm, Cs = 1, 2 mm, Cc = 1, 2 mm, Point resolution: 0, 24 nm, Line resolution: 0,10nm, Accelerating voltage: 200 kV, Holey Carbon film coated Copper grids 400 mesh (Fa. Okenshoy, Tokyo (Japan).

3.4.3. Dynamic light scattering (DLS)

DLS is also known as Photon Correlation Spectroscopy, and it can be used to determine the size distribution of nanoparticles in Brownian motion in solution. This technique is one of the most popular methods used to determine the size of nanoparticles. Measurements of particle size distributions of Ag NPs

were carried out with Malvern instruments (Zetasizer Nano-s). Samples silver nanoparticles for DLS measurements were diluted several time.

3.4.4. Dyeability and dye assays

The analysis of the surface chemical structure and surface characterization can be carried out using dye assays. The dye solution was prepared by solving 1 g of the acid dye Telon Red AFG in 1 l of water, resulting in pH = 4 - 4.5. The fabric samples were immersed in the dye solution (1 g in 50 ml) for 30 minutes at 60^{o}C. After dyeing, the samples were rinsed with distilled water and washed with non-ionic detergent (Marlipal O 13/20, Candea Chemie GmbH, 1 g/l) and Na_2CO_3 (1 g/l) in water, then rinsed with water and dried at 40^{o}C. The dye uptake (D) was calculated from the absorbance of the dye solutions before and after dyeing process, A_0 and A_1, respectively, according to the equation:

$$D\ \% = \frac{(A_o - A_1)}{A_o} \times 100$$

Absorption spectra were measured using a Cary 5E UV-Vis NIR spectrometer, and the so-called color strength K/S was measured using Data colour 3880 spectrophotometer. The colour degree is given according to Berger (light source D65/10). K/S relates the spectral reflectance (R in %) of the sample, its absorption (K) and scattering (S) characteristics according to the Kubelka – Munk equation:

$$K/S = \frac{(1 - 0.01R)^2}{2\ (0.01\ R)}$$

K/S is roughly linear proportional to the effective dyestuff concentration C on the fabric, i.e., K/S = k C, where k is a constant.

3.4.5. Wettability properties

The wettability properties of the samples were measured by two tests, TEGAWA and contact angle measurements. The wettability test according to TEGAWA was applied [166], in this test the wettability was determined by recording the drop penetration time of the drop penetration test, which was done by using an aqueous dye solution based on TEGEWA condition. Since a drop of certain volume (0.05 ml of 2% solution of the dye amino blue V-PW) from a height of 40 mm dropped on the treated sample then the penetration time was recorded as complete dipping of the drop. Contact angles (CA) were measured with 5 µl deionized water using a manual Krüss (G-1) instrument at room temperature. All the contact angles were determined by averaging the values obtained at six different points on each sample surface.

3.4.6. Amount of cationic charged on the surface and isoelectric point (IEP) for silver nanoparticles

The functional groups present on a modified textile surface can introduce a high surface charge density that is typically not present on untreated textile surfaces. When such a charged solid surface is in contact with a liquid phase, an electrical potential develops at the interface. A double layer is established, with surface bound ionizable groups and tightly bound liquid phase ions of opposite charge forming the fixed layer, and loosely bound liquid phase ions of opposite charge forming the mobile layer (Figure 3-4).

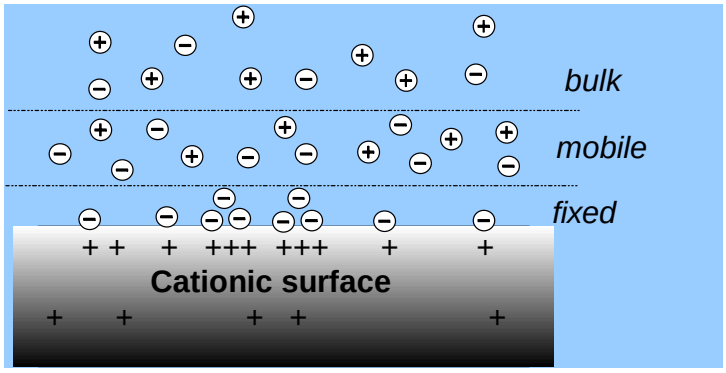

Figure 3-4: Schematic of interaction between cationic surface and opposite charged molecules.

3.4.6.1 Back titration

The amount of cationic charged group on textile surface was determined by the polyelectrolyte titration. Polyelectrolyte titration system, Particle charge detector (PCD 03 PH), was from Mütek Analytic GmbH, Herrsching, Germany, as schemed in figure 3-5.

Polyelectrolyte titrations were done with cationic charged solutions of polydiallylmethyl ammonium chloride (PDADMAC) in case of anionic systems and with anionic polyethylene sulfonic acid, sodium salt (PES-Na) in case of cationic systems as shown in Figure 3-6. A weighted sample of the fabrics was immersed in 50 ml from polyelectrolyte solution PES-Na with concentration 0.001N, after that 100 µl Marlipal was added and shacked for 2 h. During this period, the anionic PES-Na will neutralize all cationic charges of the sample.

1. plastic measuring cell
2. displacement piston
3. electrodes
4. motor and piston
5. electronics
6. display

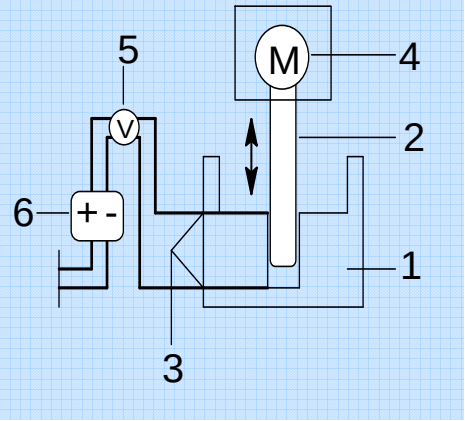

Figure 3-5: Particle charge detector (PCD 03 PH)

Since there is an excess amount of PES-Na, a residual anionic charge will remain the sample. After the reaction period screen out the sample and filtrated and take 10ml of the solution into measuring cell and titrate up to the point zero charge with PDADMAC 0.001N.

Calculation of charges amount (q) according to the following equation

$$\text{Equivalent (eq.)} = \frac{(V_2 - V_1)}{W} \times C$$

(V_2-V_1) is difference between the charge of fresh PESNa and reacted PDADMAC indicates the charge amount neutralized for 10ml in the sample C is concentration of titrant 0.001N , W is the weight of the sample

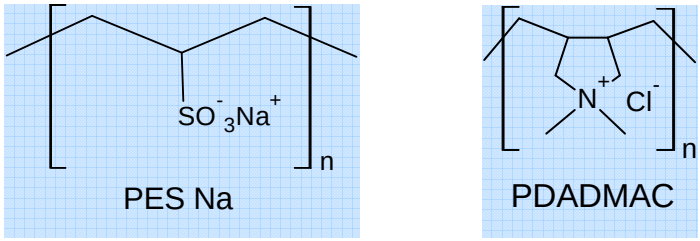

Figure 3-6: Unit structure of cationic and anionic polyelectrolyte

3.4.6.2 Determination of isoelectric point (IEP) for silver nanoparticles (acid/ base titration)

IEP is the pH dependent point of zero charge of a particle, by dropwise addition of a titrant (acid/base), the sample pH's are shifted until the point of zero charge (streaming current = 0mV) is reached.

3.4.7. Laundering durability

Laundering durability of the silver nanoparticles on the textile fabrics was evaluated by determination of the deposited amount of silver over five washing cycles in a laboratory-dyeing machine, using ICP-OES for quantitative measurement. The fabrics were washed in the bath containing 1 g/l nonionic detergent (Marlipal O 13/20 Candea Chemie GmbH) and 1 g/l sodium bicarbonate ($NaHCO_3$) at liquor to fabric ration 40: 1 after 30 minutes of washing at 40 ^oC. The fabrics were rinsed once with warm water 40 ^oC for 3 min and three times for 3 min each with cold water. Finally, the fabrics were dried at 70 ^oC.

3.4.8. Mechanical properties

Investigation of the mechanical properties (tensile strength and elongation) was carried out according to DIN 53857 1 using a Zwick 1445 Testing System, from this test we can determine the strength of the treated fabrics along with the elongation after certain tension test.

3.5. Antibacterial properties

Antibacterial efficacy of textiles was evaluated using several tests, qualitative test such as agar diffusion test and quantitative tests such as ASTM E2149-01 test and Tetrazolium/ Formazan Test. In this study, *E. coli* DSMZ 498 and *M. lutues* ATCC 9341 were used as non-pathogenic substitutes for Gram-negative and Gram-positive bacteria.

3.5.1. Preparation of microorganisms:

One well-isolated colony was transferred aseptically, using a wire loop, to a 100 ml conical flask containing 50 ml SI-medium. The flask was incubated at 37 °C for 24 h and then the grown bacteria were diluted with sterile saline to a final working concentration of 1 x 10^5 to 10^7 colony forming units (CFU)/ml.

3.5.2. Zone of inhibition test (qualitative method)

The antibacterial activity of the samples was characterized by evaluating the inhibition of the growth of *Micrococcus luteus* (*M. luteus*) and *Escherichia coli (E. coli)* bacteria. In this test, the samples were placed on top of two standard nutrient agar plates from Carl Roth GmbH. The lower layer consists of culture medium without any bacteria, while the upper layer was inoculated with the bacteria. The two-layer setup was placed in a Petri dish and was incubated for 18-24 h at 37^{o}C. The inhibition of bacterial growth on the fabric surface was characterized qualitatively by visual inspection.

To evaluate antibacterial activity of Ag NPs against *E. coli and M. luteus* and effect of concentration of Ag NPs on its antibacterial activity using the zone inhibition test as qualitative method. 100 µl of suspension of bacteria with a concentration of 10^5 to 10^7 CFU/ ml of *E. coli* and *M. luteus* were spread on a nutrient agar plate. The plates were holed with 1cm diameter and then 100 µl of Ag NPs colloid poured in the holes with different concentrations. The plates were incubated for 24 h at 37 °C.

3.5.3. ASTM E2149-01 test method (quantitative method)

A second test for quantifying the antimicrobial effect was carried out according to shake Flask method **(ASTM E2149-01)** as follows: *E coli* bacteria

were grown for 18 hours at 37 ^{o}C in a standard nutrient broth. The resulting cell suspension was diluted by the factor of 10^{7}. Textile samples (0.5 gram) were impregnated with 50 ml of the diluted solution. After that, the samples were incubated in shaker for 1 h at 37 ^{o}C. The colony forming units (CFU) in the bacteria suspension were counted. The percentage of microbe reduction (R %) was calculated using the following equation:

$$R\ \% = \frac{(B - A)}{B} \times 100$$

Here, A [CFU] is the number of colonies of the samples after 1 h and B [CFU] after zero contact time.

To calculate the lowest concentration of Ag NPs that completely inhibited bacteria growth, using minimum inhibitory concentration (MIC) test against E.coli. Broth containing was determined using the plate count method. 10^{5} CFU/ml of bacterial cells was used as a culture medium. The concentrations of Ag-NPs were zero, $3.5x10^{-5}$, $7x10^{-5}$, $14x10^{-5}$ mol/l. 100 µl with different concentrations of Ag NPs colloid mixed in 25ml of 10^{5} CFU/ml of bacterial culture. The medium was cultured in a shaking incubator at 37 ^{o}C for 3 h, and the cultured media (100 µl) was spread onto agar and incubated at 37^{o}C for 24 h. After incubation, the number of colonies grown on the agar was counted.

3.5.4. Tetrazolium/ formazan test TTC (rapid method)

The TTC-test method was used in this thesis to measure the antibacterial efficiency of textile. Tetrazolium salts as TTC and formazans have been known in chemistry for about a hundred years [167]. Tetrazolium salts and formazan are not only applied in chemistry and industrial technology, but also in histochemistry, biochemistry and biological science e.g. botany, medicine, immunology and pharmacology[168]. The TTC-test method is considered a quick method for evaluating the antibacterial activity of fabrics finished, since the absorbance of formazan, measured at 480 nm, is directly proportional to the viable active cells. Therefore, the red formazan obtained indicates the activity and viability of the cell. The tetrazolium/ formazan couple is a special redox system as described

below in Figure 3-7. Since, in the presence of bacteria, TTC is reduced to red formazan.

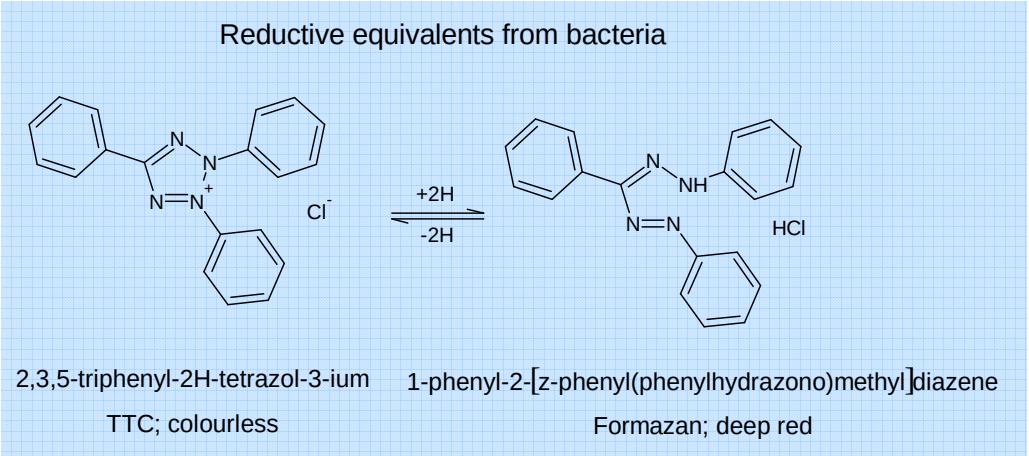

Figure 3-7: Mechanism of the tetrazolium/ formazan system.

In this test, both control and finished fabrics were cut into small size of a diameter 3.8 ± 0.1 cm of circular shape. The number of circular sample to be used was 6. Before incubation, both the control and the treated samples were sterilized at 110 °C, then all samples were placed in 40 ml nutrient broth medium flask which containing 10 µl of microorganism (10^7 CFU/ ml), then all flasks were incubated with shaking at 37 °C/200 rpm for 3 h, then 1 ml from each flask which containing the control and the finished samples was added to sterilized test tubes containing 100 µl TTC (0.5 % w/v). All tubes were incubated at 37 °C for 20 min. The resulted formazan was centrifuged at 4000 rpm for 3 min followed by decantation of the supernatants. The obtained pellets were re-suspended and centrifuged again in ethanol. The activity and viability of the cells was determined by the formazan absorbance value, which was measured by photometer at 480 nm[169].

4. Chapter 4: Surface modification of PET fabric via photo-chemical reaction of DMAPMA for antibacterial applications

4.1. Introduction

Some surface modification of synthetic fibers specially PET used to improve antibacterial activities for a variety of application such as medical applications, filtration, home furnishings and apparel products. There are lot of methods have been used to get products with antibacterial properties such as finishing and coating processes. We were interesting in finding applicable, fast, and environmentally friendly processes that could be used to modify synthetic fibers have antibacterial activity. The antibacterial activity can be introduced into the synthetic fibers either at the producing step of fibers itself by addition of antibacterial agents into polymer solution or by coating the finished product with antibacterial agents. However, the products, which physically trapped antibacterial agents, have limitation of leaching and leading to decrease antibacterial efficiency with usage time. Immobilization of antimicrobial agents through covalent bonding can be a solution of this problem and established by radiation grafting techniques for attaching polymer chain containing desired chemical groups such as quaternary ammonium groups via covalent bonding to existing polymeric backbones.

In this study, the tertiary amino group containing monomer dimethylaminopropyl methacrylamide (DMAPMA) is grafted / co-polymerized onto PET via UV irradiation. PET fabrics are used as exemplary substrates. An ensuing quaternization is done using alkyl bromides, the concept and the involved reactions are sketched in Scheme 4-1, in order to establish antibacterial properties.

4.2. Synthesis of homo PDMAPMA and quaternization of homo PDMAPMA with C_8 and C_{16}

The quaternization reactions were initially prepared for homo PDMAPMA, prior to reaction on the PET grafted PDMAPMA chains. The quaternization

reaction was confirmed by 1D and 2D 1HNMR, ATR-FTIR, DSC and Molecular weights and molecular distributions of PDMAPMA were measured by Gel Permeation Chromatograph (GPC) analysis.

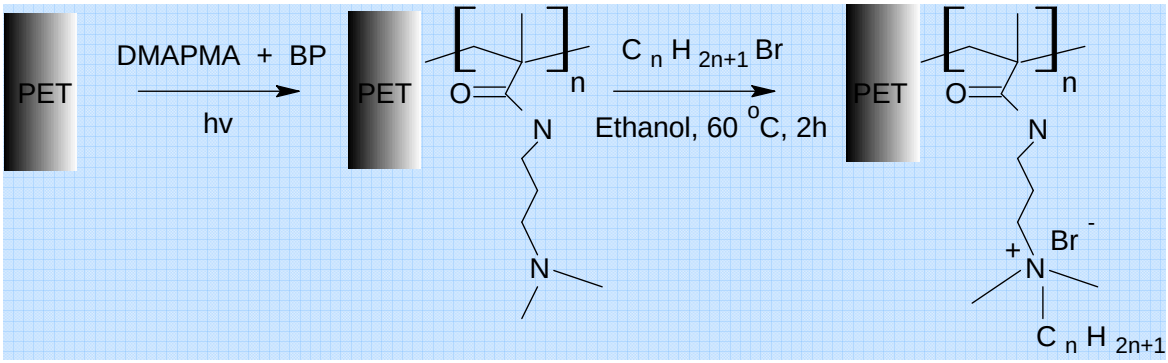

Scheme 4-1: Scheme of the photo-grafting of PET fabric with DMAPMA and the ensuing quaternization of the modified samples (designated in the following as PET-g-PDMAPMA) with alkyl bromides.

4.2.1. ^{1}H-NMR analysis

The 1D and 2D ^{1}H-NMR analysis of PDMAPMA before and after quaternization with different alkyl chain (C_8 and C_{16}), were confirmed that the pendant amino groups were successfully quaternized.

The peaks at 2.26, 2.38 and 3.18 ppm are corresponding to –N-$(CH_3)_2$, -CH_2-N- and –CH_2-NH- respectively, as shown in figure 4-1. 1D ^{1}H NMR spectra of quaternized homo PDMAPMA with C_8 and C_{16} are complex for interpretation as most of the peaks overlap. By the introduction of additional spectral dimensions, these spectra are simplified and some extra information is obtained. Thus Using 2D 1H-NMR spectra to show some peaks overlap. The Peaks of quaternized homo PDMAPMA with C_8 and C_{16} were at approximately 1.3 ppm, which are characteristic of the (-CH_2-) groups of the alkyl chains C_8 and C_{16}. Moreover, the peaks of the terminal of alkyl chain were approximately at 0.92 pmm. From these peaks, we could confirm the presence of the alkyl chains on the pendant amino groups of PDMAPMA as we see in figures 4-2 and 4-3.

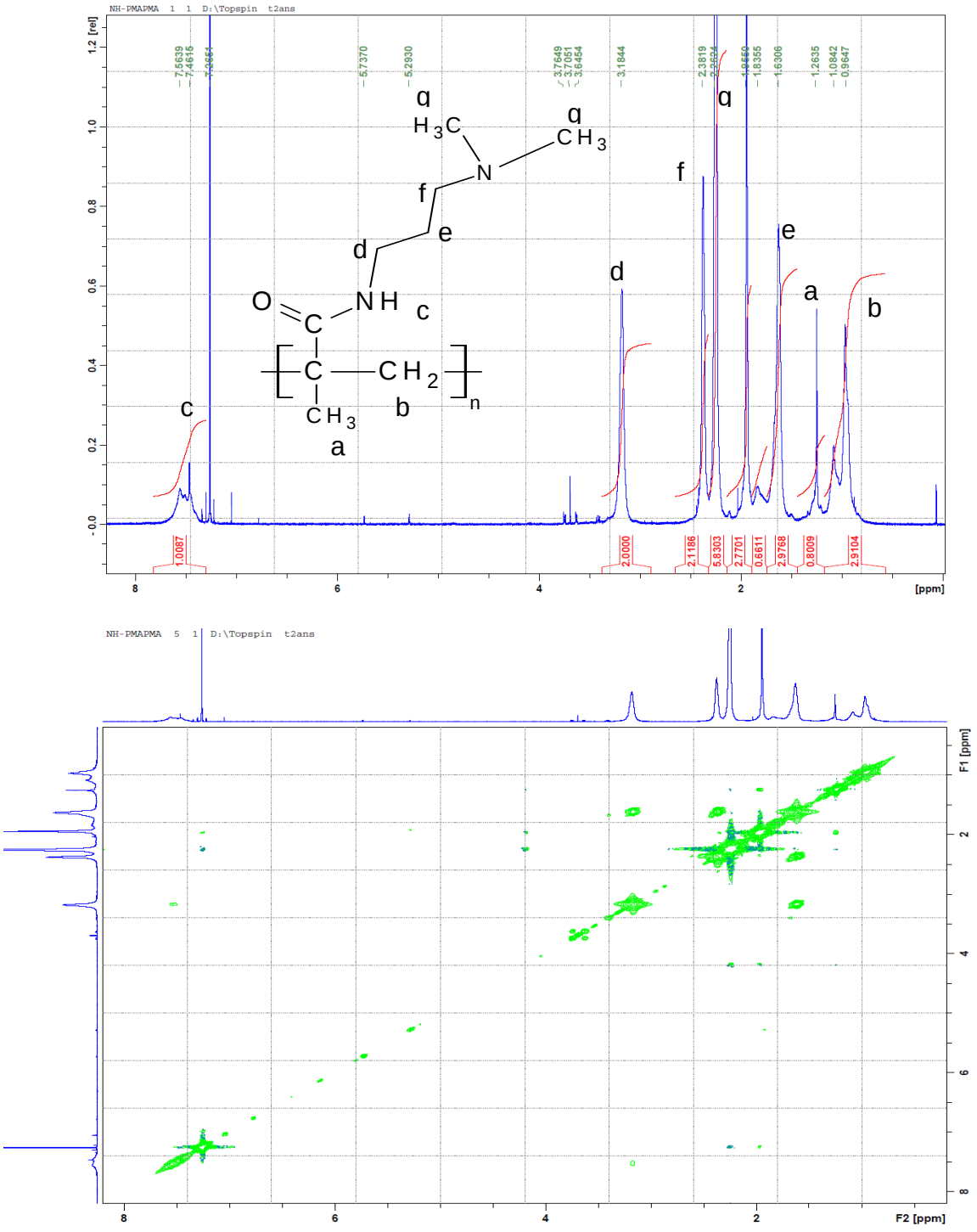

Figure 4-1: 1D and 2D ^{1}HNMR of homo PDMAPMA

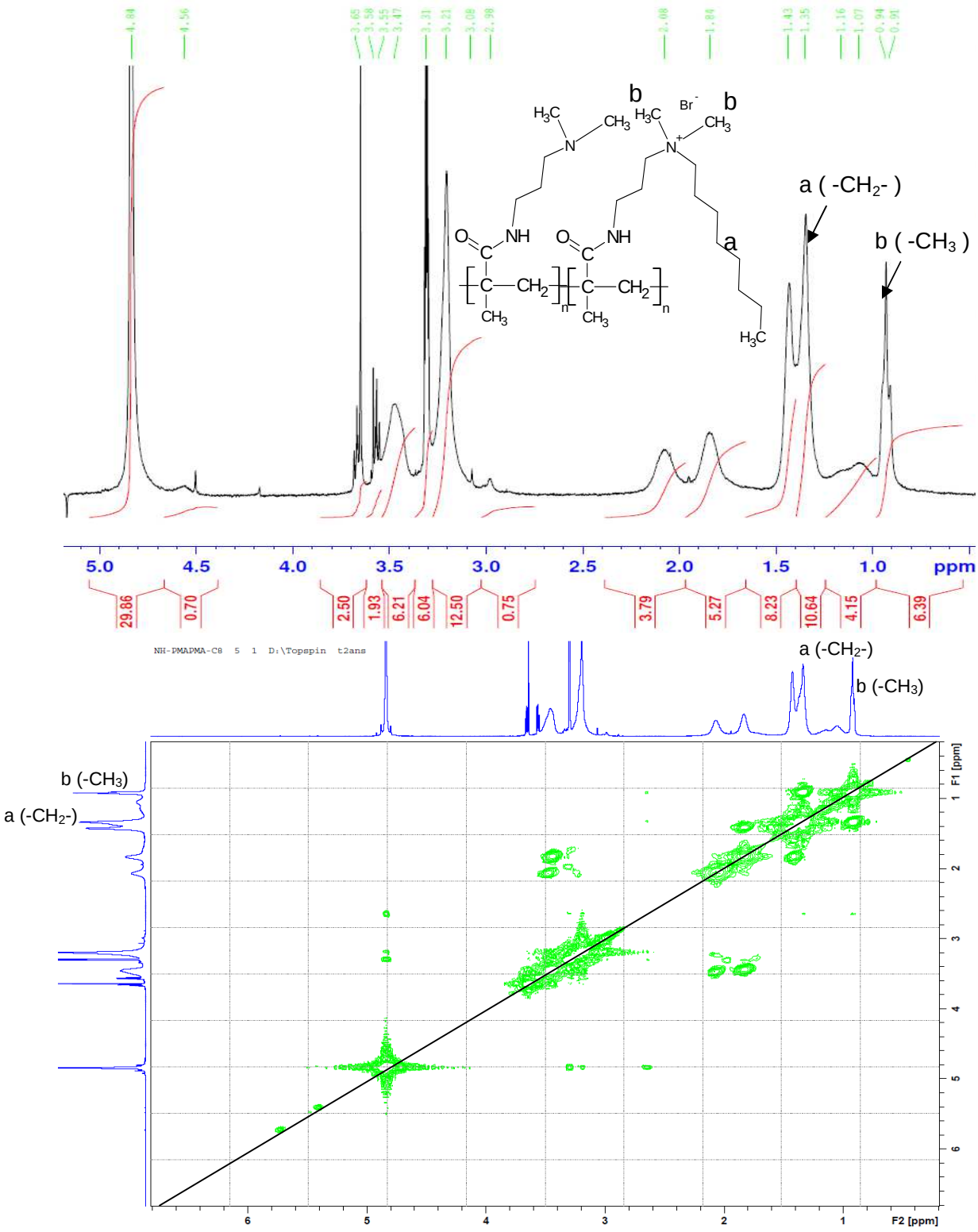

Figure 4-2: 1D and 2D ^{1}HNMR of quaternized homo PDMAPMA with C_8

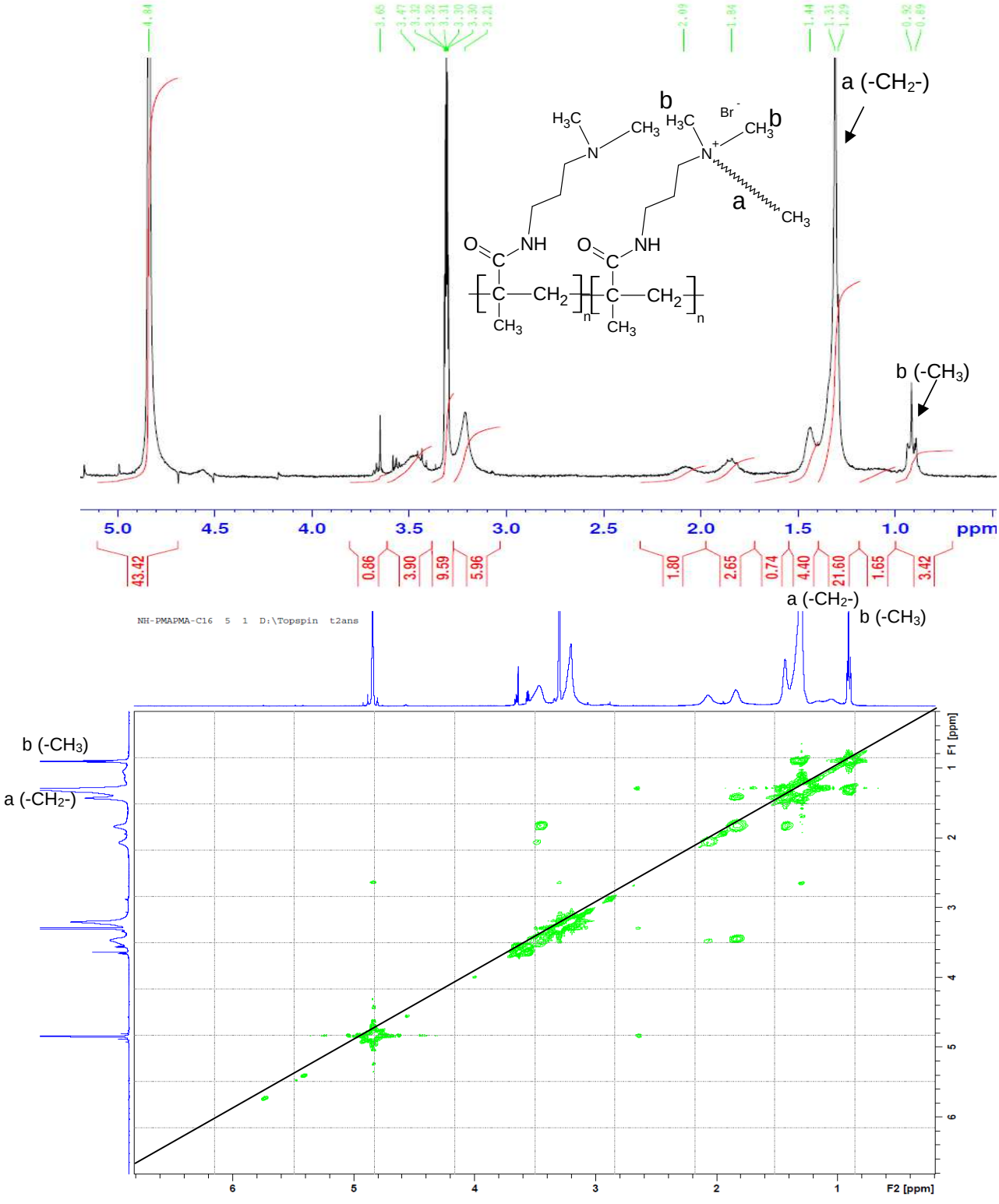

Figure 4-3: 1D and 2D ^{1}HNMR of quaternized homo PDMAPMA with C_{16}

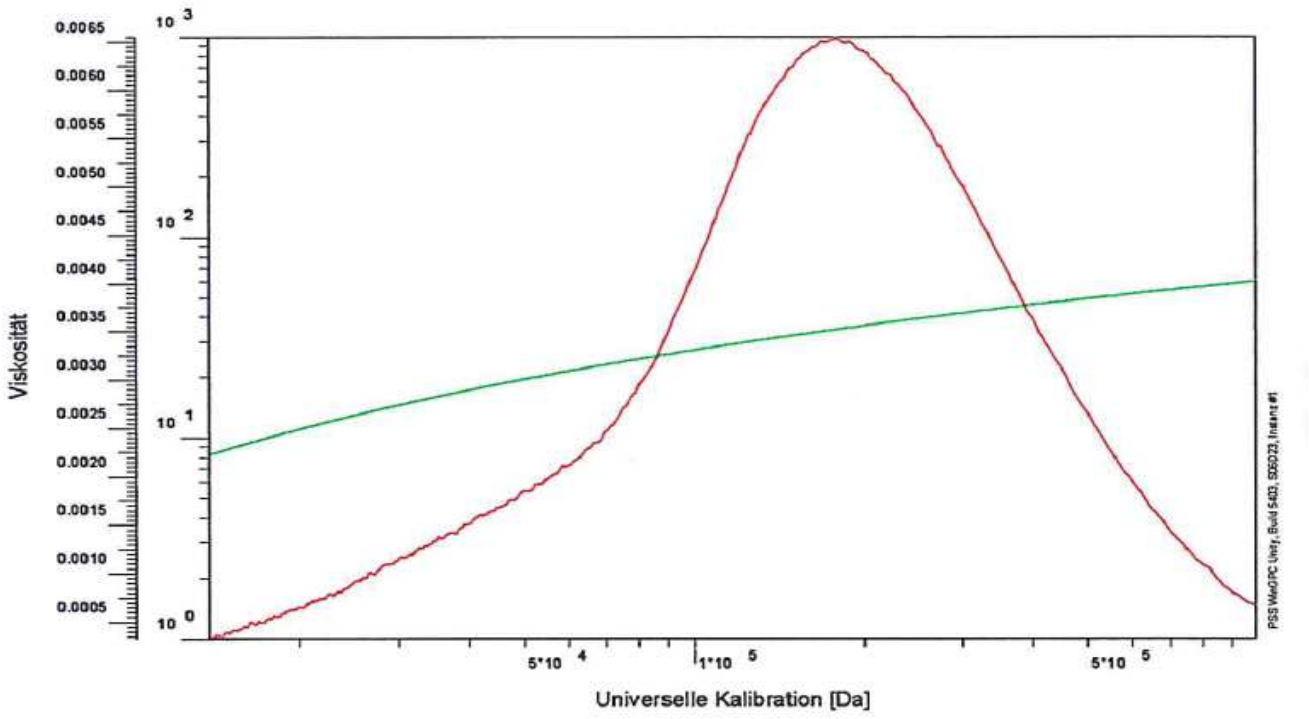

Figure 4-4: A typical size exclusion chromatogram showing the molecular weight distribution of homo PDMAPMA chains

4.2.2. GPC analysis

GPC has become the most widely used technique for analyzing polymer samples in order to determine their molecular weights and weight distributions. Therefore, the Molecular weights (Mn and Mw) and molecular distributions (Mw/ Mn) (poly dispersity index, PDI) of the homo PDMAPMA and quaternized homo PDMAPMA with C_8 were analyzed by GPC The homo PDMAPMA and quaternized homo PDMAPMA with C_8 were analyzed by gel permeation chromatograph to estimate the Molecular weights (M_n and M_w) and molecular distributions (M_w/ M_n) (poly dispersity index, PDI). M_n *(D)* and M_w (D) of the homo PDMAPMA and quaternized homo PDMAPMA with C8 were 45200, 42493 and 136000, 114200 Da, respectively. The apparent M_n *(D)* and M_w (D) were reduced due to introduce alkyl chain C_8 through quaternization reaction. This mean the swelling and solubility in DMF solvent of PDMAPMA is more than quaternized PDMAPMA with C_8. The molecular distributions of the homo PDMAPMA and

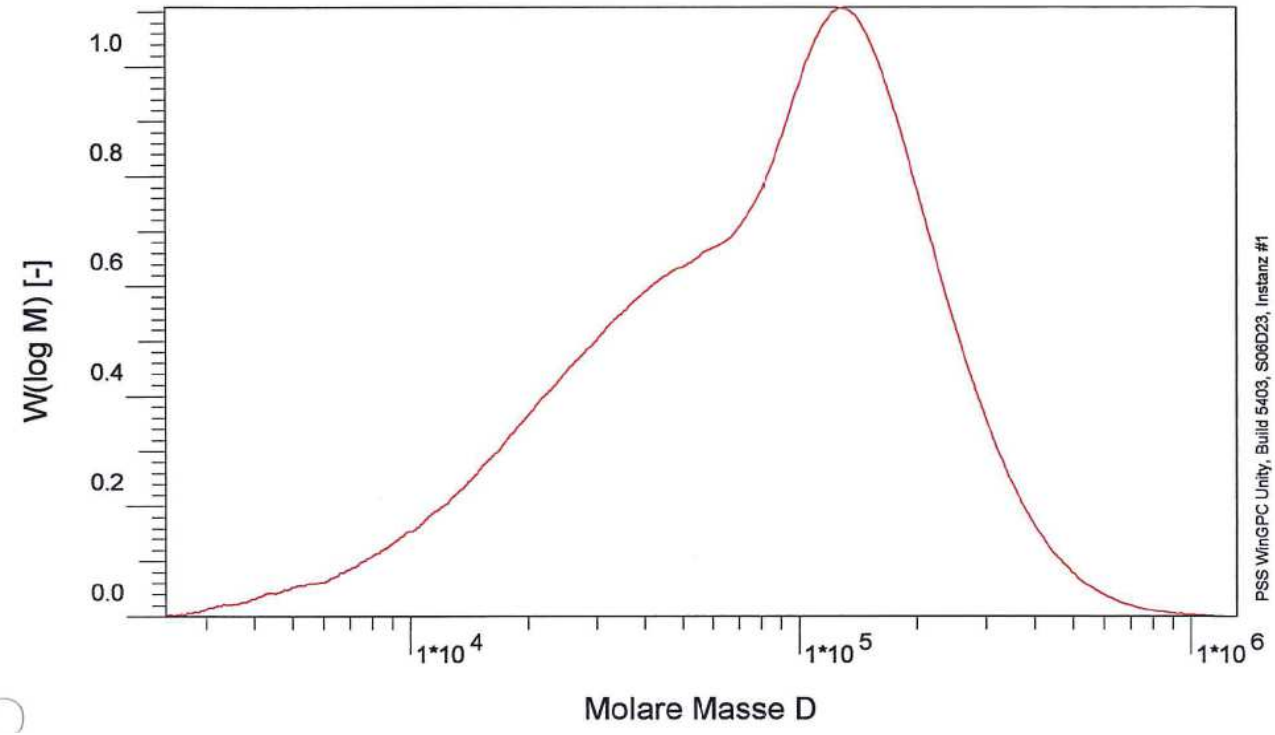

Figure 4-5: A typical size exclusion chromatogram showing the molecular weight distribution of quaternized homo PDMAPMA (C_8) chains

quaternized homo PDMAPMA with C_8 (PDI) had a broad molecular weight distribution (PDI 3.01 and 2.68) as shown in figures 4-4 and 4-5. Because of quaternized homo PDMAPMA with C_{16} sample was not soluble in DMF, due to its long alkyl chain, it was not possible to analyze the sample with gel permeation chromatograph (GPC, Jasco PU-2080) equipped with an ETA-2020 RI detector.

4.2.3. ATR-FTIR analysis

FTIR spectroscopy was also used to confirm the quaternization reaction. Since the long alkyl chain C_{16} compounds were used in quaternization, peaks in the range of 2920-2850 cm^{-1} C-H anti-symmetric and symmetric stretching of CH_3 and CH_2 group suggested the successful addition of alkyl chains to the polymer. The same peaks were also observed for quaternized homo PDMAPMA with C_8 as illustrated in figure 4-6.

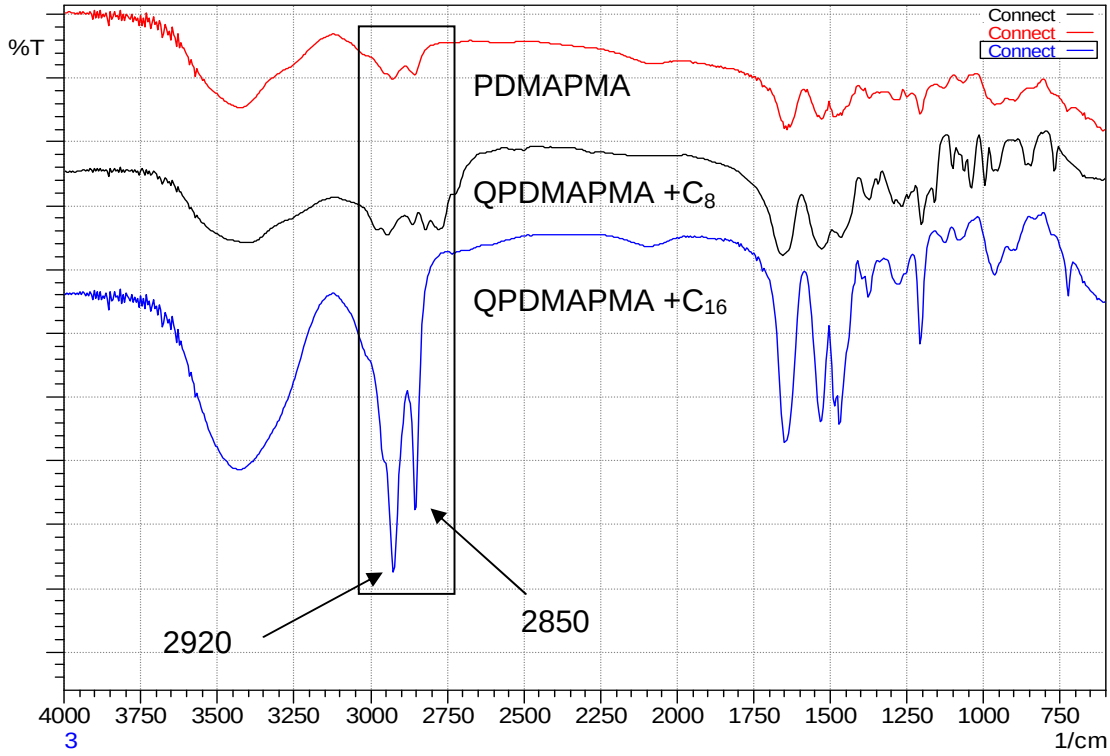

Figure 4-6: FTIR spectra of the homopPDMAPMA and quaternized homo-PDMAPMA (C_8, C_{16})

4.3. Surface modification of PET fabric via photo-chemical reaction of DMAPMA

In a second set of experiments, the grafting process was investigated. Graft yield and graft efficiency were determined by gravimetry, and Parameters influence on Graft Yield such as influence of monomer concentration, BP concentration, and irradiation time were studied. Also surface analysis and the mechanism of photochemical reaction were studied. The surface characterization of PET fabric such as morphology of the surface, dyeability, amount of positive charges on the surface, wittability properties, thermal properties, mechanicals prperties and antibactrial properties were investigated

4.3.1. Parameters influence on graft yield % (GY)

4.3.1.1 Effect of monomer concentration

The data shown in figure 4-7 indicate that the graft yield GY, i.e., the amount of the grafted DMAPMA, increases with increasing concentration of the monomer DMAPMA. The concentration of BP in these experiments was 1 %, the irradiation time 10 min. The graft yield exhibits a saturation behavior with the maximum at about 20%. Simultaneously, the graft efficiency decreases from 100 % to approximately 60 %. It may be assumed that no further monomer can be grafted onto the polymer surface at this level. The saturation behavior of photochemical reaction of monomer due to homo-polymer formation increased at high monomer concentration and surface of PET is complete coated with grafted polymer or net work polymer on the surface.

A similar behavior is observed when, at a given monomer concentration, the irradiation time is varied (figure 4-8). The maximum GY increases with increasing monomer concentration in the grafting solution. Similarly the saturation behavior prolong the time due to homo-polymer formation.

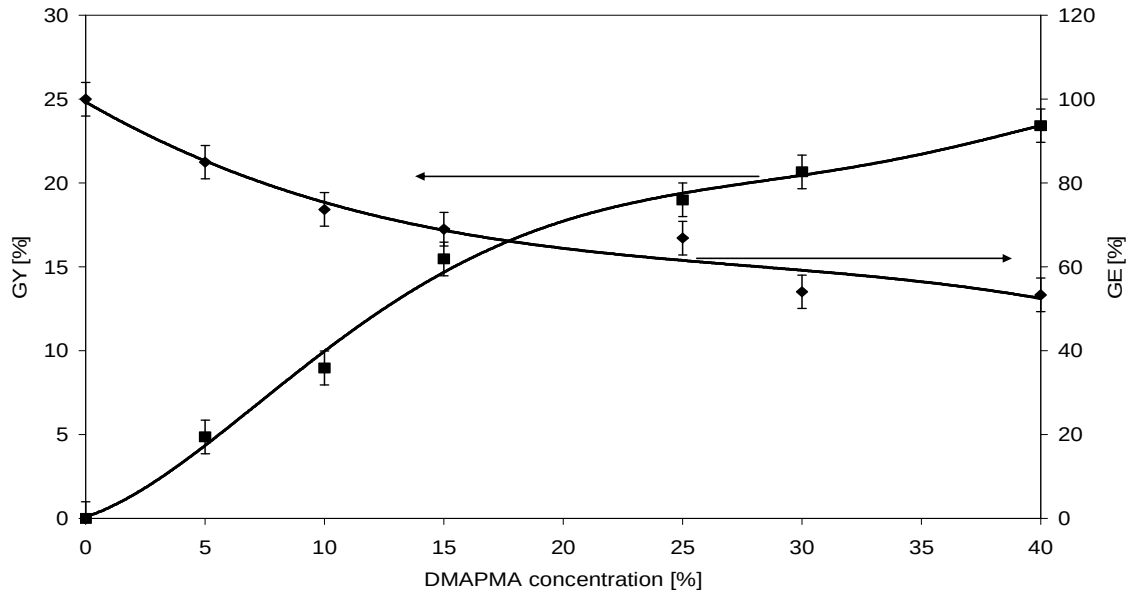

Figure 4-7: Effect of DMAPMA concentration on graft yield and graft efficiency measured as amount of PDMAPMA on the PET fabric. The BP concentration was 1 %, the irradiation time 10 min.

4.3.1.2 Effect of photo-initiator concentration

The influence of the BP concentration on the graft co-polymerization is exemplified by the data shown in figures 4-9 and 4-10. Figure 4-9 gives the dependence of graft yield on BP concentration. The UV exposure was 10 min and monomer concentration 15 %. As was observed for the variation of BP concentration (see figure 4-10), the graft yield shows a saturation behavior. A potential explanation for this behavior may be found in an increasing number of free radicals in the applied grafting solution, which promotes recombination.

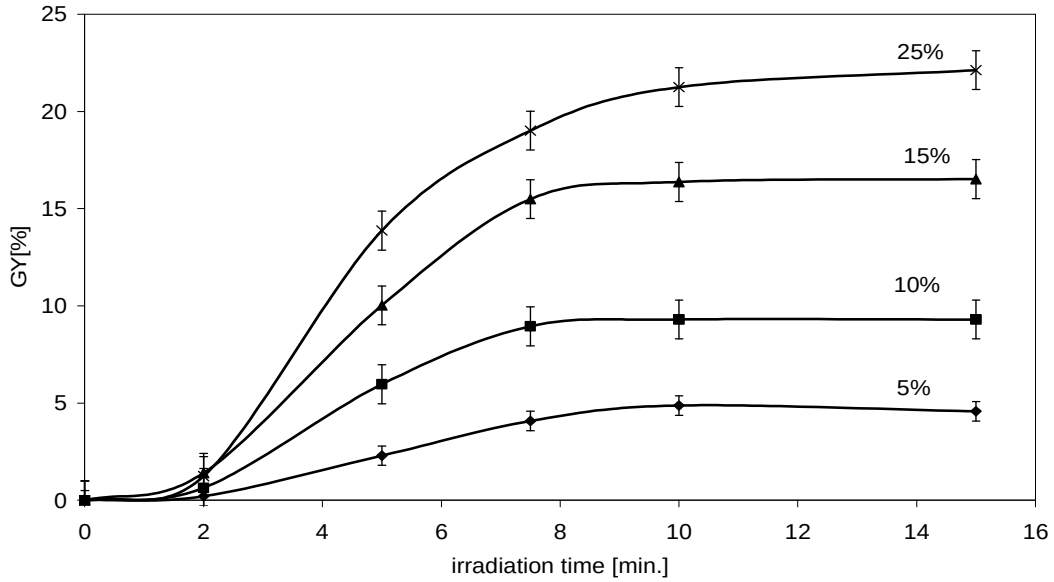

Figure 4-8: Effect of irradiation time on graft yield with different concentrations of DMAPMA measured as amount of PDMAPMA on the PET fabric. The BP concentration was 1 %

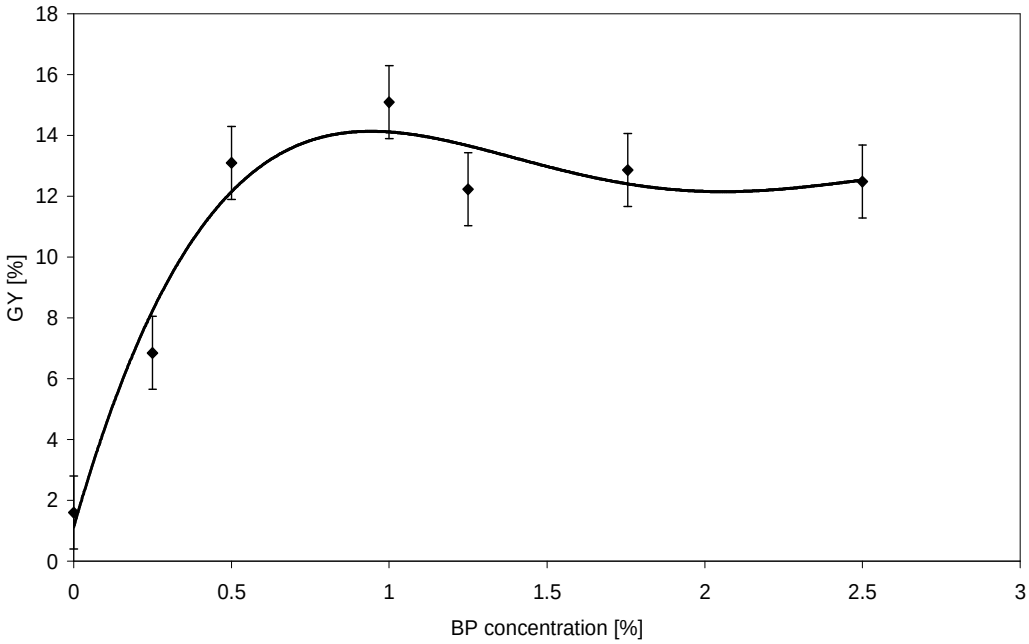

Figure 4-9: Effect of BP concentration on graft yield. Monomer concentration was 15 %, the irradiation time 10 min.

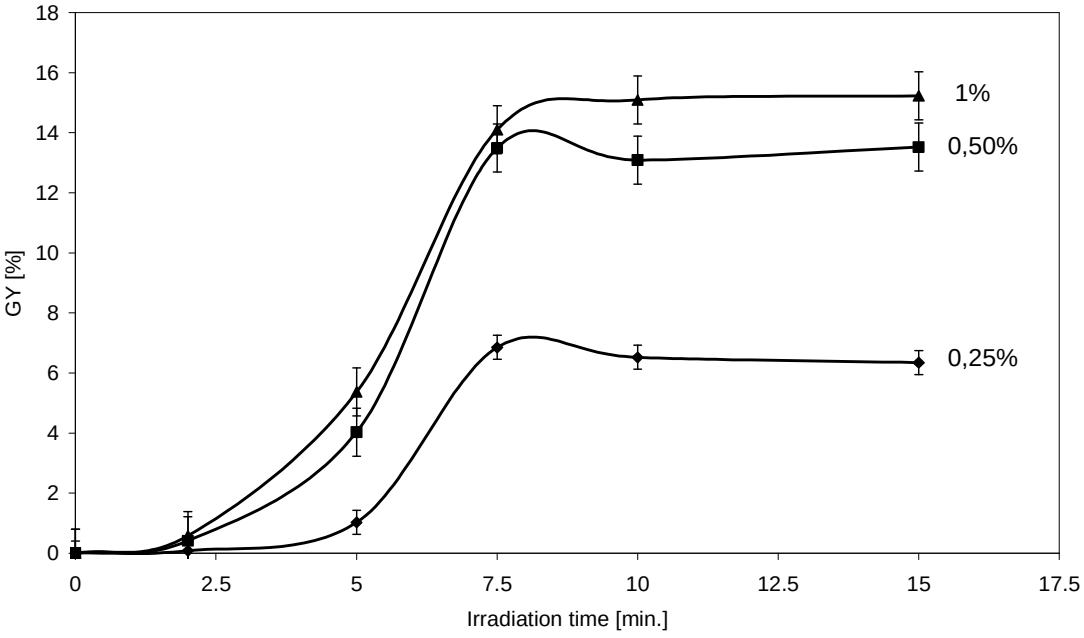

Figure 4-10: Effect of irradiation time on graft yield with different concentrations of BP. The monomer concentration was 15 %.

4.3.2. Mechanism of the photo-chemical reaction

Accordingly, the process can be assumed to involve the following Scheme 4-2. Reaction (1) is the initial formation of BP radicals. Singlet state radicals are short-lived. However, long-lived triplet-state radicals with high reactivity are also generated by intersystem crossing (ISC). Hydrogen abstraction generates a reactive polymer radical PET$^{\cdot}$ (reaction (2)), with which the monomer M can react (reaction (3)), and the less reactive ketyl radical. Potential side reactions could be: Quenching of excited BP to ground state and hydrogen abstraction from side groups of the grafted polymer or from the monomer (reaction (4)) initiate cross-linking or homo-polymerization (reaction (5)), respectively. Both reactions provide free radicals for covalent bonding, e.g., to PET. Termination can occur through typical re-combination reactions of macroradicals and cross-linked between the chains of polymer (reaction 6); dimerization of ketyl radicals yields benzpinakol (reaction 7).

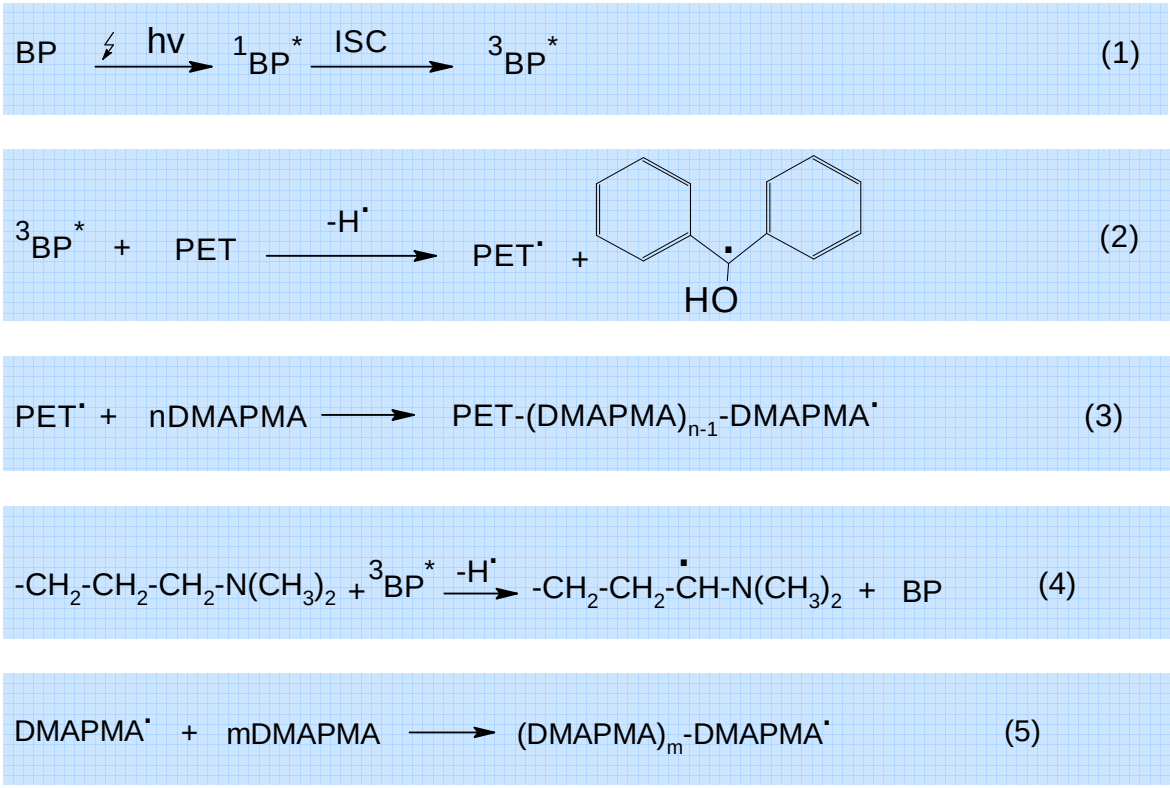

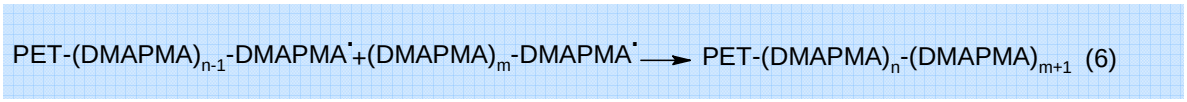

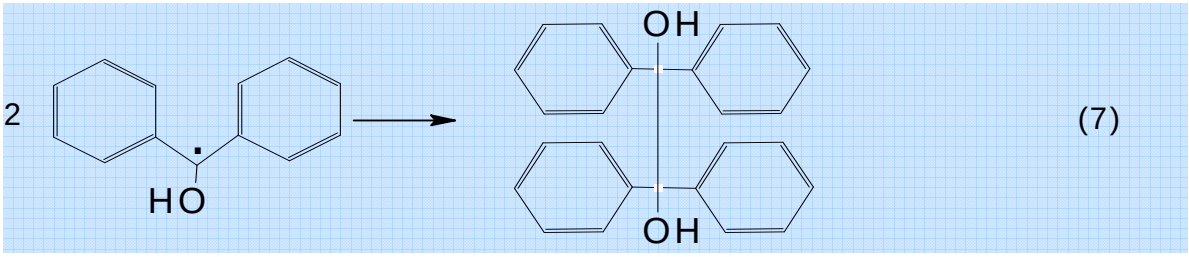

Scheme 4-2: Scheme of the photochemical reaction of PET fabric with DMAPMA

In general, we can summarize the mechanism of photochemical reaction as follows:

Benzophenone absorb a energy of photon from UV radiation then excited to singlet state, then relaxes to a triplet state with long life time. Extraction of hydrogen atoms from PET surface and from DMAPMA, resulting in free radical on PET surface and free radical on the monomer DMAPMA molecule due to chemical reactivity of amino groups. The surface radicals can react with reactive monomer DMAPMA and form grafted chains on the surface substrate; also, free radicals on the monomer DMAPMA molecules can react as cross-linker between the chains of the polymers. Finally, grafted and cross-linked of PDMAPMA, (network polymer) cover the surface of PET.

4.3.3. Quaternization of PET-g-PDMAPMA

Quaternization of PET-g-PDMAPMA reaction was described by Ramadan et al.[159,] PET-g-PDMAPMA samples were quaternized using the four different alkyl bromides, namely 1-bromohexane, 1-bromoctane, 1-bromododecane, and 1-bromohexadecane. The yield of the quaternization reaction was determined gravimetrically. Relevant results are shown in table 4-1. It can be taken from the presented data that the quaternization reaction had a high yield when bromides with shorter alkyl chain were used. This is due to the steric effect, which prevents the approach of the molecules to the tertiary groups on the fiber surfaces.

Table 4-1: Quaternization yield (QY %) for the different alkyl bromides. GY is the graft yield of PDMAPMA.

The samples		*PET-g-PDMAPMA +($C_6H_{13}Br$)*	*PET-g-PDMAPMA +($C_8H_{17}Br$)*	*PET-g-PDMAPMA +($C_{12}H_{25}Br$)*	*PET-g-PDMAPMA +($C_{16}H_{33}Br$)*
Quaternization Completion %	*GY% = 9.1*	42.1	41.02	24.3	11.9
	GY% = 21.3	46.4	43.7	28.8	14.09

In addition, the quaternzation reaction of the samples with high graft yield % and shorter alkyl chain bromides possessed a higher quaternization completion % a compared with the samples quaternized with low graft yield % and longer alkyl chain bromides as shown in table 2. This is due to the influence of geometry of the length of chain of alkyl groups (steric effect), which prevents the approach of the molecules to the tertiary groups on the fabric, and this explains the small amount of quaternization reaction product with a long chain of alkyl bromide.

4.3.4. Surface analysis

Surface chemistry and thermo-analytical of the modified samples was analyzed by ATR-FT-IR and XPS.

4.3.4.1 ATR-FT-IR analysis

Infrared spectra taken from PET (a), grafted PET (b), and grafted and quaternized PET fabrics (c to f) are shown in figure 4-11. It can be clearly seen that new absorption bands appear after grafting. The spectrum (b) shows absorption peaks at 2850 cm^{-1} for C–H stretching of – $N(CH_3)_2$ and at 2985-2905 cm^{-1} for the –NH- of amino groups which do not appear in the spectrum of untreated PET. Also, a new band appears at 1650 cm^{-1} which is characteristic for C=O stretching of amide groups from PDMAPMA. We also observed that not any new band appears after quaternization reaction with different alkyl chain as shown in spectra c to f.

4.3.4.2 XPS analysis

Results of XPS analysis were summarized in table 4-2 and figure 4-12. The balance of total element content (table 4-2) clearly shows the introduction of nitrogen following the grafting reaction and the occurrence of bromium following the quaternization. In agreement with the determined yield of the quaternization reaction, the relative bromium content after quaternization with the long alkyl bromide $C_{16}H_{33}Br$ is smaller than in the case with the shorter $C_8H_{17}Br$.

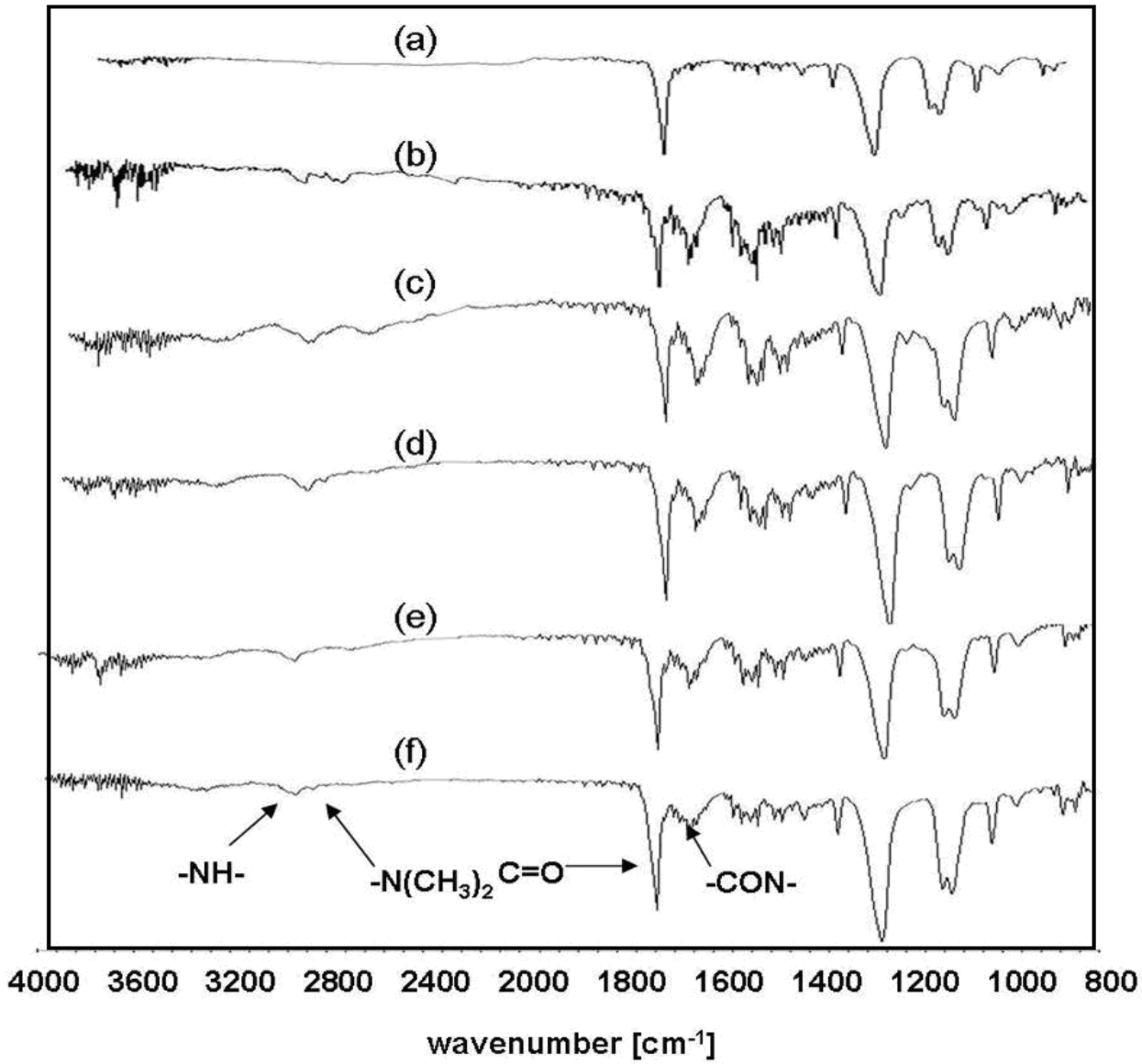

Figure 4-11: FT-IR/ATR spectra of untreated PET (a), PET-g-PDMAPMA (b), quaternized PET-g-PDMAPMA+$C_6H_{13}Br$ (c), quaternized PET-g-PDMAPMA+$C_8H_{17}Br$ (d), quaternized PET-g-PDMAPMA+$C_{12}H_{25}Br$ (e), and quaternized PET-g-PDMAPMA+$C_{16}H_{33}Br$ (f). The graft yield of the PDMAPMA-modification was 9.1 % in all cases.

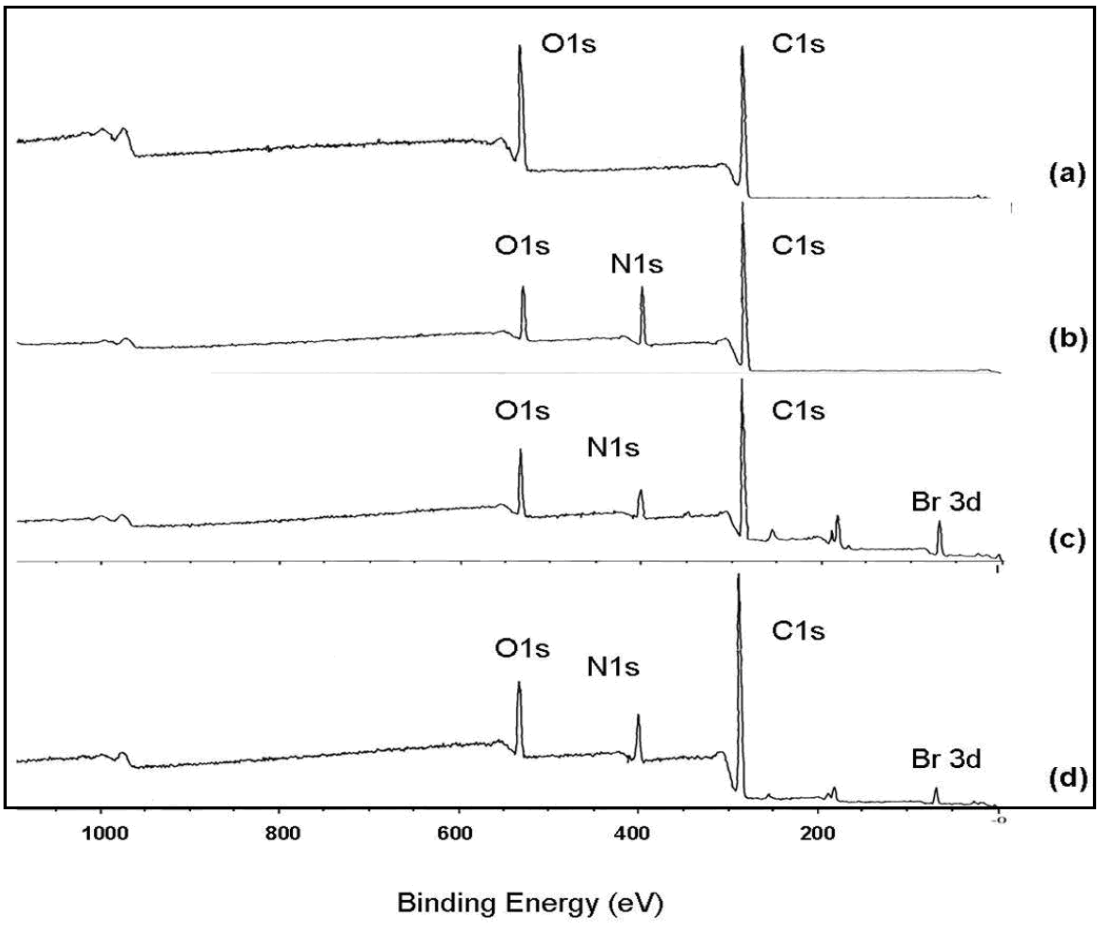

Figure 4-12: XPS spectra of untreated PET (a), PET-g-PDMAPMA (b), PET-g-PDMAPMA+$C_8H_{17}Br$(c), and PET-g-PDMAPMA+$C_{16}H_{33}Br$ (d). The graft yield of the PDMAPMA-modification was 9.1 % in all cases.

Table 4-2: Total content of elements C, O, N, and Br at the surfaces of untreated, grafted and quaternized PET as determined by XPS analysis. The graft yield of the PDMAPMA-modification was 9.1 % in all cases.

Sample	*C1s [%]*	*O1s [%]*	*N1s [%]*	*Br3d [%]*	*O1s/C1s*
PET	78.1	21.9	-	-	0.28
PET-g-PDMAPMA	77.42	8.5	13.92	-	0.11
PET-g-PDMAPMA+$C_8H_{17}Br$	74.59	10.34	10.11	4	0.14
PET-g-PDMAPMA+$C_{16}H_{33}Br$	79.25	9.27	10.17	1.31	0.11

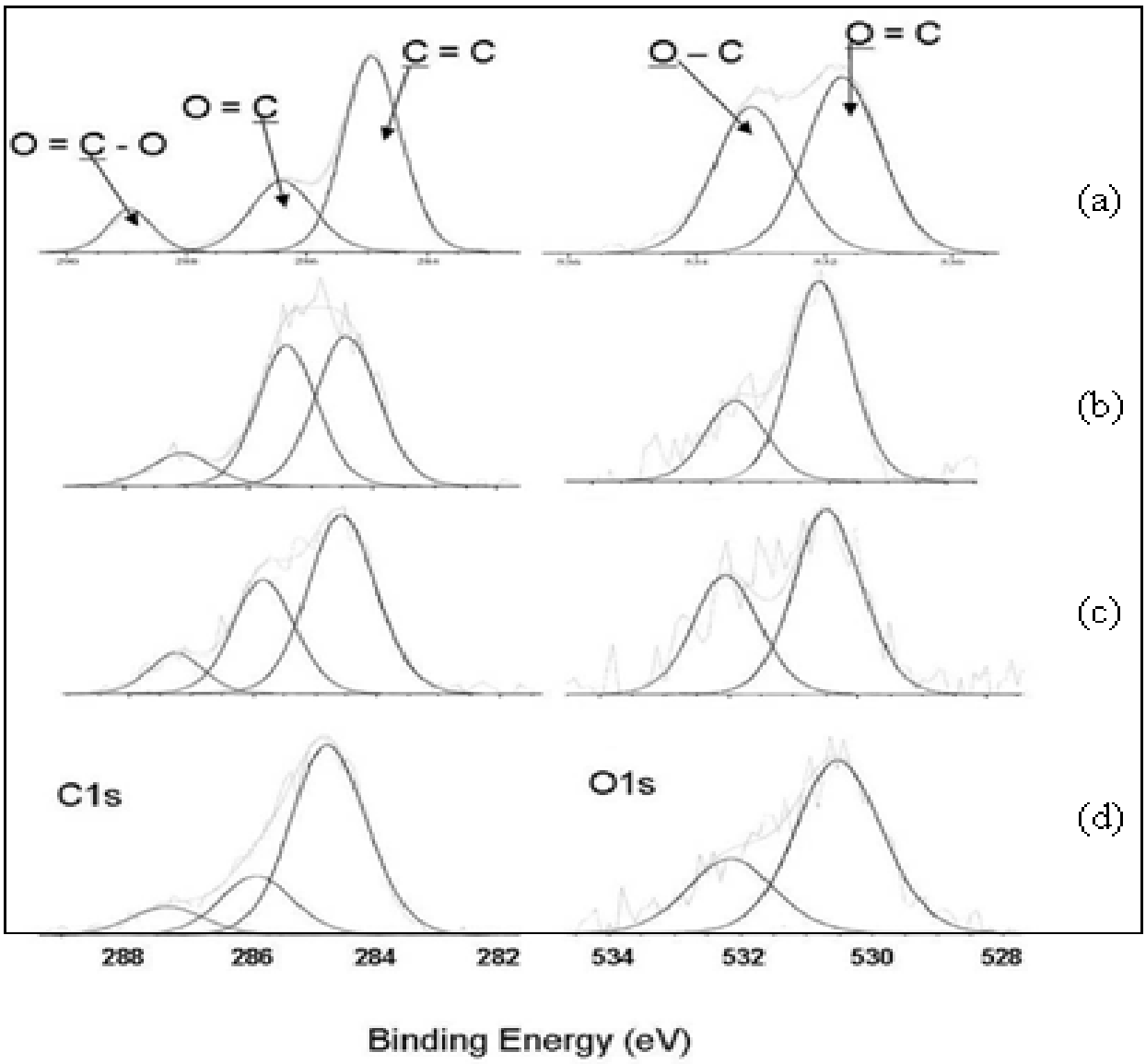

Figure 4-13: Resolved XPS spectra of C1s and O1s for PET original (a), PET-g-PDMAPMA (b), PET-g-PDMAPMA+$C_8H_{17}Br$ (c), and PET-g-PDMAPMA+$C_{16}H_{33}Br$ (d).

Highly resolved C1s and O1s spectra of the samples are shown in figure 4-13 and table 4-2. In the case of the untreated PET fabric, the main core C1s could be de-convoluted by curve fitting into three peaks at 284.89, 286.40 and 288.94 eV, corresponding to C-H or C-C in phenyl ring , C-O and C=O, respectively. This is in agreement with literature[170, 171.]

The area ratio of these peaks, however, are 5.7 : 2.3 : 1 which is not identical to theoretical values for PET film which is 30 : 10 : 1 [172]. It has to be noted, however, that the textured surface of a fabric, in contrast to the perfectly smooth surface of a film, affects the resolution of XPS spectra. The O1s spectrum shows two peaks at 531.66 and 533.08 eV, which correspond to the O=C and O-C bond, respectively. The peak area ratio of 53.9: 46.1 is in reasonable agreement with the theoretical ratio of 50: 50.

The data summarized in table 4-3 show that after UV grafting of DMAPMA, the amount of C-O and C-N bonds is increased. On the other hand, the number of C-C and C-H of bonds is reduced. This is an indication for the complete coverage of the PET fibers with PDMAPMA. After quaternization of PDMAPMA with alkylbromides of different chain lengths, the amount of C-C and C-H increases again, and the amount of C-O and C-N decreases. This is an indication for the successful reaction between the tertiary amino group of PDMAPMA and the alkylbromide and therefore for covering the PDMAPMA with the alkyl chains of the alkylation reagent.

Table 4-3: Composition from the high-resolution C1s and O1s XPS spectra of untreated, grafted and quaternized PET.

Sample	***C-H, C-C***	***C-O***	***O-C=O***	***C= O***	***C–O–C***
	285.0 eV	***286.2-286.5 eV***	***289.0 - 289.6 eV***	***532.1-532.6 eV***	***533.1-533.9 eV***
PET	63.2	25.7	11.1	53.9	46.1
PET-g-PDMAPMA	47.8	41.9	10.3	71.7	28.3
PET-g-PDMAPMA+C8H17Br	57.2	32.7	10.1	61.4	38.6
PET-g-PDMAPMA+C16H33Br	64.8	20.5	9.7	69.9	30.1

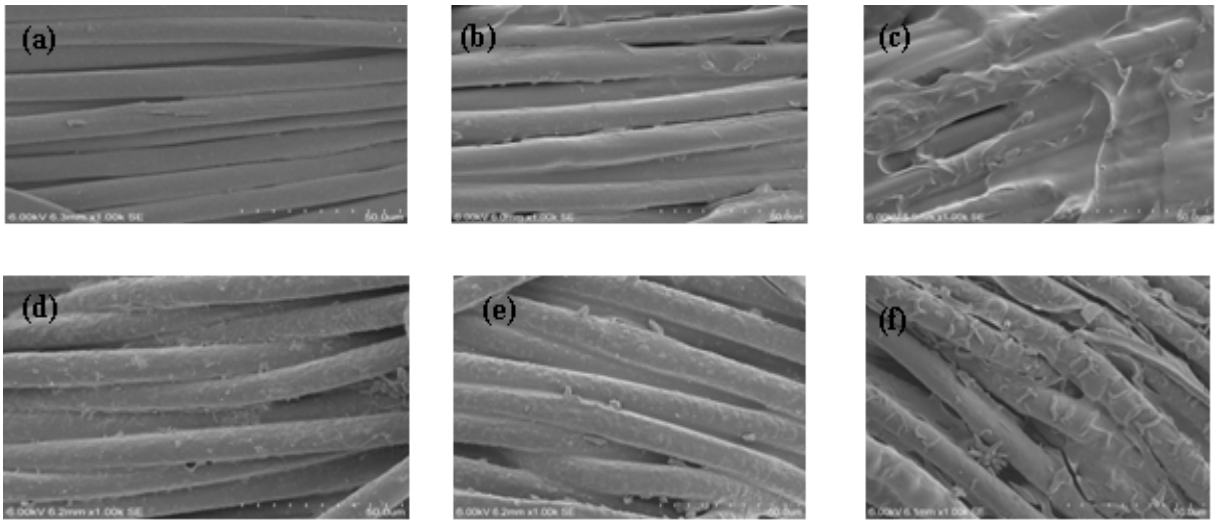

Figure 4-14: SEM images of untreated PET fibers (a), the grafted samples PET-g-PDMAPMA with GY = 9.1% (b) and PET-g-PDMAPMA with GY = 20.1% (c), and the quaternized samples PET-g-PDMAPMA+$C_6H_{13}Br$ (GY = 9.1 %) (d), PET-g-PDMAPMA+$C_{16}H_{33}Br$ (GY = 9.1 %) (e), and PET-g- PDMAPMA+$C_{16}H_{33}Br$ (GY = 20.1 %) (f).

4.3.5. Surface characterization

The surface characterization of modified PET fabric such as morphology of the surface, dyeability, amount of positive charges on the surface, wittability properties, thermal properties, mechanicals prperties and antibactrial properties were investigated

4.3.5.1 SEM images

Surface topography of original PET, grafted, and quaternized PET fabric were analyzed by SEM images which are given in figure (4-14 (a-f)). The images of SEM of After grafting, a rather homogeneous layer of PDMAPMA covers the smooth PET fibers. With increasing graft yield, this layer completely shields the fibers (figure 39 c). The samples quaternized with different alkyl bromides exhibit a significant surface roughness (figures 4-14 (d-f)).

4.3.5.2 Hydrophilic and hydrophobic properties

The surface wettability was examined by drop penetration time (TEGAWA test) and contact angle measurements. The results were shown for PET fabrics

before and after grafting with PDMAPMA and quaternized with different alkyl chain bromide. Untreated PET fabrics had been hydrophobic properties; the wettability was 120 s and 75^{o}. according to TEGEWA test and contact angle was been. After the samples grafted by PDMAPMA the surface of the samples became hydrophilic properties. As observed that the PET-g-PDMAPMA after quaternization with different alkyl chain bromide C_6, C_8, the surface of samples become more hydrophilic properties due to the positive charges of quaternary ammonium groups increase hydrophilic properties and the length of alkyl groups are shorter as compared to C_{12} and C_{16}. The surface of samples with C_{12} and C_{16} alkyl chains, retain again to hydrophobic properties. the drop penetration time were 60 s and 1200 s and contact angles were 70 ^{o} and 120 ^{o} respectively due the long chain of alkyl groups have been hydrophobic properties and cross linked between the chain of polymer during photo-chemical reaction, as was schemed in figure 4-15.

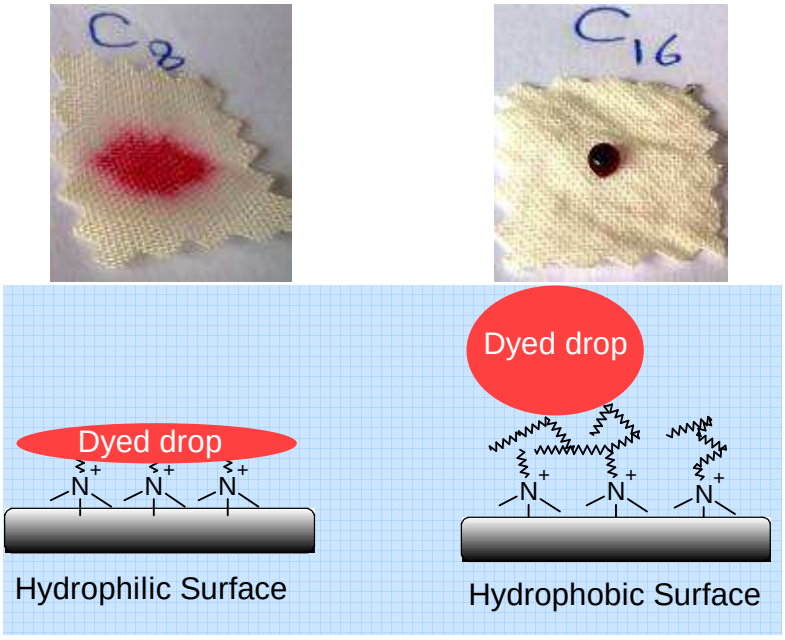

Figure 4-15: Dyed drop penetration for PET grafted with PDMAPMA fabrics after quaternized with different alkyl chain bromide (C_8 and C_{16}).

4.3.5.3 Dyeability with acidic dyes

To test the effect of the modified PET surface on dyeability, samples were dyed with the acidic dye Telon Red AFG. The dye uptake is plotted in figure 4-16 against dyeing time. As expected, there is little or no dye uptake by the untreated PET fabric. PET has no or very little reactive groups for acidic dyes. A significant increase in dye uptake is observed in the case of the grafted and quaternized PET, in the example using octylbromide (PET-g-PDMAPMA+$C_8H_{17}Br$).

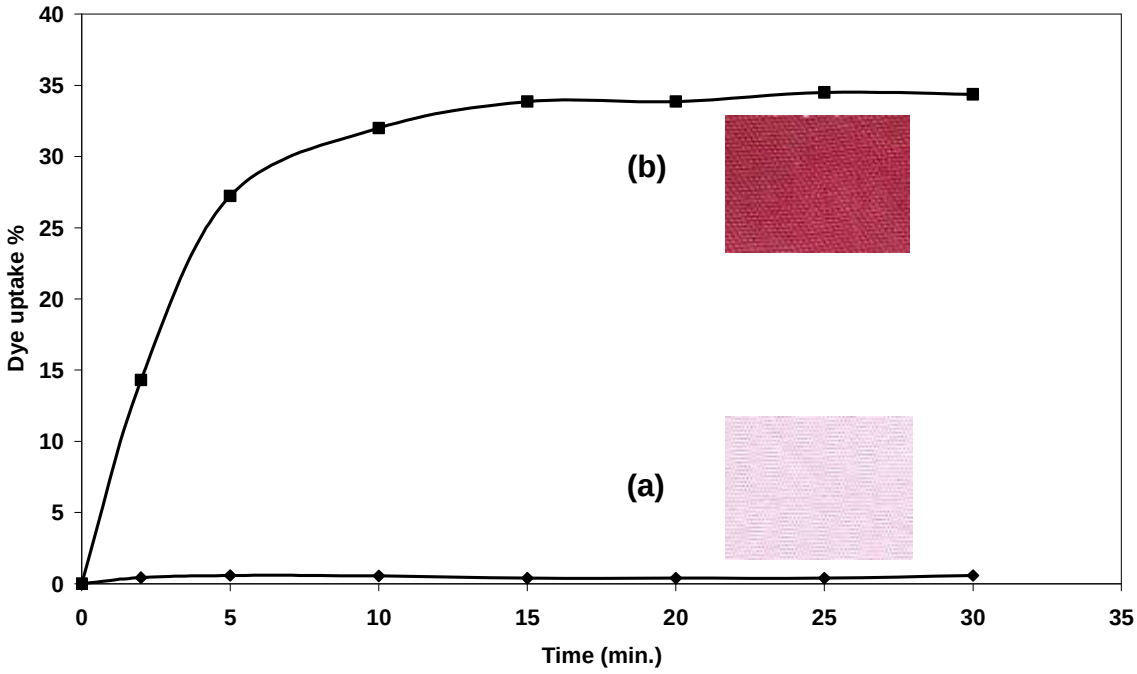

Figure 4-16: Uptake of the acidic dye Telon Red AFG by untreated PET (a) and by quaternized PET-g-PDMAPMA +$C_8H_{17}Br$ (b) as a function of dyeing time.

The corresponding K/S values describing color strength are 0.3 for untreated PET and 2.56 for the quaternized PET-g-PDMAPMA+$C_8H_{17}Br$. This remarkable increase in K/S and dye uptake can be related to tertiary amine and quaternary ammonium groups introduced by the photochemical surface modification. These groups improve the affinity of the acidic dye due to ionic and polar interactions between positive charges on the grafted and quaternized fiber surfaces and the negative charge of the acidic dye.

4.3.5.4 Amount of charges on the grafted surface

Polyelectrolyte titration test was used to determine the amount of charged available on the grafted surface of textile, which gives more information about degree of the crosslinking, and chain segment mobility of grafted polymer on the surface of textile. A polyelectrolyte titration measurement and the nitrogen content of the PET-g-PDMAPMA and quaternized PET-g-PDMAPMA were represented in Tables 4-4 and 4-5. It was found that the amounts of cationic charges of the PET-g-PDMAPMA increased with increasing the amount of nitrogen content as shown in table 4-4 due to the presence amino groups on the treated surface. The amounts of cationic charges were lower than the expected value, because all nitrogen content are not charged and not available for the polyelectrolyte titration, also a polyelectrolyte titration measurement are detected only the charges on the surface.

Table 4-4: Polyelectrolyte titration and nitrogen content of the treated fabrics PET-g-PDMAPMA

The samples add on% by weight	***Amount of N%***	***Add on % by N%***	***Amount of cationic charges [meq/g fabric]***
0	-	-	0
0.22	0.03	0.19	0.059 ± .003
1.41	0.21	1.33	0.065 ± .006
5.97	0.78	4.82	0.075 ± .007
9.4	1.29	8.03	0.078 ± .008
16.37	2.11	13.04	0.093 ± .007
21.25	2.48	15.35	0.121 ± .011

Table 4-5: Amount of cationic charges of PET-g-PDMAPMA and quaternized PET-g-PDMAPMA

The samples	*add on% by weight*	*Amount of cationic charges [meq/g fabric]*
PET	-	-
PET-g-DMAPMA	9.4	0.078 ± .008
PET-g-DMAPMA	21.2	0.121 ± .011
PET-g-DMAPMA Q- C6 Br	9.4	0.102 ± .005
PET-g-DMAPMA Q- C6 Br	21.2	0.127 ± .013
PET-g-DMAPMA Q- C8 Br	9.4	0.098 ± .008
PET-g-DMAPMA Q- C8 Br	21.2	0.117± .010
PET-g-DMAPMA Q- C12 Br	9.4	0.087 ± .005
PET-g-DMAPMA Q- C12 Br	21.2	0.078 ± .004
PET-g-DMAPMA Q- C16 Br	9.4	0.076 ± .003
PET-g-DMAPMA Q- C16 Br	21.2	0.110 ± .009

From data as shown in table 4-5, the amount of cationic charges on the surface of PET-g-PDMAPMA and quaternized PET-g-PDMAPMA is affected with alkyl chain lengths of the quaternary ammonium groups. The electrostatic interaction between positive charged site on the surface and negative charged of polyelectrolyte solution PES-Na, which used in the titration, was affected with alkyl chain lengths of the quaternary ammonium groups. This is due to the steric effect of the alkyl chain lengths, which prevents the approach of negative charged molecules to the positive charged sites on the fiber surfaces. Therefore the amounts of cationic charge measured on the textile surface by polyelectrolyte titration are in order 1-bromohexane (C_6) >= 1-bromooctane (C_8) > 1-bromododecane (C_{12}) > 1-bromohexadecane (C_{16}).

4.3.5.5 Mechanical properties

The tensile strength and elongation % at break of untreated PET and PET-g-PDMAPMA are given in figure 4-17. The small changes in tensile strength and elongation % of the PET fibers with a little statistical meaning, the elongation % of PET-g-PDMAPMA increased by 2% compared with untreated PET, also little increased in tensile strength by 0.25N for PET-g-PDMAPMA compared with

untreated PET due to the photografting reaction, resulting from increased fiber to fiber friction through cross-linking effect of PDMAPMA.

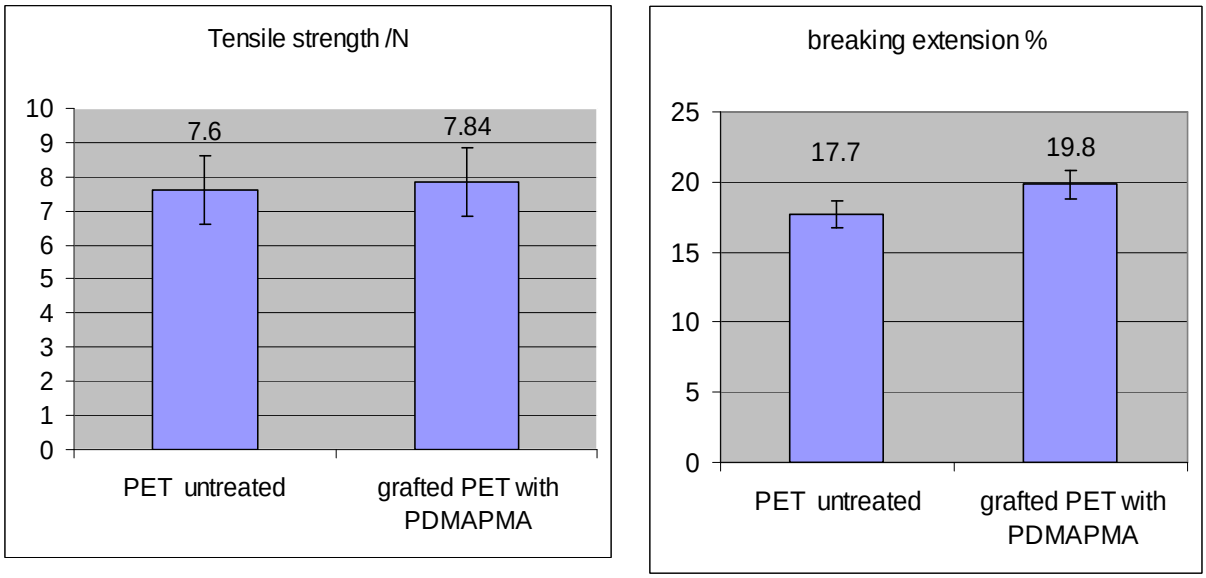

Figure 4-17: Tensile strength and breaking extension of untreated PET and PET-g-PDMAPMA

4.3.6. Antimicrobial properties

The antibacterial activity of the samples was characterized by evaluating the inhibition of the growth of *E. coli* bacteria. In this test, untreated fabric as well as samples, which were grafted and quaternized using alkyl bromides of different chain length (C_6 - C_{16}), were placed on top of two standard nutrient agar plates. The lower layer consisted of culture medium without any bacteria, while the upper layer was inoculated with the bacteria. The two-layer setup is placed in a Petri dish and incubated for 18- 24 h at 37^{o}C. Visual inspection after incubation gave no evidence of an 'inhibition zone around the fabric samples as shown in figure 4-18 A. This indicates that no diffusion of quaternary ammonium compounds (QACs) took place. However, after removal of the fabric sample, no bacteria were detected below the modified samples. This observation proves the antimicrobial effect of the grafted and quaternized PET as well as the effective fixation of the QACs on the fiber surfaces. A photographic top-view of the agar

plate after removal of the fabric samples is given in Figure 4-18 B. The visual inspection shows a lighter shade of the agar where the circular samples were removed indicating a reduction of bacteria density at theses places.

Qualitatively, this effect is strongest for the quaternized PET-g-PDMAPMA + $C_{12}H_{25}Br$ (sample no. 5). In contrast, the sample which was only grafted with PDMAPMA but not quaternized (sample no. 2) does not exhibit any antibacterial effect. Also, there is no indication of an inhibition zone around the fabric samples, with the exception of sample no. 2 where a small inhibition zone appears to be evident. These observations prove the antimicrobial effect of the grafted and quaternized PET, but also – based on the lack of inhibition zone – the effective fixation of the QACs on the fiber surfaces.

Quantitative data on the antimicrobial activity of the original PET, grafted PET-g-PDMAPMA and quaternized PET-g-PDMAPMA were obtained by means of the ASTM E2149-01 method, again using *E. coli.*

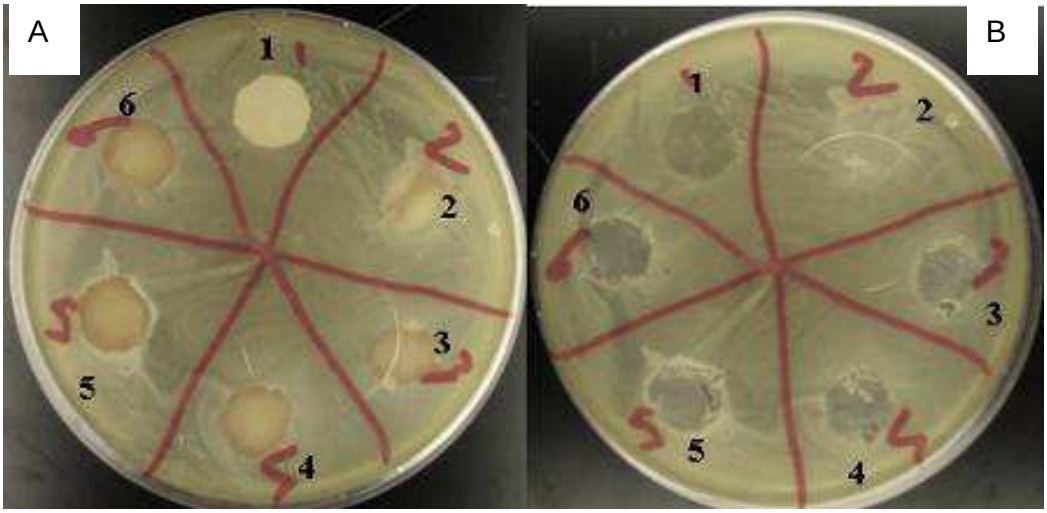

Figure 4-18: Result of the 'agar test'. The photographic top-view shows the agar plate before (A) and after (B) removal of the fabric samples. The numbers indicate the position of the original PET (1), PET-g-PDMAPMA (2), quaternized PET-g-PDMAPMA + $C_6H_{13}Br$ (3), quaternized PET-g-PDMAPMA + $C_8H_{17}Br$ (4), quaternized PET-g-PDMAPMA + $C_{12}H_{25}Br$ (5), and quaternized PET-g-PDMAPMA + $C_{16}H_{33}Br$ (6). The graft yield of the PDMAPMA modification was 9.1% in all cases.

Table 4-6: Antimicrobial activity with regard to E. coli of original PET, PET-g-PDMAPMA (GY 9.1%) and quaternized of PET-g-PDMAPMA with different alkyl chain length.

Samples	***Average of colony forming units E. coli after 0 time***	***Average of colony forming units E. coli after 3 time***	***R%***
Control (without sample)	35×10^5	40×10^5	-
Original PET	35×10^5	25×10^5	28.5
PET-g-PDMAPMA	35×10^5	18×10^5	48.5
PET-g-PDMAPMA +($C_6H_{13}Br$)	35×10^5	16×10^4	95.4
PET-g-PDMAPMA +($C_8H_{17}Br$)	35×10^5	10×10^4	97.1
PET-g-PDMAPMA +($C_{12}H_{25}Br$)	35×10^5	11×10^5	68.5
PET-g-PDMAPMA +($C_{16}H_{33}Br$)	35×10^5	12×10^5	65.7

As shown in Table 4-6, the antimicrobial activity of all samples is not very high with maximum microbe reduction of R = 97.1%. The reduction of the *E. coli* varies strongly with the alkyl chain lengths of the pendant QAGs. In contrast to qualitative agar test, the ASTM E2149-01 test shows the highest effect for the samples quaternized with 1-bromohexane (C_6) and 1-bromooctane (C_8). An increase in the alkyl chain lengths of the quaternary ammonium groups of the PET-g-PDMAPMA appears to reduce the antibacterial effect again. This observation is in agreement with results published by Dizman et al.[171] who reported that the antibacterial activity of polymers with pendant quaternary ammonium groups against Gram-negative bacteria such as *E. Coli* decreased with increasing alkyl chain length. A reason for this behavior might be seen in the effect of the alkyl chain lengths of the quaternary ammonium groups on the wettability properties of the PET fabrics. As could be established by contact angle measurements as well as drop penetration measurements, the originally hydrophobic PET fabric becomes increasingly hydrophilic following grafting and

quaternization with 1-bromohexane (C_6) and 1-bromooctane (C_8). In contrast, quaternization with bromides with long alkyl chain, i.e. 1- bromododecane (C_{12}) and 1-bromohexadecane (C_{16}) increased the hydrophobicity of the fabrics. In addition network and cross-linked of grafted copolymer, which is resulted by photochemical reaction of monomer DMAPMA, which is caused that the biocidal functions (QAGs) prevent (steric effect), to reach to bacteria cell and antibacterial activity decreased. In addition, the amount of positive charged on the modified PET decreased (from polyelectrolyte titration test data, table 4-5) with increasing alkyl chain length after quaternization reaction on the PET-g-PDMAPMA. Beside the quaternization yield % (as shown in table 4-1) decreased after quaternization reaction with increasing alkyl chain length due to steric effect. Thus, electrostatic interaction decreases between the negatively charged cell surface of the bacteria and the surface of modified PET (antibacterial activity).

5. Chapter 5: Ag NPs and its application as antibacterial agent

5.1. Synthesis of Ag NPs by photochemical reduction

5.1.1. Introduction

In recent years Ag NPs have been found to exhibit interesting antibacterial activities due to the large surface to volume ratio, thus they can penetrated into inside cell of bacteria and destroyed it[64, 65]. Due to high antibacterial properties of Ag NPs, they have been applied for various medical applications such as surgical products and wound dressing [173], [174]. Many methods have been reported for the preparation of Ag NPs such as chemical reduction of silver ions in aqueous solutions with or without stabilizing agents [175], chemical reduction and photo-reduction in reverse micelles [176], and radiation chemical reduction [177], electrochemical synthesis, or by exposure to UV or γ-radiation. Most of these methods are extremely expensive and involve the use of toxic, hazardous chemicals, which may pose potential environmental and biological risks. Since noble metal nanoparticles are widely applied to areas of human contact[61], there is a growing need to develop environmentally friendly processes for nanoparticle synthesis that do not use toxic chemicals. Addition of water-soluble polymers may control particle growth and stabilize intermediates. One of the most frequently applied additives is the sodium salt of poly (methacrylic acid) (Na PMAA). The mechanism for the formation of Ag nanoparticles - under UV irradiation in aqueous solutions of PMAA is through reduction of Ag^+ by reactive species (reducing agents) from the photochemical reaction of Na PMAA. Using Na PMAA offers numerous advantages due to its physical and chemical properties. Furthermore, it does not show any toxic chemical effect. Moreover, it fulfils the ever-increasing demand for safe, eco-friendly and low- cost processing of materials [8-12].

In this work, the synthesis and characterization of silver nanoparticles with low molecular weight of sodium salt of poly (methacrylic acid) (PMAA) as stabilizing agent by photochemical reduction method reported. The antibacterial activity of silver nanoparticles colloid was evaluated against two bacteria *E. coli* (Gram negative) and *M. luteus* (Gram positive) using the agar disc diffusion method.

5.1.2. Properties of Ag colloids formed by UV irradiation of silver nitrate

Structural characterization of Ag NPs, formed by UV irradiation, was studied by UV-visible spectroscopy. Initially, the solution of $AgNO_3$ and Na PMAA was colorless, but, following UV irradiation with increasing time, obvious color changes from colorless to light yellow, then to brown, and finally to dark brown were observed. As shown in Figure 5-1, before the irradiation, the solution showed no absorption in the wavelength range from 350 to 800 nm. After 1 minute of UV irradiation, a weak absorption band centered at 500 nm appeared. When further extending the irradiation time from 1.5 to 5 min, the intensity of this absorption band increased significantly due to localized surface plasmon resonance (LSPR) of spherical nanostructure of Ag NPs. When the spherical nanostructure of Ag NPs are smaller than the wavelength of light incident, the free electrons can be displaced from the lattice of positive ions (consisting of nuclei and core electrons) and collectively oscillate in resonance with the light[178] as illustrated in figure 5-2. This is known as a localized surface plasmon resonance (LSPR). This indicates that spherical nanostructure particles are formed (nucleation of Ag NPs).

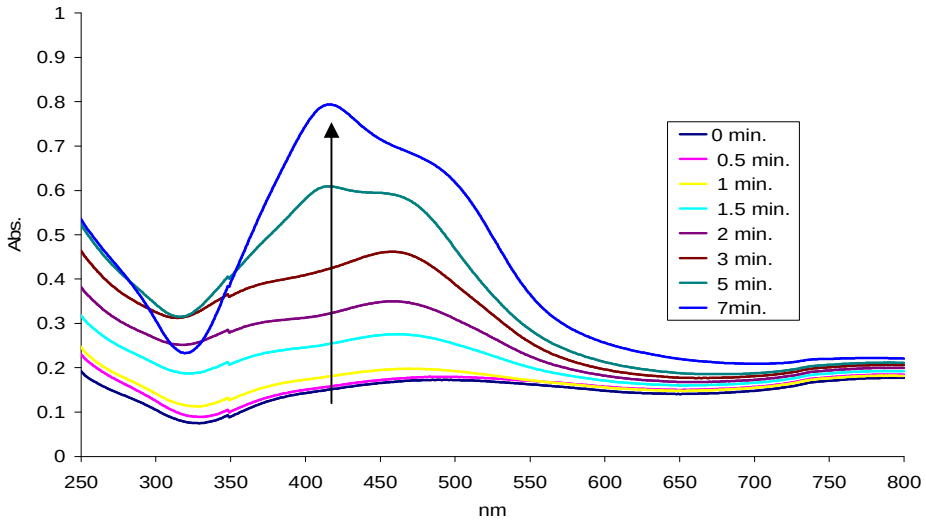

Figure 5-1: Absorption spectra of silver nanoparticle colloids produced from a $AgNO_3$ solution with a concentration of silver of $[Ag^+] = 7x10^{-5}$ mol/l by UV irradiation under variation of exposure time

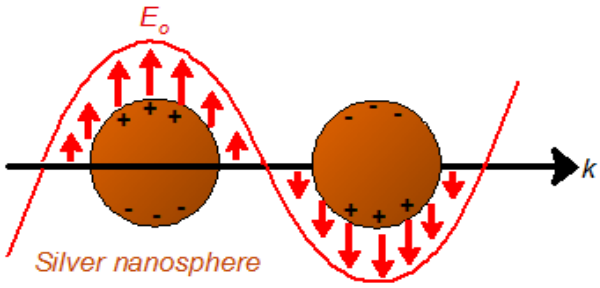

Figure 5-2: Schematic of localized Surface Plasmon Resonance (LSPR) of spherical silver nanoparticles as excited by the electric field (*Eo*) of incident light with wave-vector (*k*).

In figure 5-3 the number of size distribution of Ag NPs obtained by DSL increased with prolong time of UV irradiation. From above results, it was found relationship between absorbance of Ag NPs due to surface plasmon resonance of Ag NPs (nucleation of Ag NPs) and growth of Ag NPs during time of UV irradiation. A shoulder peak at ca. 430 nm was also observed upon the irradiation, and the increasing in the absorbance of the absorption peaks indicated the gradual growth of Ag nanoparticles upon prolonged UV irradiation.

According to Mie theory we can described relationship between LSPR and size of spherical Ag NPs[179]

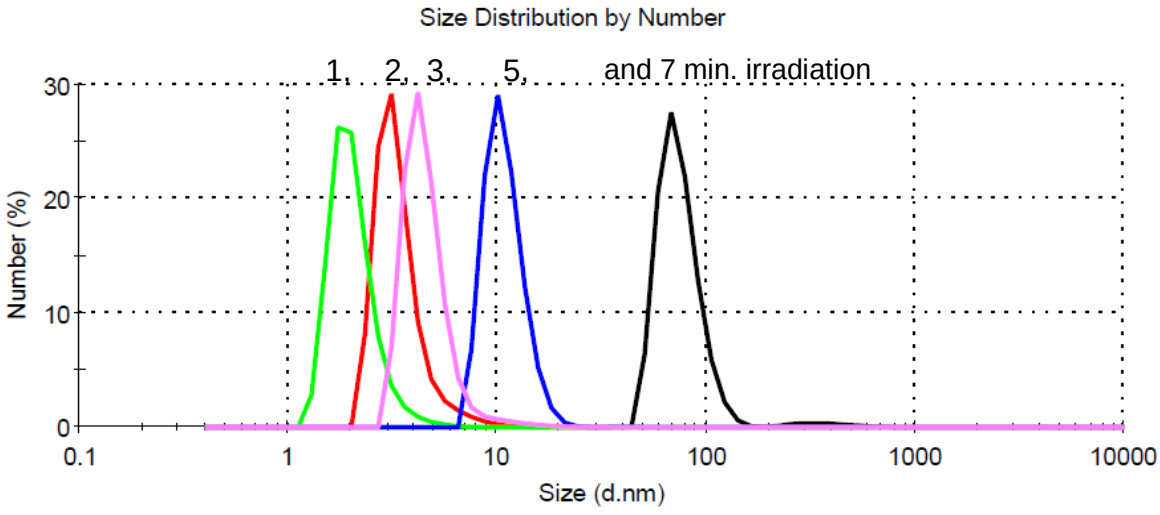

Figure 5-3: Number size distribution of Ag NPs, formed by UV irradiation under variation of exposure time, by dynamic light scattering (DLS) (5% PMAA and concentration of Ag+ = 7x10-5)

$$C_{ext} = \frac{24\pi^2 R^3 \varepsilon_m^{3/2}}{\lambda}\left[\frac{\varepsilon_i}{(\varepsilon_r + 2\varepsilon_m)^2 + \varepsilon_i^2}\right]$$

Where C_{ext} is the extinction (absorption or scattering) cross section of spherical structure Ag NPs, R is the radius of the spherical Ag NPs, ε_m is the relative dielectric constant of the medium surrounding the spherical Ag NPs, ε_r is the relative dielectric of spherical particles, ε_i relative dielectric of ions and λ is excitation wavelength. This equation shows that the interaction between a metal nanoparticle and light depends strongly on its dielectric properties (ε_r and ε_i). In addition, the molar extinction coefficient of spherical Ag NPs increases linearly with increasing size of the nanoparticles, i.e. optical absorption spectra of the Ag NPs depend directly on the size of the nanoparticles [180].

The peak in the spectrum at 450-500 nm is assumed to be due to interactions of Na PMAA with Ag nanoparticles as sketched in Figure 5-4. Initiation of Ag NPs formation by UV irradiation depends on the reactivity between the Ag^+ ions and PMAA molecules and on the molecular weight of PMAA [181]. The mechanism of Ag NPs formation under UV irradiation in aqueous solutions of PMAA carried out through reduction of Ag^+ ions by reductive (reactive) species i.e. reducing agents which result from the photochemical reaction of Na PMAA.

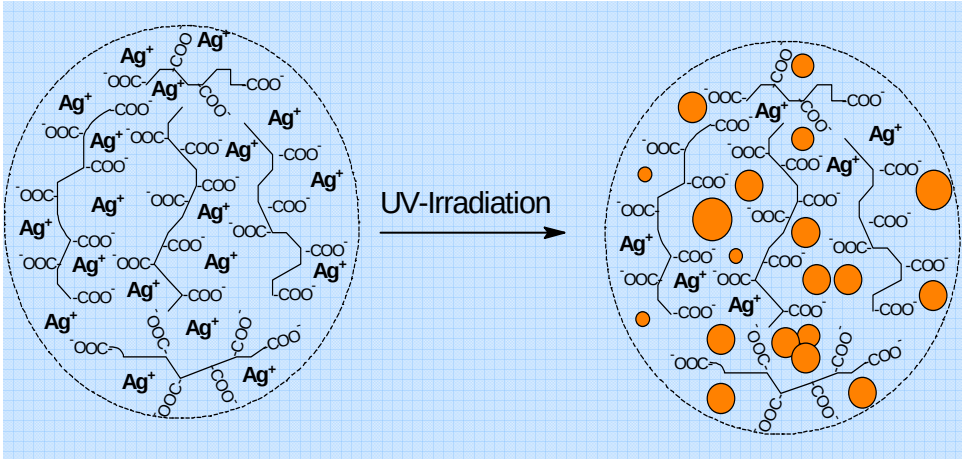

Figure 5-4: A possible sketched for the interaction between Ag^+, Ag nanoparticles and Na PMAA

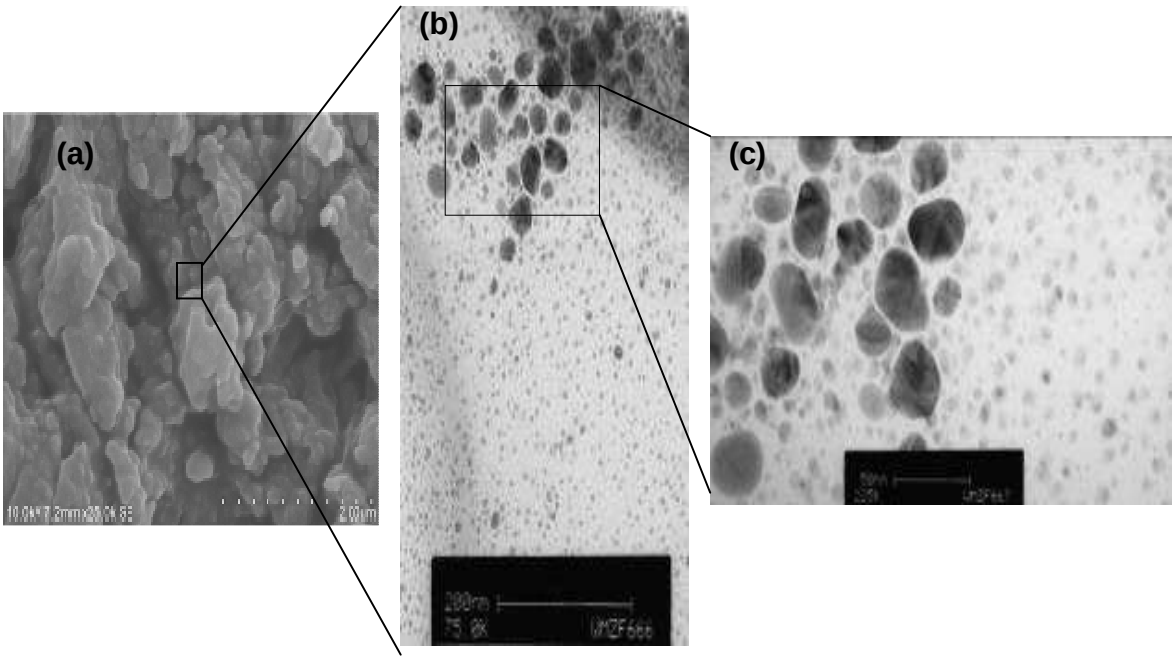

Figure 5-5: SEM of Ag nanoparticles stabilized by PMAA (a), TEM images of silver nanoparticles (b and c) (5 min. time of irradiation, 5% PMAA and concentration of Ag^{+} = $7x10^{-5}$)

Size and morphology of silver NPs were studied by TEM and DSL techniques. In Figure 5-5 shows typical SEM and TEM images of Ag nanoparticles with PMAA obtained after 5 min UV irradiation. A size distribution of the Ag nanoparticles was obtained by analysis of the TEM image and showed diameters ranging from 3 nm to 35 nm. More than 70% of the Ag NPs have a size smaller than 15 nm and no particles larger than about 35 nm were observed in the TEM image shown in at Figure 5-6. This is in agreement with the nanoparticles size distribution (number distribution) obtained by DSL (Figure 5-7).

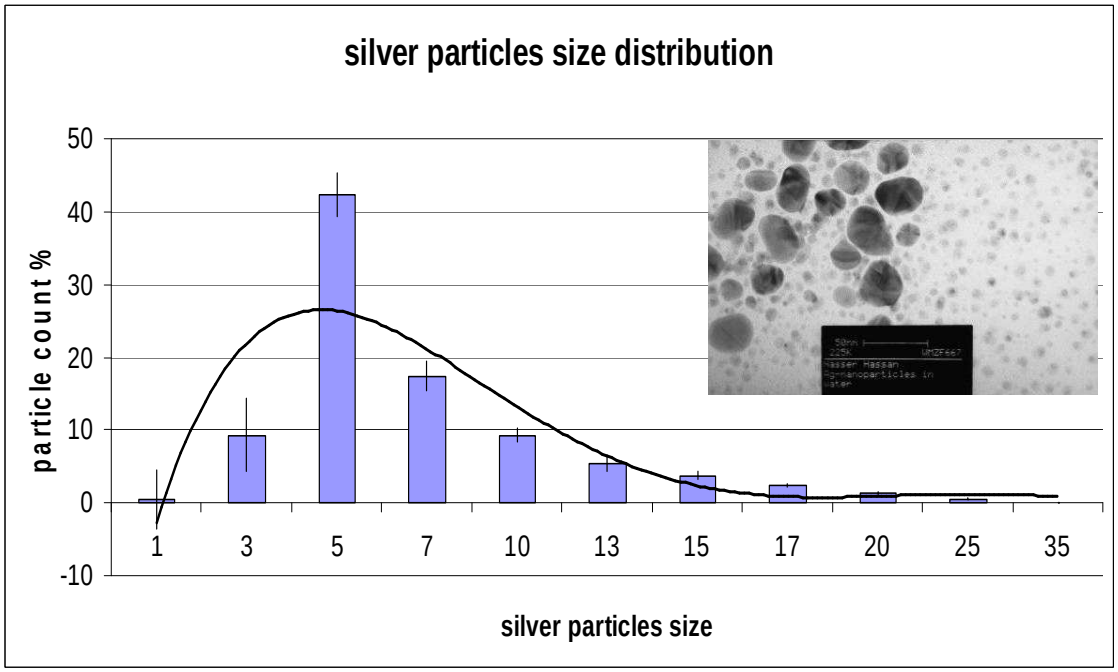

Figure 5-6: Silver nanoparticles size distribution obtained by count and TEM image.

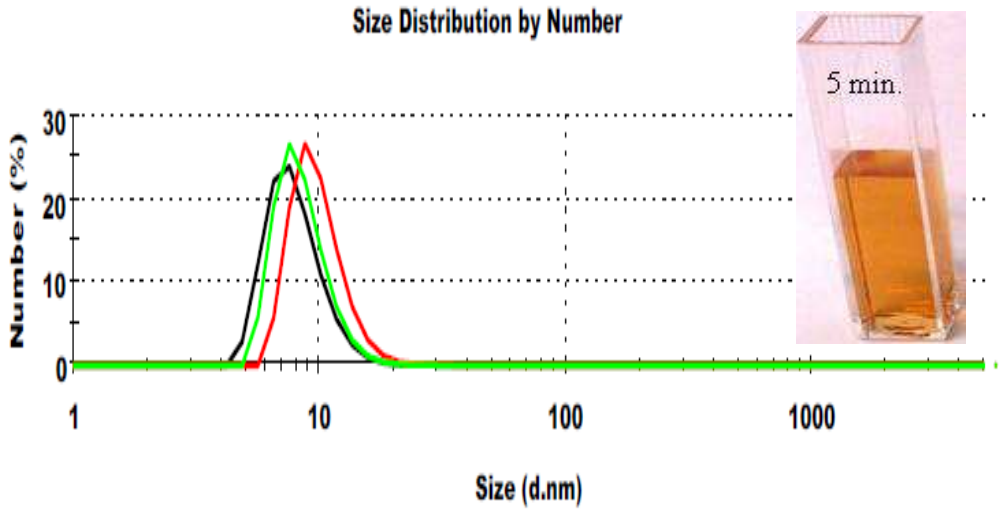

Figure 5-7: The number size distribution of silver nanoparticles obtained from DSL, three times, insert photograph of Ag NPs colloid after dilution (5 min. time of irradiation, 5% PMAA and concentration of Ag^{+} = $7x10^{-5}$.

5.1.3. Stability of Ag NPs colloid against pH

The stability of the Ag colloid against the pH changes is significance when using Ag colloid in appropriate applications especially when applied with textile such

as antibacterial finishing, and find out the optimum conditions for this treatment and can be determined using Isoelectric Point (IEP) measurements. Streaming potential is the net surface charge of the nanoparticles when they are inside a solution. The fact that particles push each other and their agglomeration behavior depends on large negative or positive streaming potential.

A plot of streaming potential of Ag NPs versus pH (3-10) is shown in figure 5-8. It was noted that the streaming potential versus pH curve is negative, the sample pH's are shifted until the point of zero charge (streaming potential = 0mV) is reached. The streaming potential of Ag NPs decrease with decreasing pH. However, from the figure 5-8, it is apparent that the Ag NPs colloid is stable at pH values more than 6 (sufficient negative charge is present). The isoelectric point has been observed at pH values of 3.5- 4, due to carboxylic groups COOH is weak acid and proton ions exchanged, therefore, insufficient negative charge on the Na PMAA and Ag NPs agglomerated.

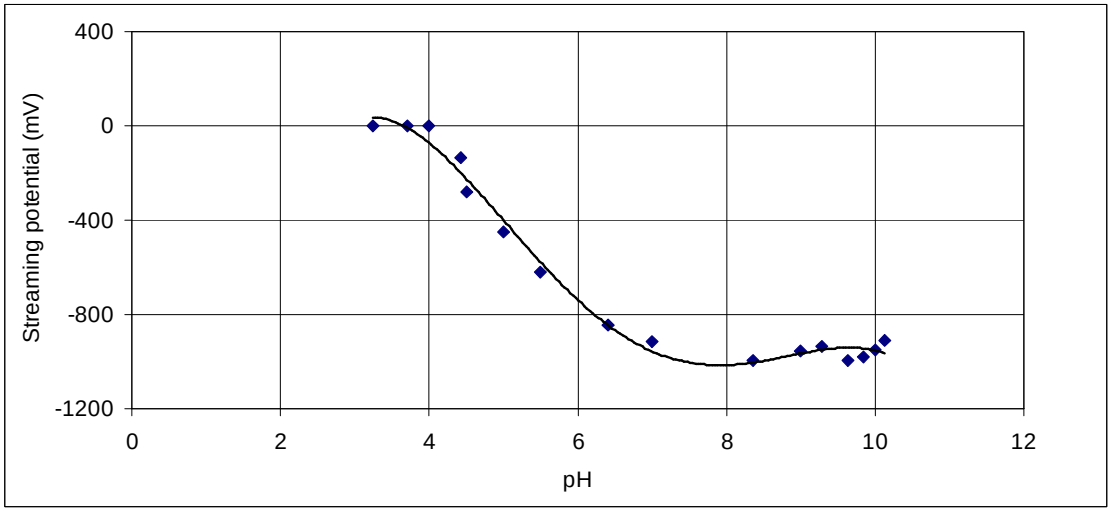

Figure 5-8: Streaming potential as function of pH value for silver nanoparticles colloid (5 min. time of irradiation, 5% PMAA and concentration of Ag^{+} = $7x10^{-5}$)

5.1.4. The antibacterial activity of the Ag NPs colloid

To evaluate antibacterial activity of Ag NPs against *E. coli and M. luteus* and effect of concentration of Ag NPs on its antibacterial activity using the zone inhibition method as qualitative method. 100 µl of suspension of bacteria with a concentration of 10^5 to 10^7 CFU/ ml of *E. coli* and *M. luteus* were spread on a nutrient agar plate. The

plates were holed with 1 cm diameter and then 100 µl of Ag NPs colloid poured in the holes with different concentrations. The plates were incubated for 24 h at 37 °C.
In figure 5-9, the antibacterial activity of the Ag nanoparticles colloid was tested against *M. Luteus* and *E. coli* by the inhibition zone method. As observed the growth inhibition could be observed as clear zones surrounding the holes on the Petri dish, and antibacterial efficiency increased with increasing Ag NPs concentration.

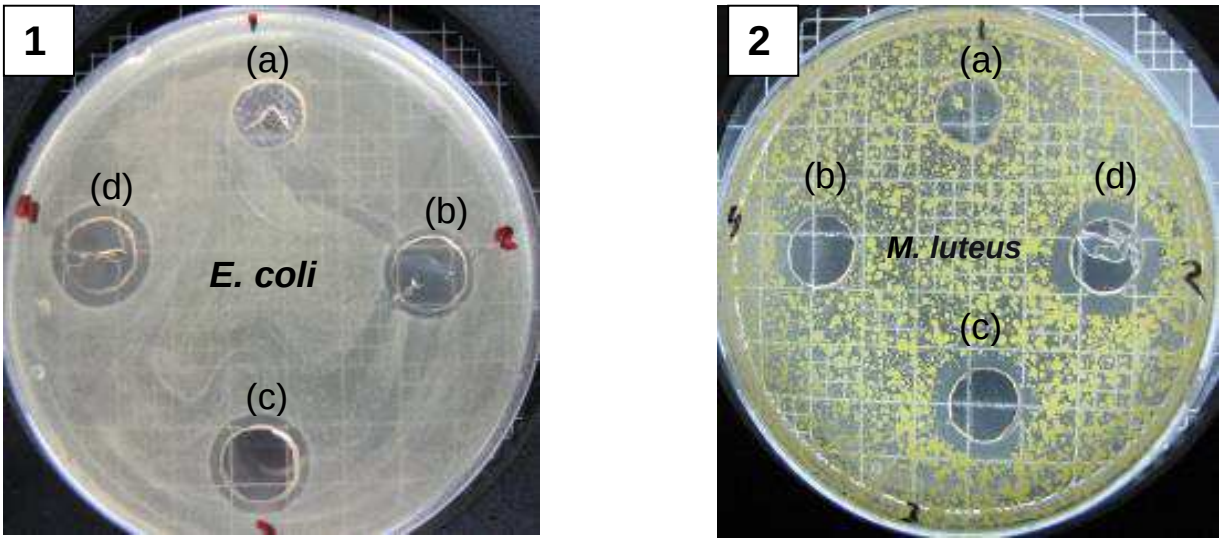

Figure 5-9: Zone inhibition test against *E. coli (1)* and *M. luteus (2)* (a) Blank without silver (b) solution of Ag nanoparticle $3.5x10^{-5}$ (c) solution of Ag nanoparticle $7x10^{-5}$ and (d) solution of Ag nanoparticle $14x10^{-5}$ mol/L

To calculate the lowest concentration of Ag NPs that completely inhibited bacteria growth, using minimum inhibitory concentration (MIC) test against E.coli. Broth containing was determined using the plate count method. 10^5 CFU/ ml of bacterial cells were used as a culture medium. The concentrations of Ag-NPs were zero, $3.5x10^{-5}$, $7x10^{-5}$, $14x10^{-5}$ mol/l. 100 µl with different concentrations of Ag NPs colloid mixed in 25ml of 10^5 CFU/ml of bacterial culture. The medium was cultured in a shaking incubator at 37 ^oC for 3h, and the cultured media (100 µl) was spread onto agar and incubated at 37^oC for 24 h. After incubation, the number of colonies grown on the agar was counted. The minimum inhibitory concentration (MIC) was defined as the lowest silver nanoparticles concentration resulting in the lack of visible

microorganism growth. As shown in figure 5-10, The MIC of Ag-NPs against E. coli was 100µl at 7x 10^{-6} mol/l. The results showed that the spherical shape of Ag NPs have high antibacterial activity, with a broad size distribution (3- 35nm) which observed by TEM images. This indicate that small size of Ag NPs have antibacterial activity, which can penetrate easily into cell membrane of the bacteria and large surface area per mass of Ag NPs, where a large number of atoms are in immediate contact and available for reaction with biological components of the cell, and caused destroyed the cells of bacteria.

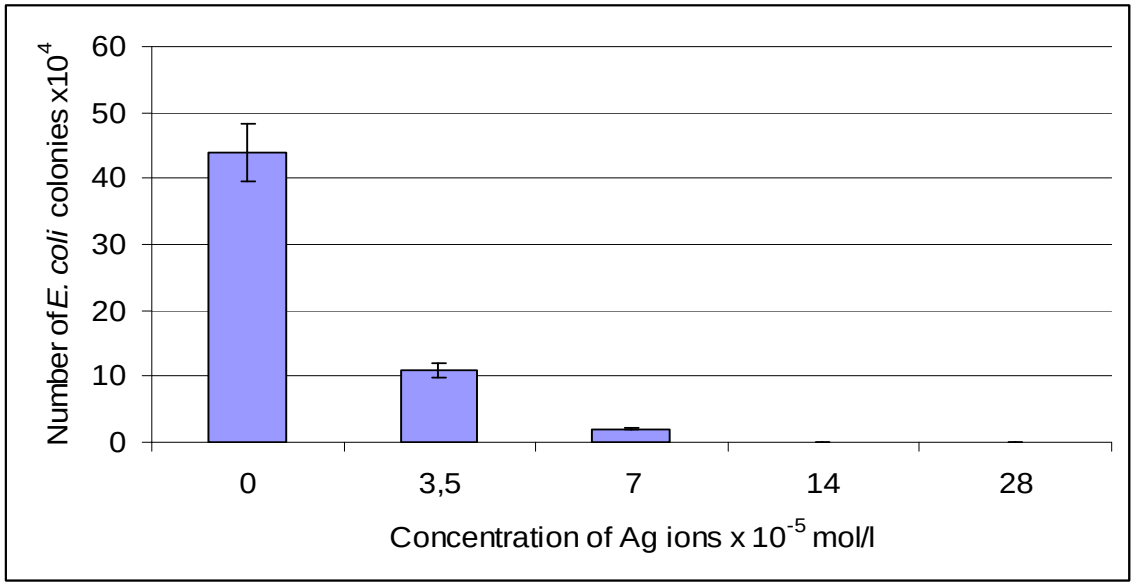

Figure 5-10: Number of *E. coli* colonies against concentration of Ag ions

5.2. Antibacterial properties of PET impregnated with photochemically synthesized Ag NPs

Due to stability and high antibacterial properties of Ag NPs has been reported. The minimization and control of bacterial growth on the surface textile is among the fastest growing sectors in the textile research. The antibacterial activity of the textile open and make possible new application such as medical textile, healthcare application, housing , and a large number of other applications.[182]

5.2.1. Treatment PET with Ag NPs colloid

After finishing PET fabrics with Ag NPs colloid, the silver loading of the PET fabrics is reflected in the visual appearance. This is shown in figure 5-11 for an untreated fabric and fabrics with different amount of particles.

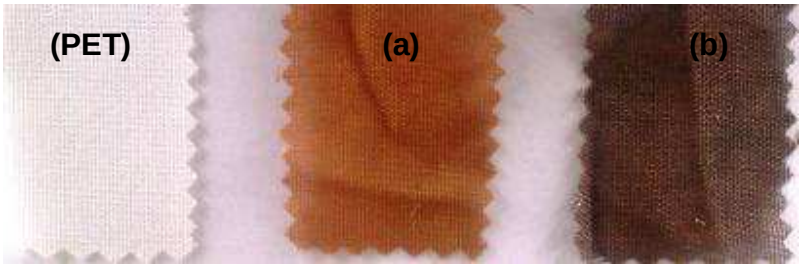

Figure 5-11: Photographs of Ag NPs loaded PET fabrics after treatment with Ag colloid (a) amount of Ag on the fabric 15 mg/ kg (b) amount of Ag on the fabric 30 mg/ kg

Fabrics finished with the silver nanoparticle colloid were ensuing studied by ICP-OES. The relevant data shown in figure 55 indicate an increase in silver content on the fabric with increasing UV exposure of the $AgNO_3$.solution. This can be due to larger particles produced by the irradiation, as would be suggested by the absorption spectra in figure 5-12. However, a saturation behavior is observed in the ICP data. Accordingly, in spite of larger particles, no further increase in the loading on the fabric can be achieved. This proven that amount of Ag NPs increased prolong time of irradiation until all silver ions Ag^+ were reduced to silver metal Ag^0 and formation Ag NPs. A similar behavior is observed when the silver nanoparticles are prepared from

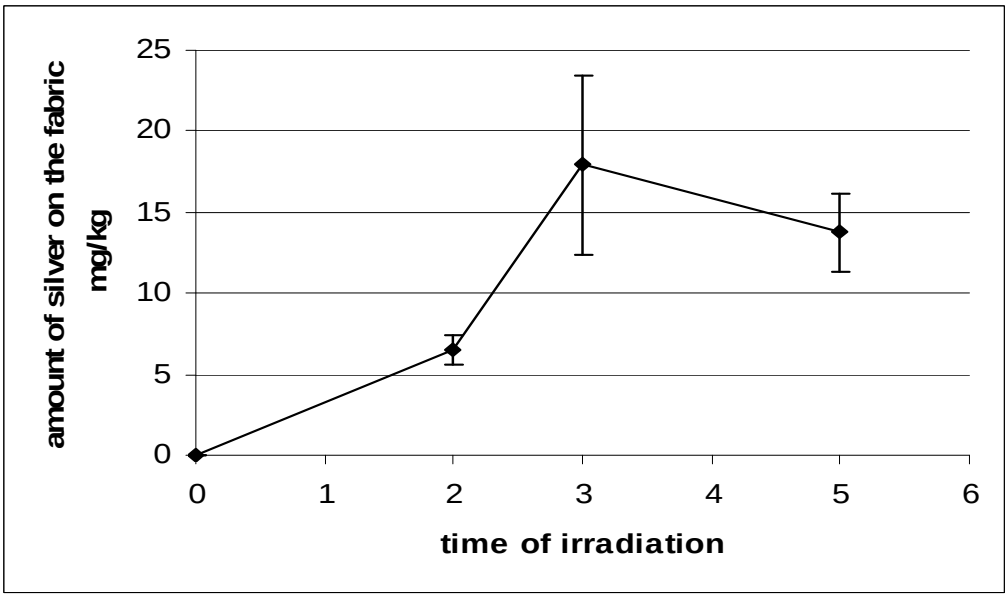

Figure 5-12: Amount of silver on fabrics finished with silver colloids prepared [Ag^+] = $7x10^{-5}$ mol/l with different irradiation time

solutions with varying $AgNO_3$ concentration (figure 5-13). As increasing silver ions Ag^+ amount of Ag NPs increased at certain time irradiation and amount of Ag NPs deposited on the PET surface increased until all surface of PET completed and saturated with Ag NPs , the surface of PET could not more adsorbed excess of Ag NPs from the solution (leveling of Ag NPs on the PET surface).

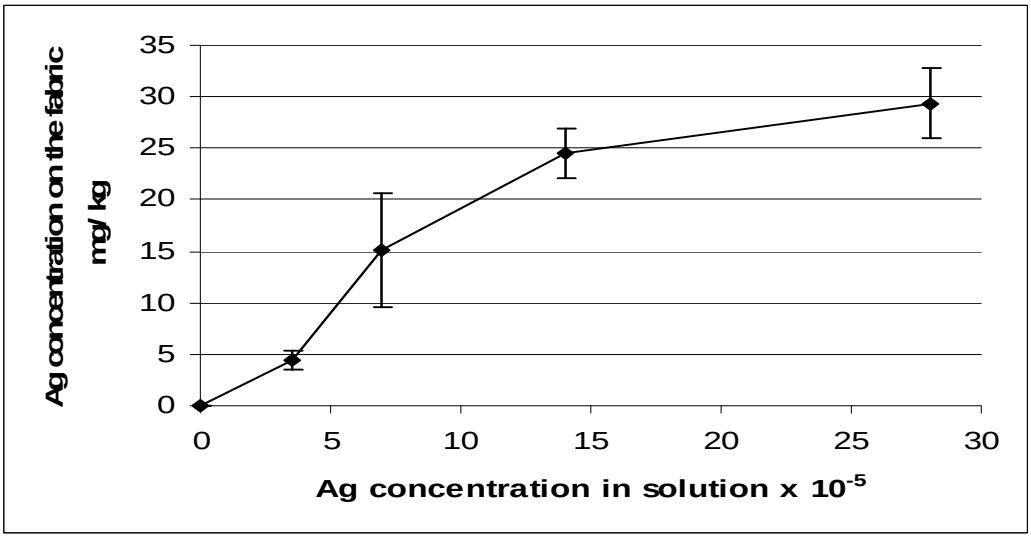

Figure 5-13: Amount of silver on fabrics finished with silver colloids prepared with different silver ion concentrations and 5 minutes irradiation time.

5.2.2. Surface analysis

The deposition of silver nanoparticles from the colloid on the fiber surface was then analyzed by scanning electron microscopy. The SEM images of fibers from the untreated PET fabric and from a fabric loaded with 15 mg/kg silver on the fabric (figure 5-14) revealed unevenly distributed silver nanoparticles on the fiber surface. Energy-dispersive X–ray spectroscopy (EDX) was employed to establish the chemical identity of the observed particles. It can be clearly seen from EDX mapping (figure 5-15b) and the integral EDX spectrum (figure 5-15c) that particles found on the surface are silver nanoparticles or agglomerates

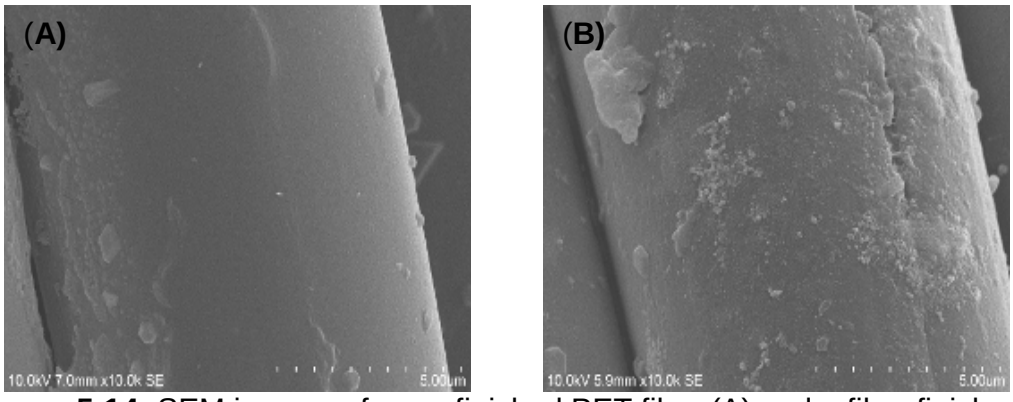

Figure 5-14: SEM images of an unfinished PET fiber (A) and a fiber finished with Ag nanoparticles (B)

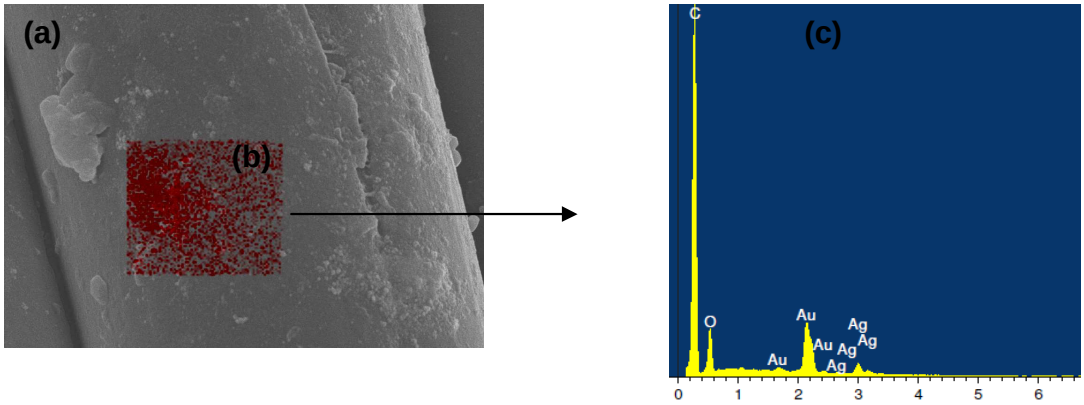

Figure 5-15: SEM images of Ag nanoparticles on the surface (a), spots of high silver content indicated by EDX mapping, (b), EDX spectrum (c).

.

SEM micrographs of PET fabric loaded with 15 and 30 mg/kg are shown in figure 5-16a, the higher deposition clearly detectable in figure 5-16b. EDX analysis mirrored the different loading. It should be noted, however, that the ratio of silver contents detected by EDX (4:1) did not relate to the ratio of total silver contents in the fabrics as detected by ICP-OES (2:1). Due to ICP-OES instrument can be detected all silver in the fabrics i.e. All silver in surface, pores and capillaries of PET. While EDX has some limited, i.e. the date refers to silver adsorbed on the surface only. It can be concluded that the Ag NPs are widely distributed in the surface and capillaries system of the fabrics, not only on the surface of the fabrics.

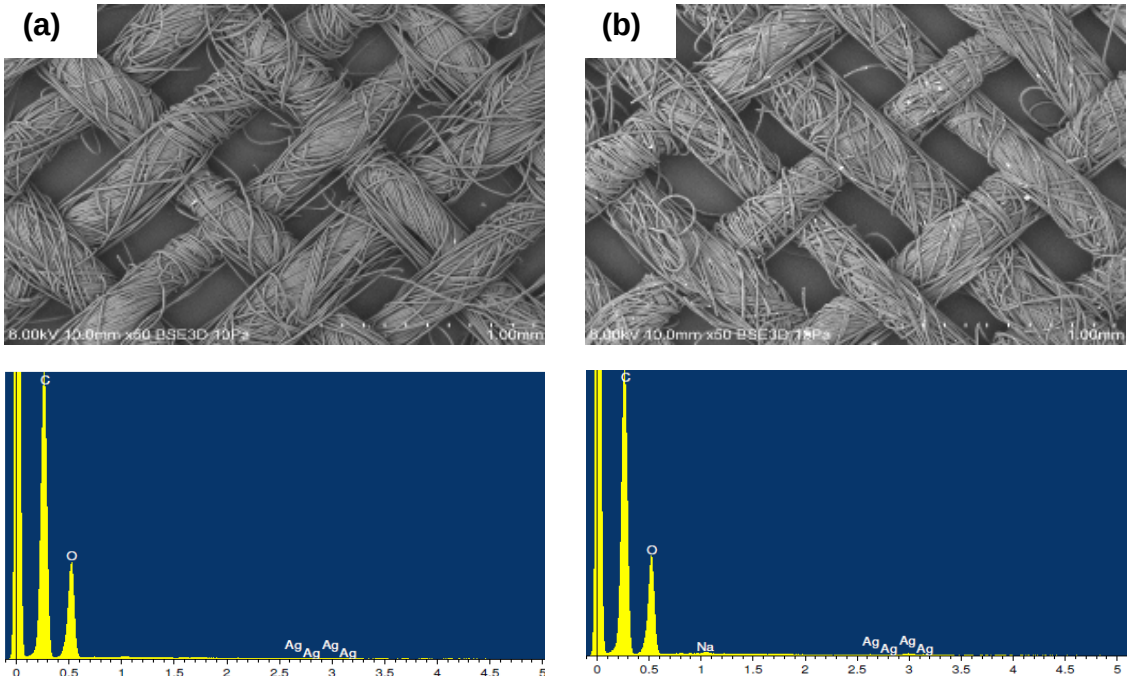

Element	Massen%	Atom%
C K	63.05	70.18
O K	35.45	29.63
Ag L	1.50	0.19

Element	Massen%	Atom%
C K	59.56	69.23
O K	34.18	29.83
Na K	0.27	0.17
Ag L	5.99	0.78

Figure 5-16: SEM images of PET fabrics loaded with different concentrations of silver nanoparticles and the relevant EDX spectra; (a) amount of silver on the fabric 15 mg/kg (b) amount of silver on the fabric 30 mg/kg

5.2.3. Laundering durability

Laundering durability of the Ag NPs on the PET fabric was evaluated by determination of the deposited amount of silver over five washing cycles in a laboratory-dyeing machine, again using ICP-OES for quantitative measurement. In this specific measurement, the fabric was originally loaded with 15 mg/kg Ag NPs. The data shown in figure 5-17 indicate that most of the silver nanoparticles were removed from the fabric after five times laundering. It may be assumed that, due to the hydrophobic nature of the PET fiber, the adhesion of the silver nanoparticles is weak. It is know that Ag NPs dispersed in aqueous solution have negative charged (from streaming current data), due to Ag NPs a rounded with Na PMAA as sketched in figure 5-4, and surface of PET is inert surface i.e. it has not functional groups to attaché with Ag NPs structure. Thus, adhesion forces between Ag NPs and surface of PET is week.

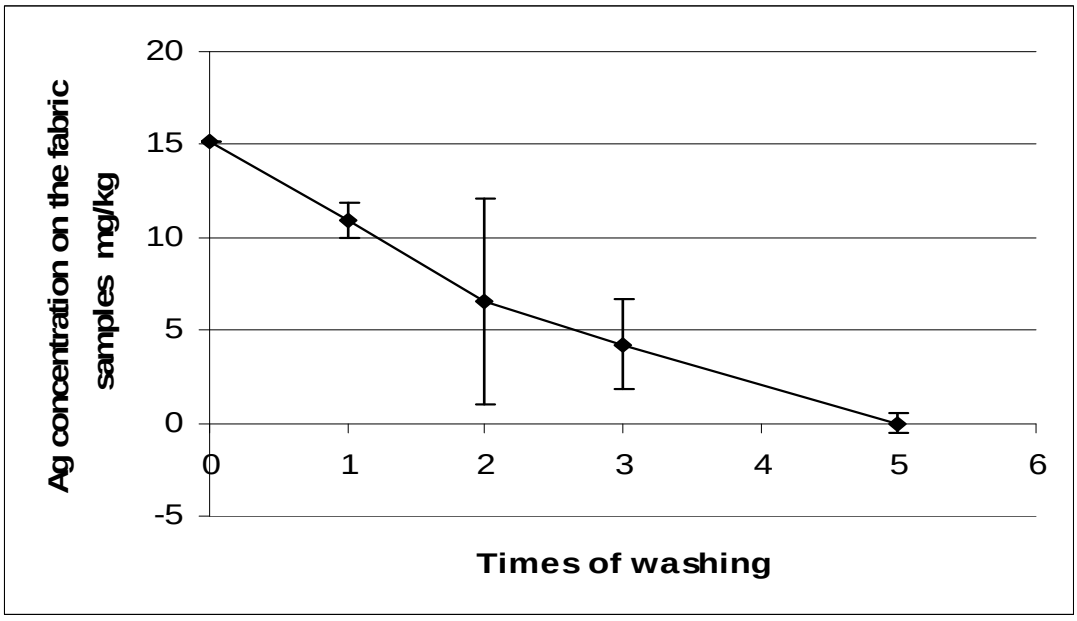

Figure 5-17: Amount of silver nanoparticles on a fabric originally loaded with 15 mg/kg of silver nanoparticles as a function of washing cycles

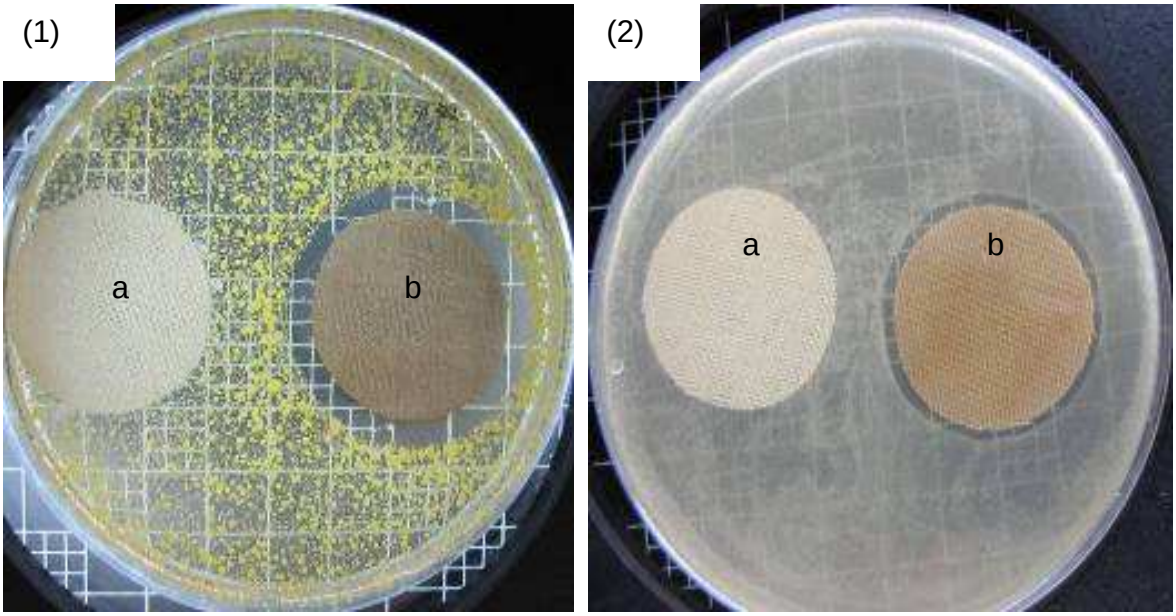

Figure 5-18: Antibacterial efficiency of Ag nanoparticles loaded PET fabric amount of silver on the fabric 15 mg/ kg *(1) Micrococcus luteus* (*M. luteus*), *(2) Escherichia coli (E. coli)* (a) PET original, (b) PET with Ag nanoparticle

5.2.4. Antibacterial efficiency of Ag loaded PET fabrics

In the zone of inhibition test, the samples of PET loaded with silver nanoparticles to an amount of 15 mg/kg show more antibacterial activity against both Gram positive *Micrococcus luteus* (*M. luteus*), and Gram negative *Escherichia coli (E. coli)* bacteria than untreated PET fabrics. A clear inhibition zone with no bacteria growth is observed around the treated samples (figure 5-18).

The data derived from the ASTM E2149-01 test, which are summarized in table 5-1, show that after two washing cycles the PET fabric preserved the antibacterial activity. The referring amount of deposited silver nanoparticles at that stage is approximately 7 mg/kg and higher. After the third washing cycle the samples lost antibacterial properties In that state, the residual amount of silver is below 5 mg/kg.

Table 5-1: Antibacterial efficiency of Ag loaded PET fabrics according to the ASTM E2149-01 test after 1, 2 and 3 washing cycles.

Samples	*Average colony units of E. coli after 0 time incubation (CFU)*	*Average colony units of E. coli after 1 h incubation (CFU)*	*R (%)*
PET	35 x 10^7	25x 10^7	28.57
PET with Ag NPs	14 x 10^3	<1	99.99
PET with Ag NPs (1)	12 x 10^3	2	99.98
PET with Ag NPs (2)	11 x 10^3	3 x 10^2	97.77
PET with Ag NPs (3)	12 x 10^3	5 x 10^3	58.33

5.3. Antibacterial properties of plasma activated synthetic fibers impregnated with photochemically synthesized Ag NPs

5.3.1. Introduction

Synthetic fibers especially PET and polyamide-6 (PA 6) fabrics have been widely used in medical and surgical applications. For centuries, silver ions in different form have been use for healing of burns and wounds. So, recently silver ions and Ag NPs are considered of the most important antibacterial agents used in medical textile products. The loading of the textile products with Ag NPs carried out by two different ways: Ag NPs can be embedded into the fibers during the spinning process or by deposition on the surface during finishing processes. The effect of plasma pre-treatment on wettability and on particle adhesion on the textile surfaces was studied[13]. The treatment was effected by atmospheric air plasma, which can be applied in the production line without the need for vacuum. Deposition of colloidal silver nanoparticles onto synthetic fabrics such as PA 6 and PET fabrics provides excellent antibacterial effect. Plasma treatment positively affected the loading of Ag NPs as well as antibacterial activity and laundering durability of this textile nanocomposite materials [57-60]

In this work, Ag NPs were prepared by a simple and inexpensive single step synthesis based on UV activation of a solution of $AgNO_3$ and Na PMAA. Ag NPs were applied to a PET and PA 6 fabric by finishing the fabric with the resulting colloid of silver nanoparticles. The effect of plasma pre-treatment on wettability and on particle

adhesion on the surface, as suggested by[13], was studied. The treatment was effected by atmospheric air plasma, which can be applied in the production line without the need for vacuum.

5.3.2. Plasma pre-treatment on PET fabrics

In order to study the effect of plasma pre-treatment on wettability and on particle adhesion on the surface, a number of samples were treated by atmospheric air plasma. In general, the intensity of the plasma treatment ("dose") is determined by plasma power and exposure time (or in our case by processing speed i.e. time of plasma treatment on the surface of textile) the distance between samples and plasma source is fixed, thus the processing speed was controlled by the speed of the moving samples. The experiments showed that the dose was critical. Thermal damage to the fibers was found, if the dose was too high, as is exemplarily shown in the SEM images in Figures 5-19.

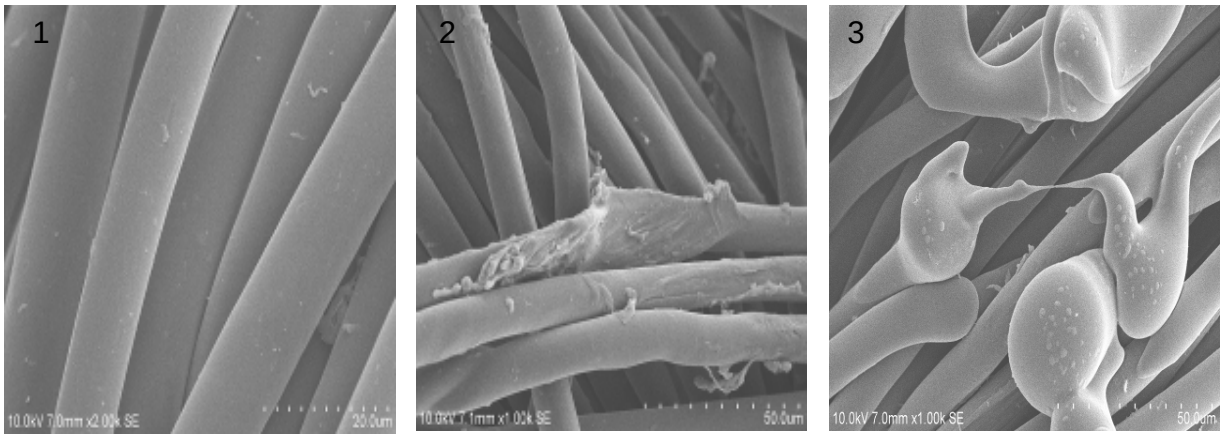

Figure 5-19: SEM images of (1) Original PET. (2) PET activated with plasma 0.3 cm/s. (3) PET activated with plasma 0.16 cm/s.

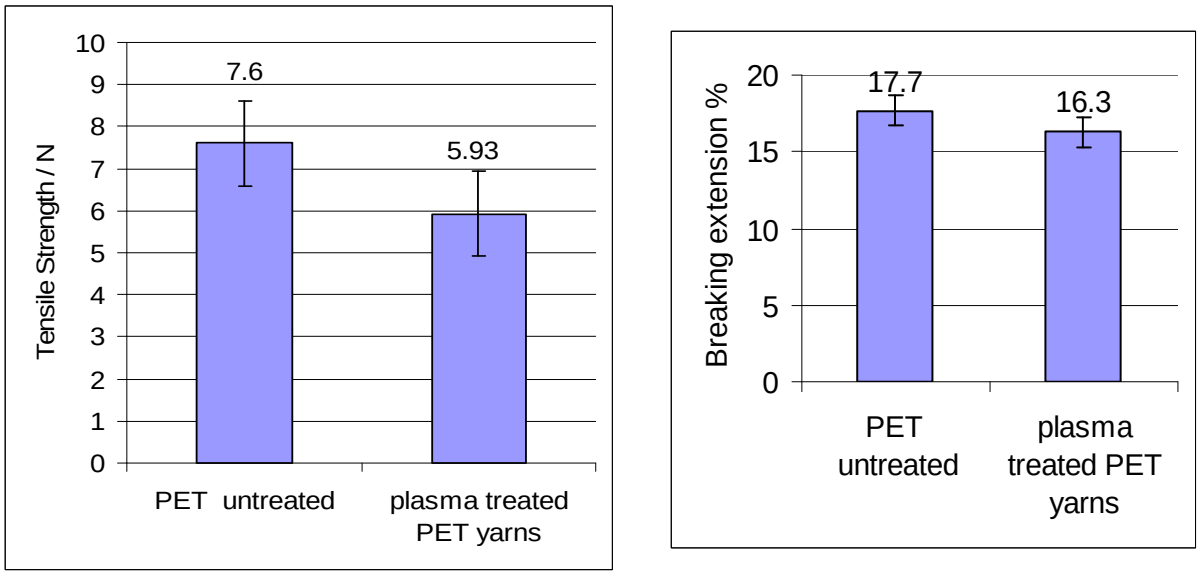

Figure 5-20: Tensile strength, breaking extension of untreated, and plasma activated PET fabrics 0.3 cm/s

5.3.3. Surface Properties of PET Fabrics after plasma treatment

Tensile strength and breaking extension of PET fabric before and after plasma treatment are shown in figures 5-20. The breaking extension of the plasma treated sample decreased by 1.5 % compared with the untreated PET fabric, also little change in tensile strength by 1.6 N compared with the untreated PET fabric was observed. The plasma treatment results have revealed reduction in both tensile strength and breaking extension of PET fibres, because the induced fluency of energetic particles, which come from plasma, on the surface create weak points to the fibres eventually reduce both tensile strength and breaking extension as shown in the SEM images in Figures 5-19.

As was expected, the concentration of carboxyl groups on the surface was increased by the plasma treatment. The quantitative determination using the methylene blue test indicated a linear dependence of the carboxyl concentration on the relative plasma dose, which was estimated as the inverse of the sample speed during the treatment (figure 5-21). The carboxyl groups have a large effect on the wettability of the PET fabric, as can be taken from the spreading behaviour of a droplet applied to the surface (Figure 5-22).

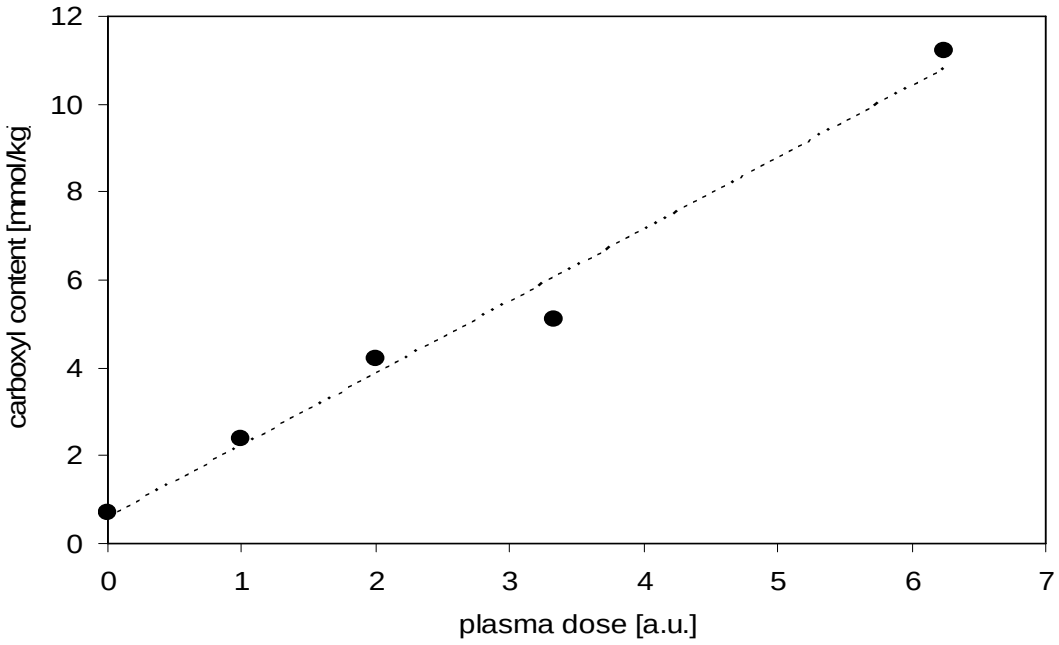

Figure 5-21: Carboxyl content on the PET surface as a function of sample speed during the plasma treatment

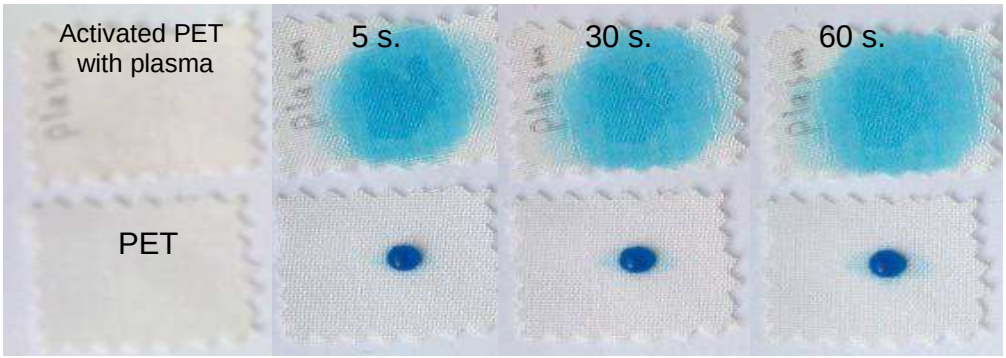

Figure 5-22: photographs of diffusion of dyed drop after 5, 30 and 60 second through untreated and treated polyester with plasma 0.3 cm/s

5.3.4. Treatment PET with Ag nanoparticles colloid

The effect on deposition and adhesion was characterized by quantitative determination of the silver concentration before and after laundering, again using ICP-OES for quantitative measurement. A standard laundering procedure was employed by running three washing cycles in a laboratory-dyeing machine. In this specific measurement, the fabric was originally loaded with Ag NPs. As is shown in Figure 5-

23, plasma activation yields a higher amount of deposited silver nanoparticles on the fabric surface. The increase from 8.9 to 13.0 mg/kg (as compared to the untreated fabric) can be explained by the improved wettability, which gives better excess to the capillary system of the fabric and yarn. After the washing, most of Ag NPs were removed from the fabrics. Silver concentration is reduced to approximately 3 mg/kg on both untreated and plasma treated samples, this indicates that the adhesion of the silver nanoparticles on the surface is weak, and that the plasma treatment has no effect on this.

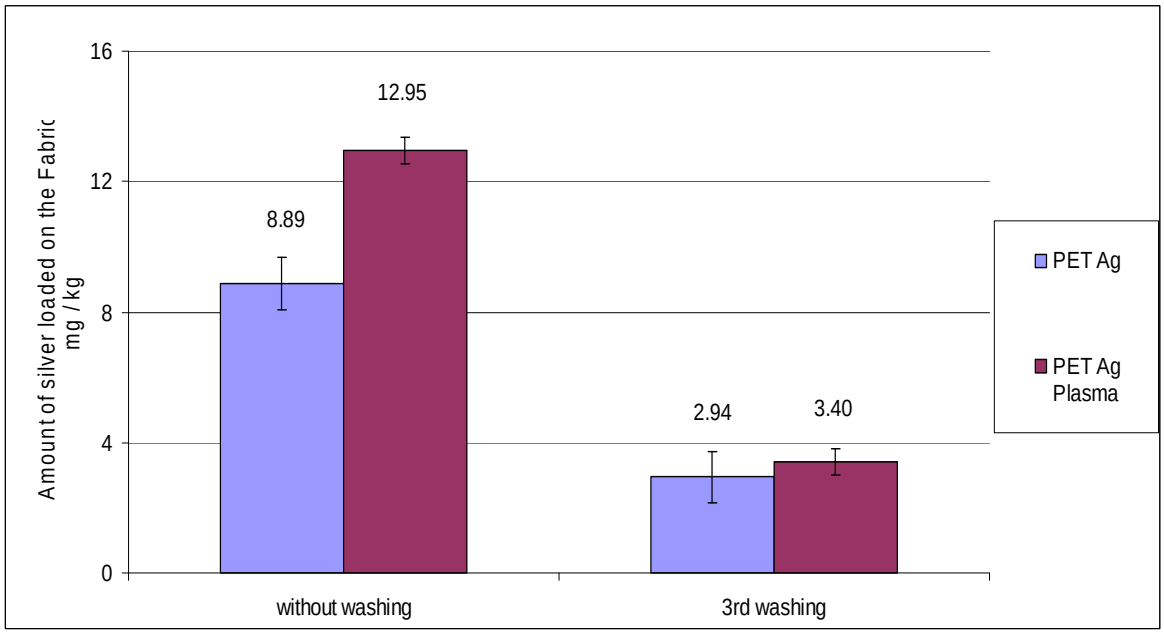

Figure 5-23: Amount of silver loaded on the PET fabrics (untreated and pre-treated with plasma) before washing and after 3rd cycles washing

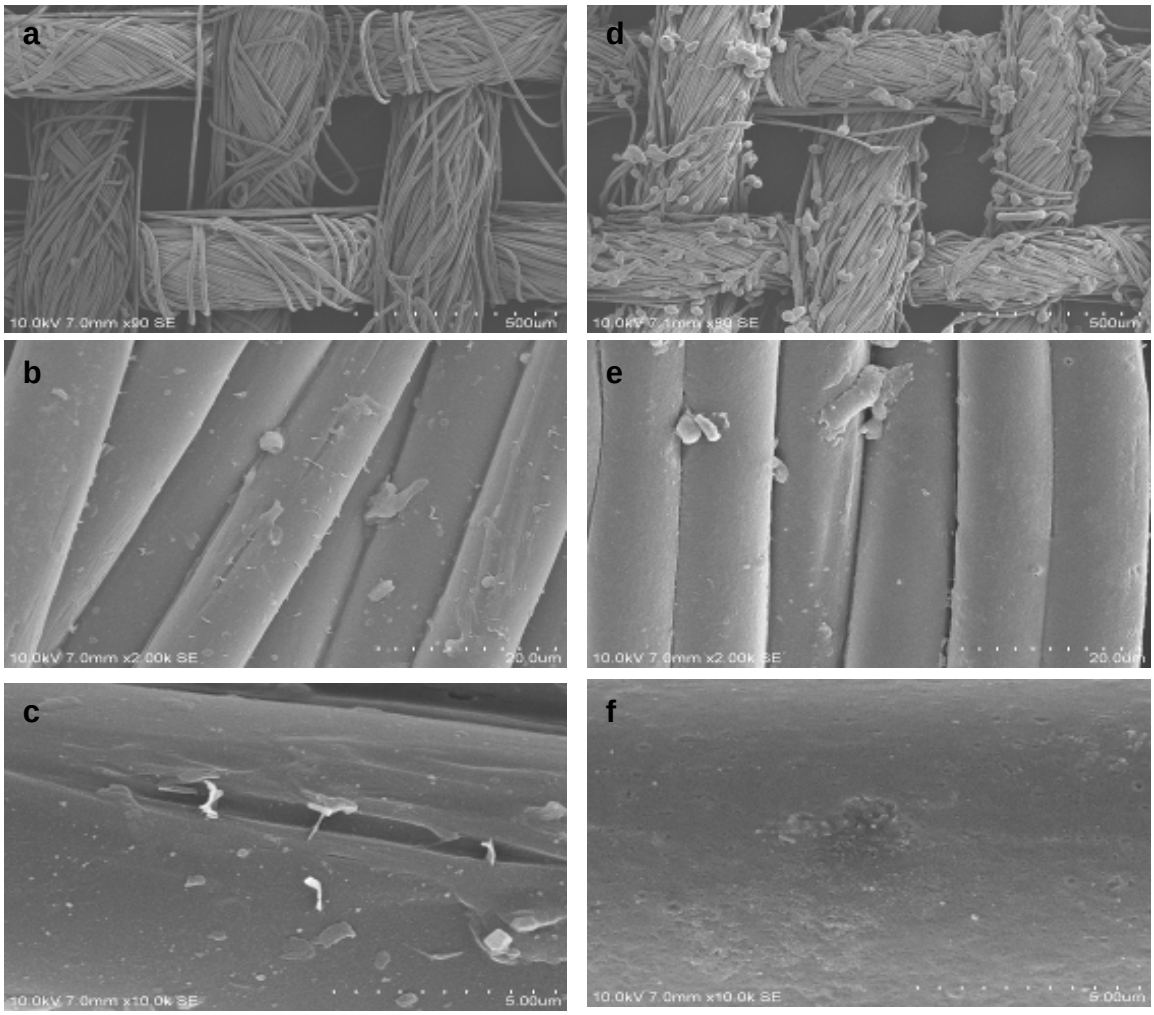

Figure 5-24: SEM images with different magnification of (a), (b) and (c) Original PET Loaded with **Ag NPs**. (d), (e) and (f) PET activated with plasma 6 sec. cm^{-1} loaded with **Ag NPs**.

5.3.5. Surface characterization of PET fabrics after deposition of Ag NPs

5.3.5.1 SEM images of PET fabrics

Topologies the fiber surface of the deposition of Ag NPs from the colloid were analyzed by SEM images. In SEM images of untreated PET fabrics loaded with Ag NPs as shown in figure (5-24 a, b and c) with different magnification, revealed a low yield of unevenly distributed agglomerates of Ag NPs on the fibers surface. The plasma treatment positively affected the loading of Ag NPs onto PET surface. Remarkable uniform and dispersed of Ag NPs on the surface after pretreated with

plasma. The increased wettability and capillary properties of the fabrics after plasma treatment indicates the compatibility between PET surface and Ag NPs as shown in figures (5-24 d, e and f).

5.3.5.2 ATR-FTIR analysis of PET fabrics

ATR-FTIR spectra of PET original, PET activated with plasma and activated PET loaded with Ag NPs are shown in figure 5-25. The formation and development of a weak absorption shoulder on the lower wave number side of 1750 cm^{-1} peak corroborates with the formation of carboxylic acid. The formation of a broad band was observed in the region 3200-3600 cm^{-1} of the spectrum for activated PET loaded with Ag NPs, because the formation of hydrogen bonded (H-bond) between carboxylic groups of polymethacrylic acid PMAA and polar groups (carboxylic or alcohol groups) on the PET surface.

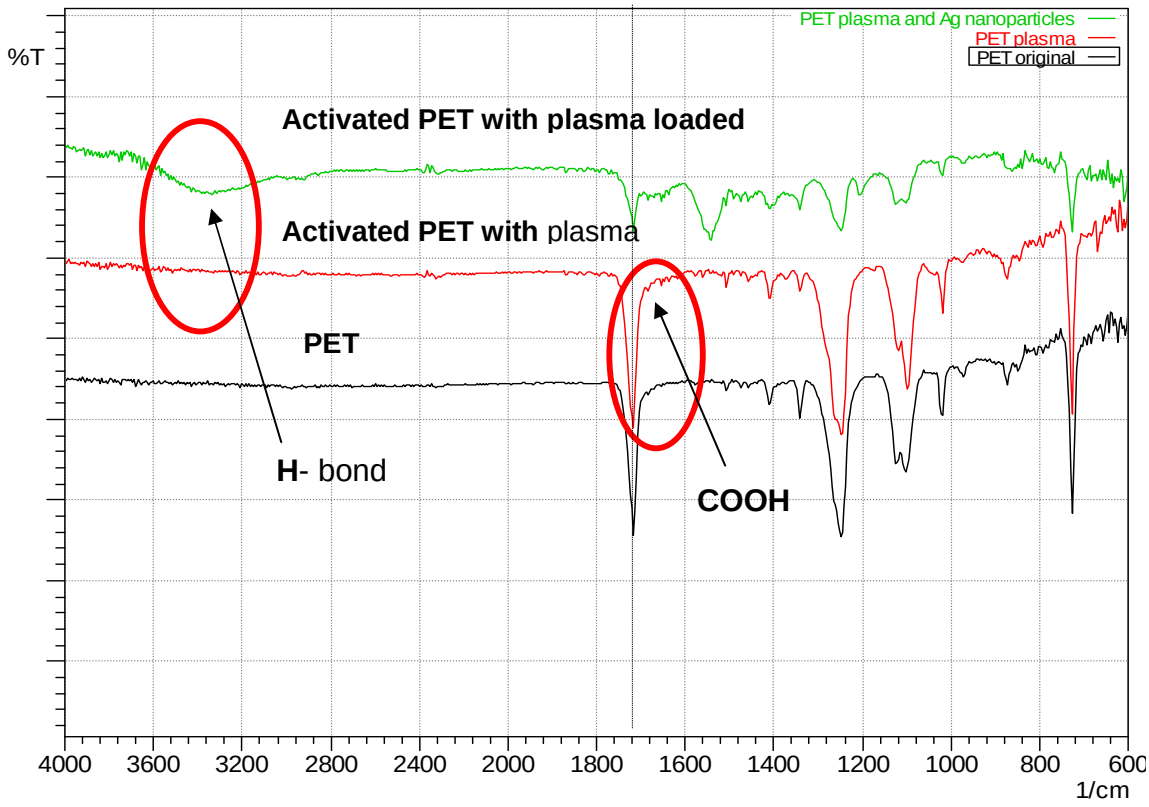

Figure 5-25: FTIR-ATR spectra PET original, PET activated with plasma 0.3 cm/s and activated PET loaded with Ag NPs

5.3.6. Antibacterial activity of PET fabrics

Tests of antibacterial activity were performed (Figure 5-26). In both images, the zone of inhibition effect can be clearly seen around samples 2 and 3. In the zone of inhibition test, the samples of PET loaded with Ag NPs with amounts of 8 mg/kg and 12 mg/kg for activated PET with plasma. All samples loaded Ag NPs showed an efficient zone inhibition against both Gram positive *Micrococcus luteus* (*M. luteus*) and Gram negative *Escherichia coli (E. coli)* bacteria, which is not found in the case of untreated PET with silver (Figure 5-26).

The antibacterial activities of the samples measured according to ASTM E2149-01 are shown in Table 5-2. Values are shown for original PET and samples loaded with silver nanoparticles, both before and after three washing cycles. All samples loaded with Ag exhibited high bacterial reduction before and after washing. There is no significant difference between untreated and plasma pretreated fabrics.

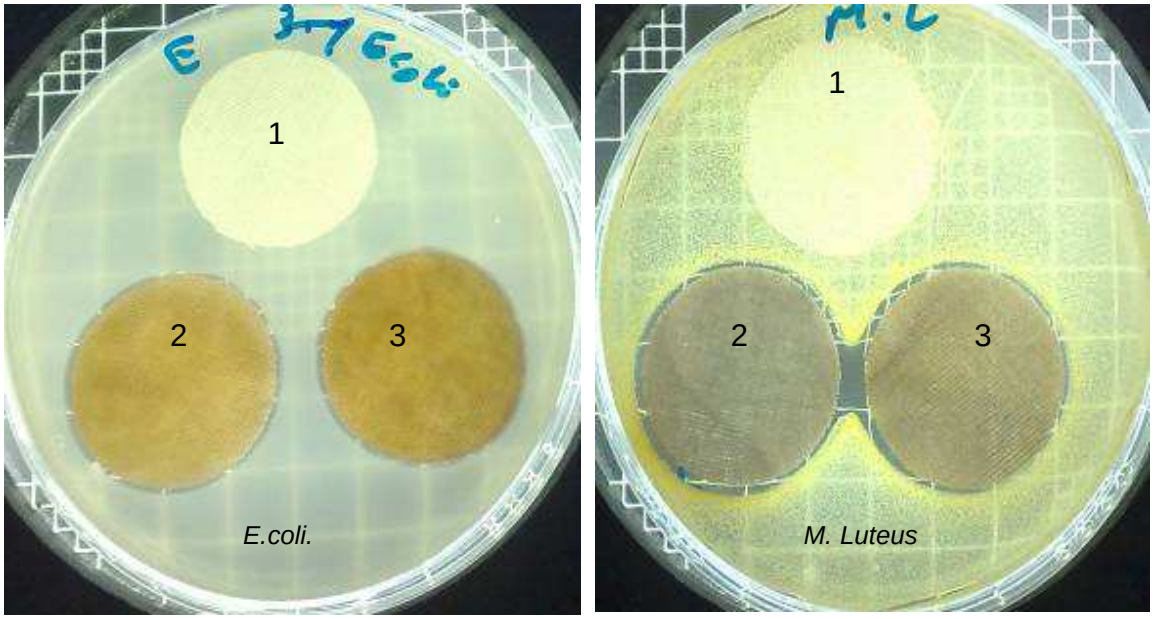

Figure 5-26: Antibacterial efficiency of Ag nanoparticles loaded PET fabric with *Micrococcus luteus* (*M. luteus*) and *Escherichia coli (E. coli)* (1) PET original, (2) PET with Ag nanoparticle and (3) activated plasma 0.3 cm/s PET with Ag nanoparticles

The efficient bactericidal effect of the samples even after the laundering procedure, where silver content is reduced to about 3 mg/kg, In other words, the samples only lost antibacterial properties, if the residual amount of Ag NPs fell significantly below 3 mg/kg.

In the TTC test, the antibacterial activity is related to amount of absorbance of formazan, which is directly proportional to the amount of living cell bacteria. The results show strong reduction of living cell bacteria due to presence Ag NPs on the surface of the fabrics before and after three cycles washing (Figure 5-27). These results are agreement with the results which were shown before.

Table 5-2: Antibacterial efficiency of Ag loaded PET fabrics according to the ASTM E2149-01 test after 3 washing cycles.

Samples	*Average colony units of E. coli after 0 time incubation (CFU)*	*Average colony units of E. coli after 1 h incubation (CFU) before washing*	*R (%)*	*Average colony units of E. coli after 1 h incubation (CFU) after 3 cycles washing*	*R (%)*
Control PET	33×10^7	25×10^7	24.2	28×10^7	15.1
Activated PET with plasma 0.3 cm/s	38×10^7	31×10^7	18.4	33×10^7	13.1
Untreated PET loaded with Ag NPs	12×10^5	5	99.9	4×10^4	96.6
Activated PET with plasma and loaded with Ag NPs	18×10^5	1	99.9	2×10^4	98.8

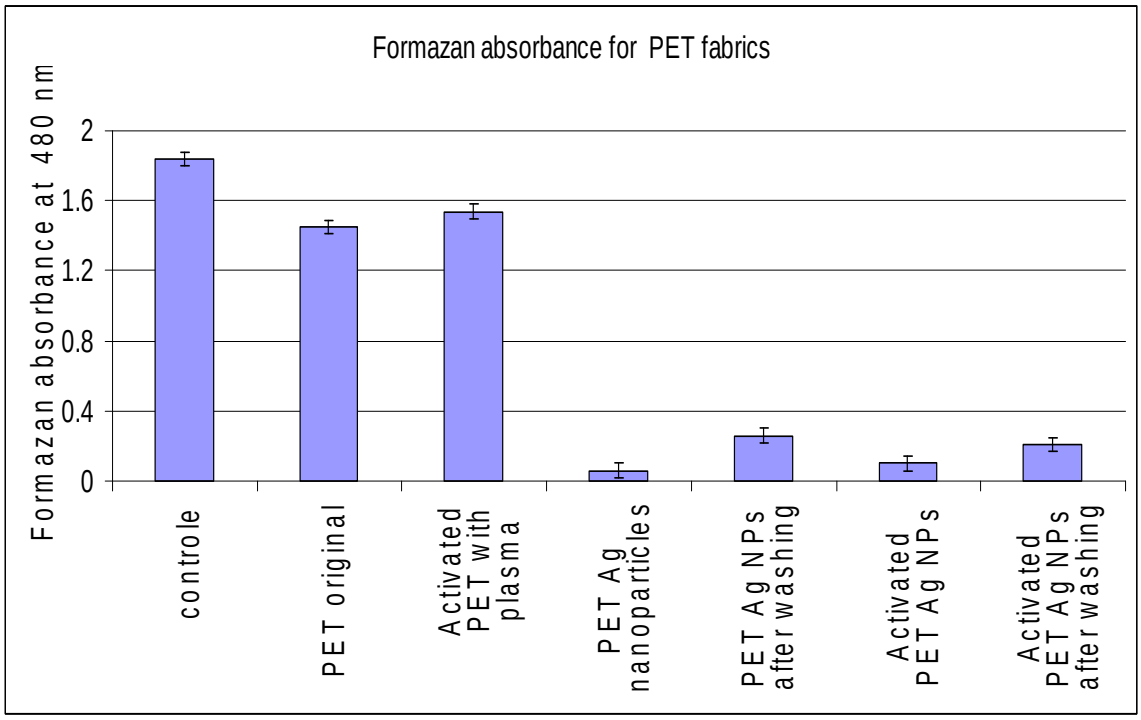

Figure 5-27: Absorbance of formazan for PET fabrics and PET loaded with silver nanoparticles (Ag NPs) before and after washing

5.4. Antibacterial properties of plasma activated PA 6 fabric impregnated with photochemically synthesized Ag NPs

5.4.1. Plasma Pre-treatment on PA 6 Fabrics

Plasma treatment is a surface treatment, influencing only the top layer. As shown in figure 5-28. SEM images show two types of fibers of PA 6 warp and weft fibers before and after plasma treatment. The images of SEM show that topographical of PA 6 surface changed, due to the different characteristics and properties between warp and weft. This difference is attributed to the different fabrication steps the warp and weft yarns underwent and which lead to slightly different surface conditions such as orientation of the fibers and contamination with environments.

The mechanical properties of PA 6 yarn for warp and weft before and after plasma treatment are shown in figures 5-29 and 5-30. The breaking extension % of the PA 6 yarn for warp and weft after plasma treatment was decreased from 27 to 24.2 % and 41.9 to 20.1% respectively (figures 5-29). The tensile strength of PA 6 for

warp and weft yarns also decreased from 5.6 to 5.1 N and 10.7 to 5.7 N respectively as shown in figure 5-30. Because the induced of plasma high energy influences on the surface of PA 6 which creates more weak points on the fibres and reduce both strength and extensibility, distinguished the values between warp and weft, due to the different characteristics and properties between warp and weft.

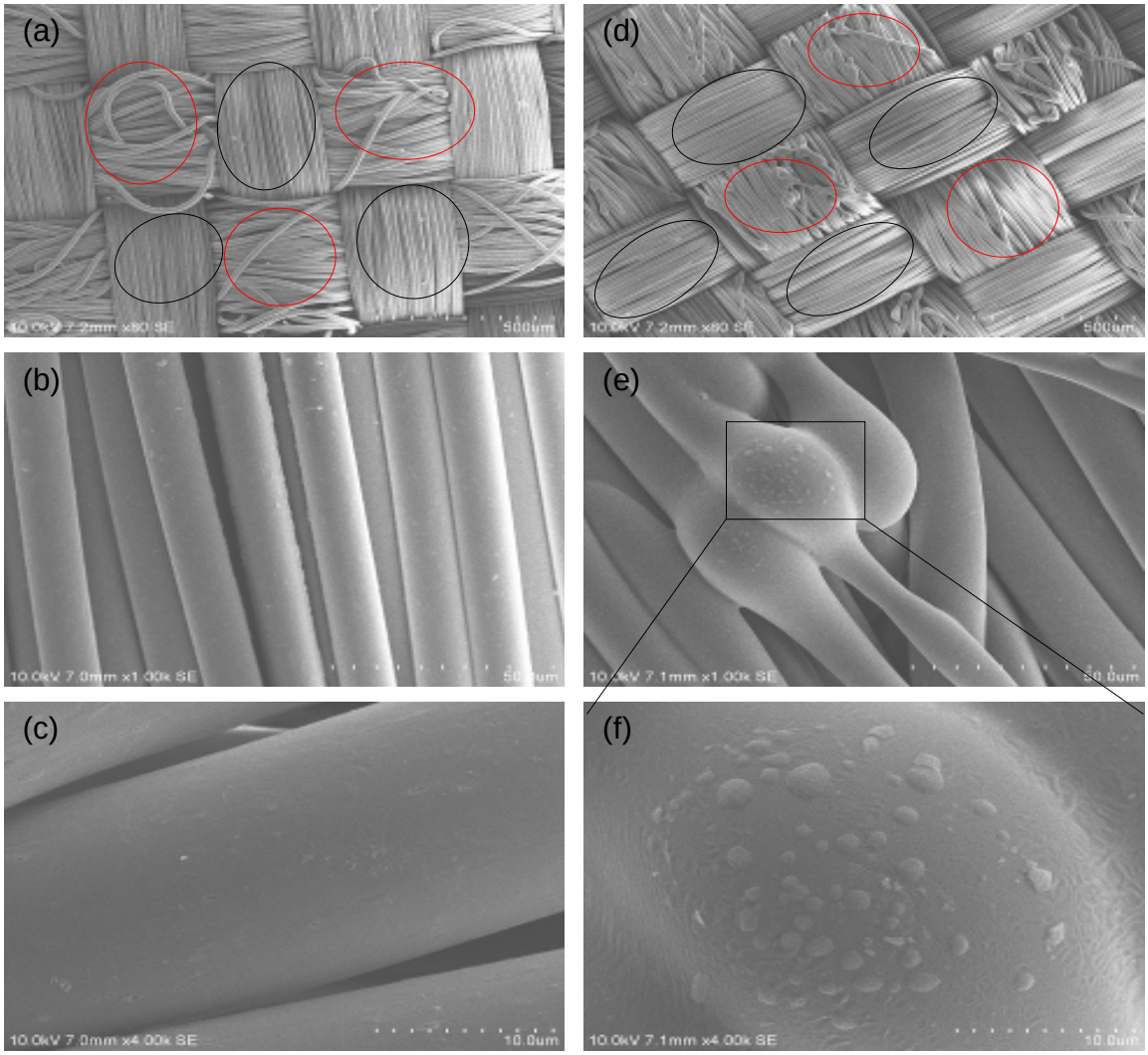

Figure 5-28: SEM images of (a), (b) and (c) Original PA 6 (d), (e) and (f) PA 6 activated with plasma 0.16 cm/s

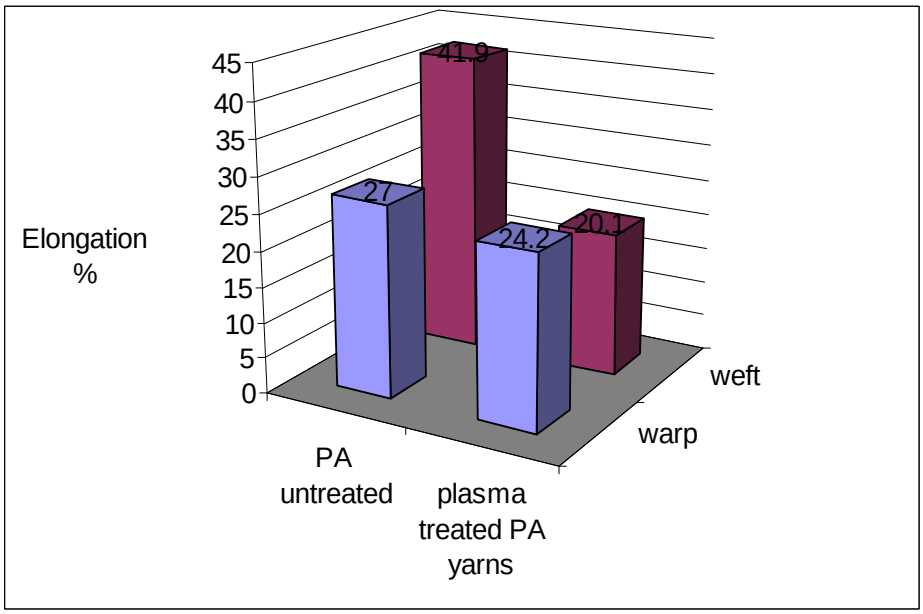

Figure 5-29: Elongation % of untreated and plasma activated PA 6 fabrics 0.3 cm/s

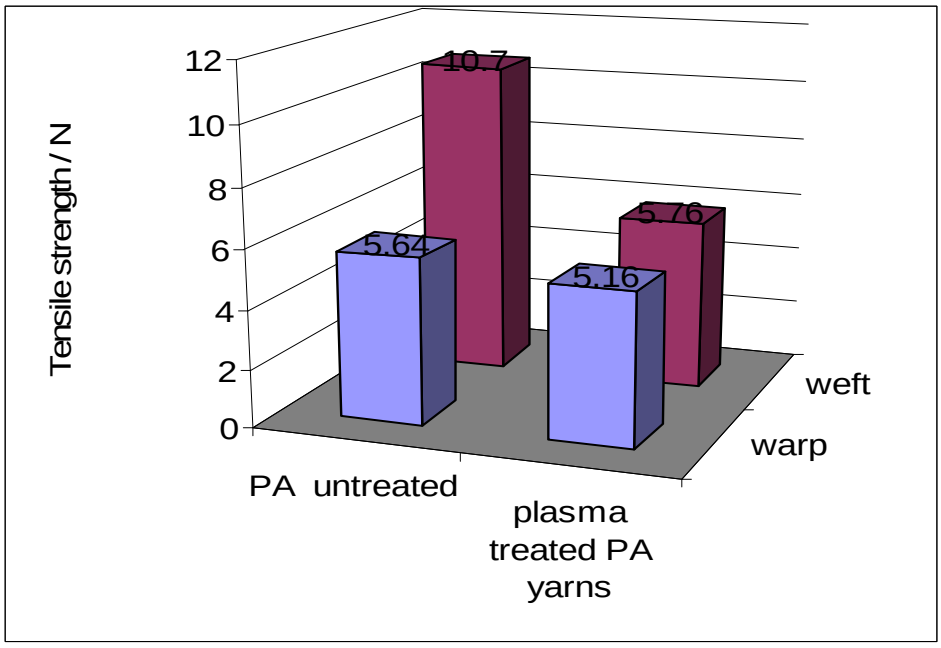

Figure 5-30: Tensile strength of untreated and plasma activated PA 6 fabrics 0.3 cm/s

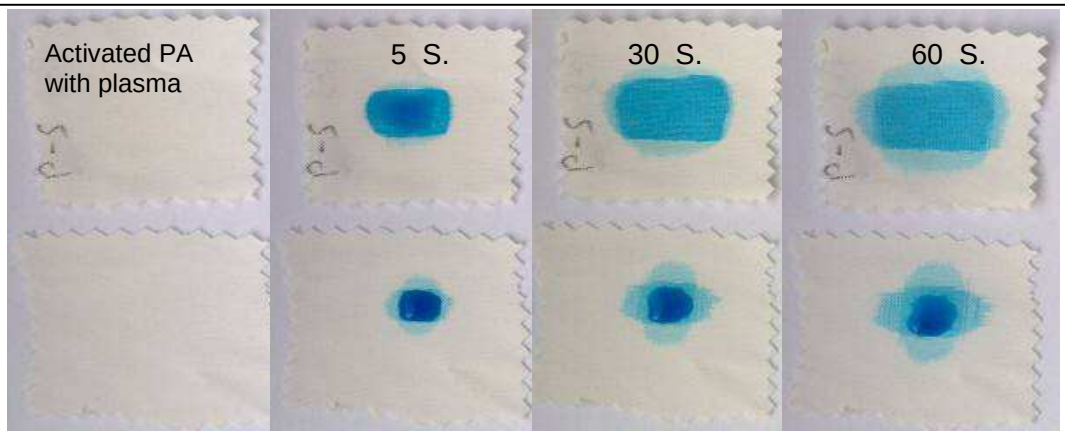

Figure 5-31: Photographs of diffusion of dyed drop through untreated and treated polyamide with plasma 0.3 cm/s

As shown in figure 5-31, the rate of spreading of dyed drop placed on PA 6 surface increased after plasma treatment. The dyed drop did not spread well compared to treated PA 6 fabrics with plasma, this indicates that increase in wettability of fabrics after activation with plasma also increase the capillary properties of the fabrics.

5.4.2. Treatment PA 6 fabrics with Ag nanoparticles colloid

Laundering durability of Ag NPs on the PA 6 fabrics was evaluated by determination amounts silver deposited on the PA 6 fabrics before washing and after one and three time cycles washing in a laboratory-dyeing machine, using ICP-OES instrument for quantitative measurement. As shown in figure 5-32, deposition of Ag NPs on the surface of PA 6 after activation with plasma increased from 8 to 82 mg/kg fabric, i.e. approximately 10 times more. The treatment with Ag NPs solution has to be as close as possible after activation with plasma, due to improve hydrophilic and wettability properties on the surface. After the washing, the most of the silver nanoparticles were removed from the fabric after three times laundering, due to the adhesion of the Ag NPs on the surface is weak. This behavior is similar to behavior PET fabrics with Ag NPs after pretreatment plasma and Laundering durability.

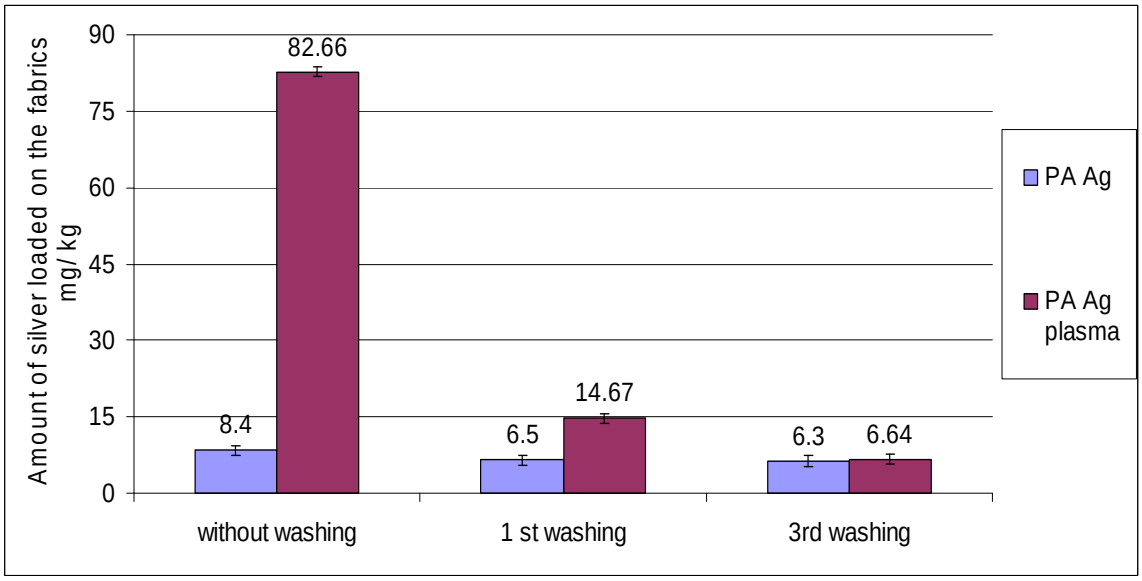

Figure 5-32: Amount of silver loaded on PA 6 the fabrics (untreated and pre-treated with plasma) after 1 and 3 cycles washing.

5.4.3. Surface characterization of PA 6 fabrics after deposition of Ag NPs

5.4.3.1 SEM images of PA 6 fabrics loaded with Ag NPs

Topology of PA 6 loaded with Ag NPs before and after pretreated plasma was analyzed by SEM. In SEM images of untreated PA 6 fabrics loaded with Ag NPs as shown in figure (5-33 a, b and c) with different magnification, revealed a low yield of unevenly distributed agglomerates of Ag nanoparticles on the fibers surface. The plasma treatment positively affected the loading of Ag NPs onto PA 6 fabrics. In addition, we observed, increasing in the dispersion and uniform Ag NPs on the PA 6 surface after treated with plasma. The increased wettability and capillary properties of the fabrics after plasma treatment indicates the possibility of a strong interaction between PA 6 fabrics and Ag NPs as shown in figures (5-33 d, e and f) with different magnification.

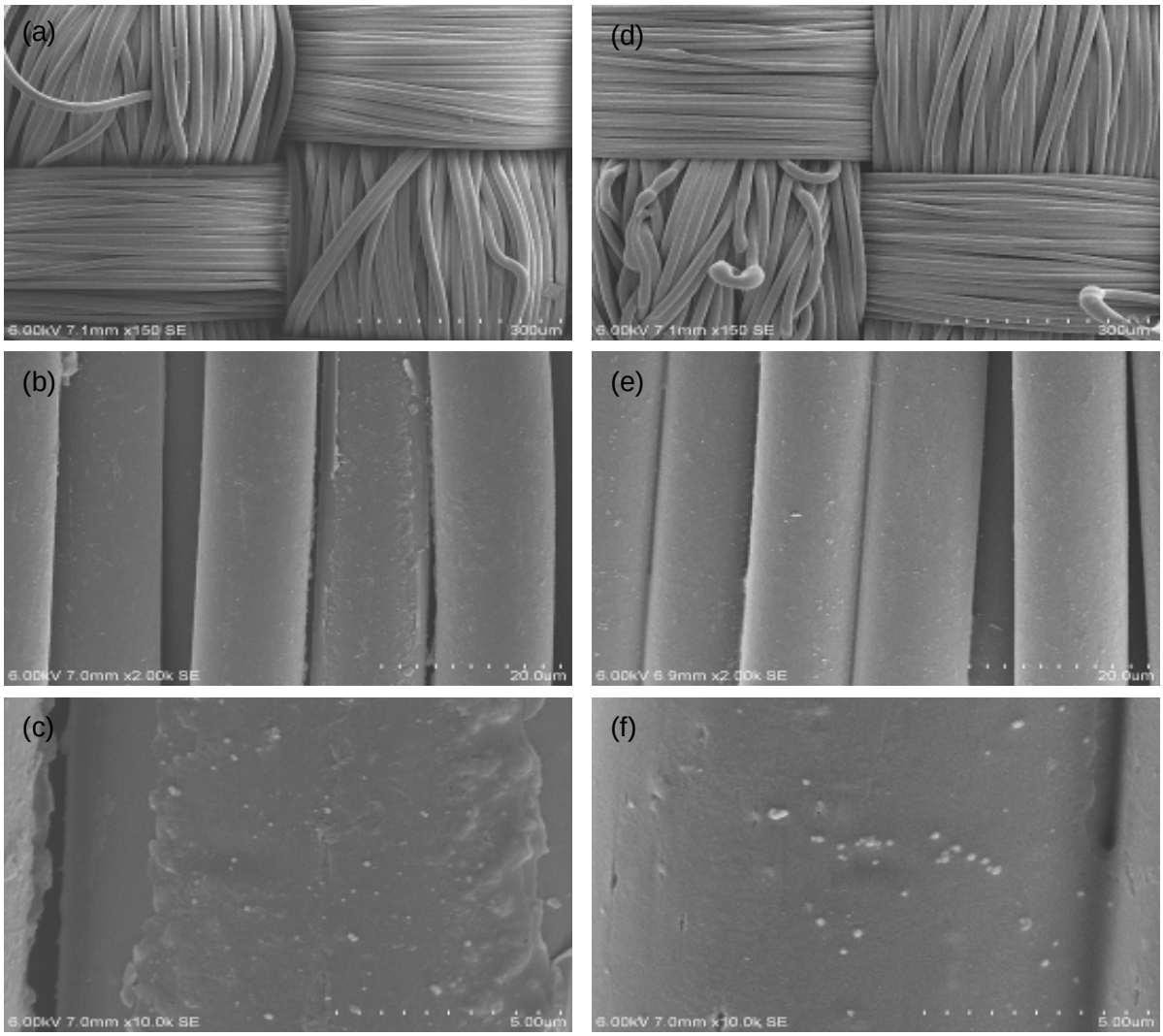

Figure 5-33: SEM images of (a), (b) and (c) Original PA 6 Loaded with Ag NPs. (d), (e) and (f) PA 6 activated with plasma 0.3 cm/s loaded with Ag NPs.

5.4.3.2 ATR-FTIR analysis of PA 6 fabrics

FTIR-ATR spectra of PA 6 before and after plasma pre-treated with plasma as shown in figure 5-34, does not show different in absorption bands between them, but the absorption bands can be explained the types of functional groups on polyamide-6 surface. However at 3750 cm^{-1} a small band appears that may corresponding to O-H groups , the band at 3300 cm^{-1}, corresponding to N-H groups, the band at 2930 and 2850 cm^{-1}, corresponding to symmetric and asymmetric C-H vibration, respectively.

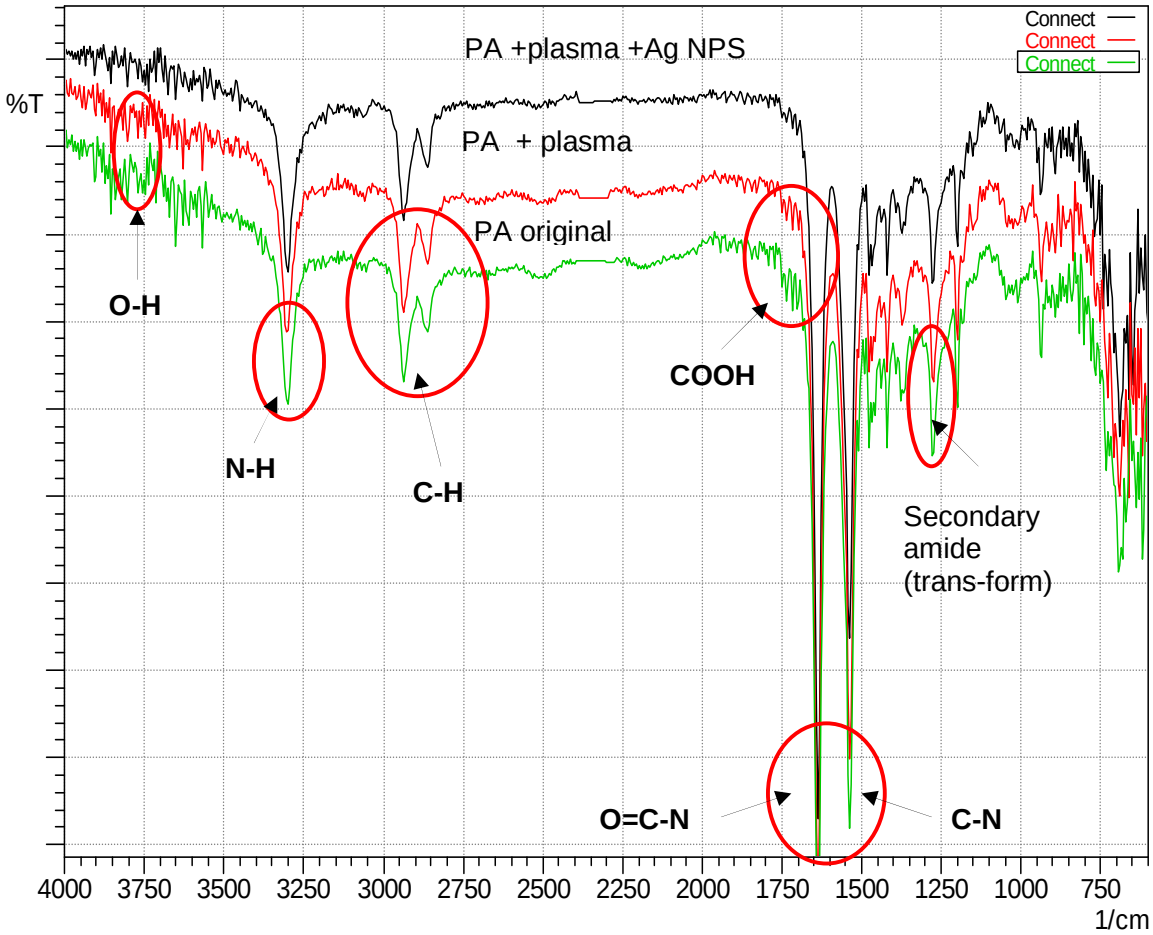

Figure 5-34: FTIR-ATR spectra PA 6 original, PA 6 activated with plasma 0.3 cm/s and activated PA 6 loaded with Ag NPs

At 1740 cm^{-1} a small band is observed, indicating the formation of carboxylic groups on the surface. The absorption band at 1630 cm^{-1} corresponding to C=O of amide groups, and band at 1525 cm^{-1} corresponding to C-N of amide groups. The intensity of the bands at 1265 cm^{-1}, corresponding to secondary amide (trans- form)

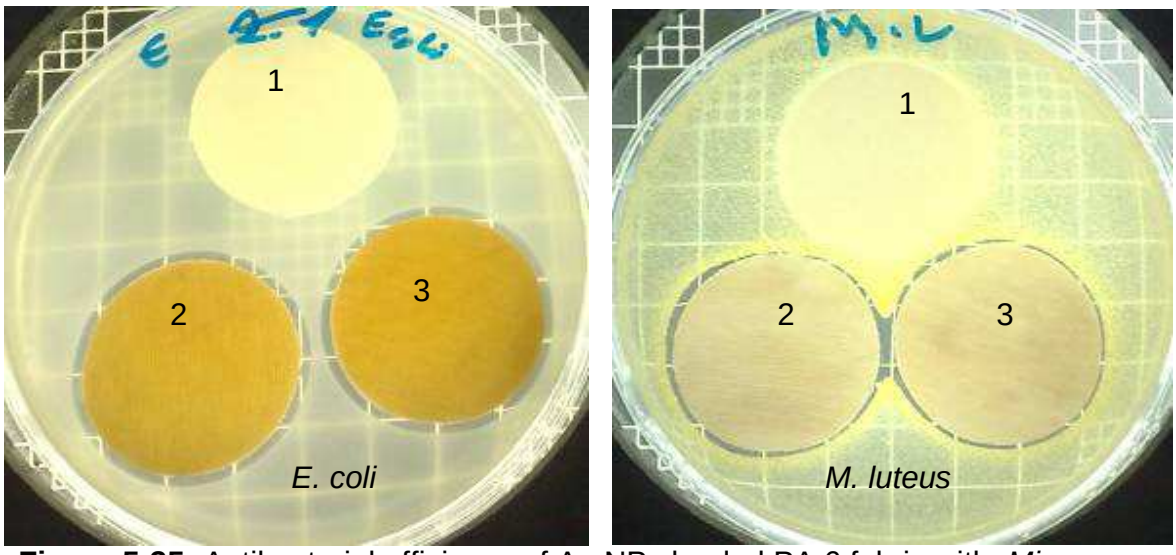

Figure 5-35: Antibacterial efficiency of Ag NPs loaded PA 6 fabric with *Micrococcus luteus* (*M. luteus*) and *Escherichia coli (E. coli)* (1) PA 6 original, (2) PA 6 with Ag NPs and (3) activated plasma 0.3 cm/s PA 6 with Ag NPs.

5.4.4. Antibacterial activity of PA 6 fabrics

The antibacterial activity of silver nanoparticles loaded on the PA fabrics against *Micrococcus luteus* (*M. luteus*) and *Escherichia coli (E. coli)* was evaluated by three methods. In the zone of inhibition test, the samples of PA 6 loaded with Ag NPs to amounts of 8 mg/kg and 82 mg/kg for activated PA 6 with plasma. All samples loaded silver nanoparticle appeared zone inhibition around them compared to untreated PA 6 with silver against both Gram positive *Micrococcus luteus* (*M. luteus*) and Gram negative *Escherichia coli (E. coli)* bacteria. A clear inhibition zone indicates to no bacteria growth in this area, it was observed around the treated samples with silver nanoparticles (figure 5-35).

According to ASTM E2149-01 test, antibacterial activity of the samples loaded with Ag NPs before and after three washing cycles is shown in table 5-3.

Table 5-3: Antibacterial efficiency of Ag NPs loaded PA 6 fabrics according to the ASTM E2149-01 test after 3 washing cycles.

Samples	*Average colony units of E. coli after 0 time incubation (CFU)*	*Average colony units of E. coli after 1 h incubation (CFU) (before washing)*	*R (%)*	*Average colony units of E. coli after 1 h incubation (CFU) (after 3 cycles washing)*	*R (%)*
Control PA 6	$50x\ 10^7$	43×10^7	14	44×10^7	12
Activated PA 6 with plasma 0.3 cm/s	54×10^7	48×10^7	11.1	50×10^7	7.4
Untreated PA 6 and loaded with Ag NPs	25×10^5	7	99.9	3×10^4	98.8
Activated PA 6 with plasma and loaded with Ag NPs	28×10^5	5	99.9	38×10^4	86.4

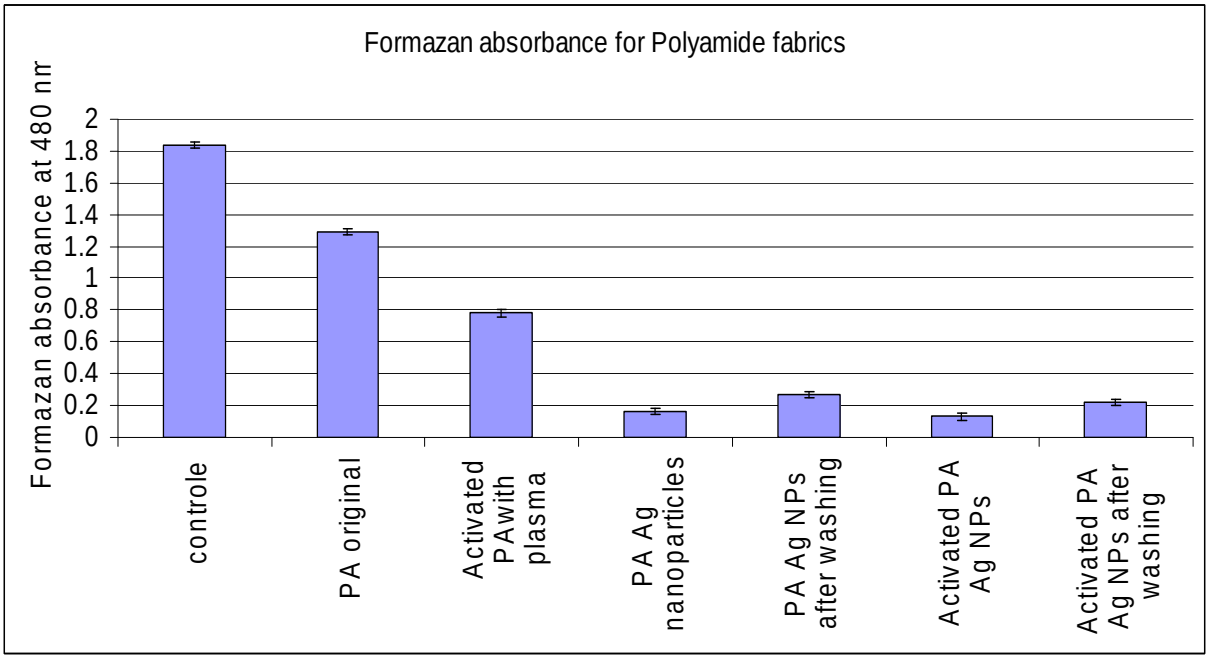

Figure 5-36: Absorbance of formazan for PA 6 fabrics and PA 6 loaded with Ag NPs before and after washing

All samples loaded Ag NPs exhibited higher bacterial reduction before and after washing, there is no significant difference between untreated, and plasma pretreated fabrics. After the third washing cycle, the samples lost antibacterial properties. In that state, the residual amount of silver is below 6 mg/kg.

In the TTC test, (figure 5-36) the antibacterial activity is related to amount of absorbance of formanzan which is directly proportional to the amount of living cell bacteria. The results were shown strong reduction of living cell bacteria due to presence silver nanoparticles on the surface of the fabrics before and after 3 cycles washing; these results are agreement with the results which were shown before.

6. Chapter 6: Summary and conclusion and recommendations for future work

6.1 Summary and conclusion

Modification of synthetic fibers specially, Poly (ethylene terephthalate) (PET) and polyamide-6 (PA 6) and production of high value- added products such as medical, healthcare and hygiene products has increased and renewed rapidly in the last years for antibacterial finishing of textile materials. There are a lot of functional materials that can give antibacterial properties, such as quaternary ammonium compounds (QACs) and silver nanoparticles (Ag NPs).

The photochemical reaction by UV irradiation of synthetic textile fibers is considered an important way to modify fabric surface properties without changing the bulk properties of the polymer matrix, and offer practical solutions and rapid reduction of the environmental problems as well as save time and reduce the cost of treatment processes.

To improve and change synthetic fibers surface properties and therefore to extend its applications for antibacterial applications using QACs as chemically bounded antibacterial agent , the surfaces of PET fibers were modified by UV photo-grafting of dimethylaminopropyl methacrylamide (DMAPMA), and graft yield increased with increasing irradiation time and monomer concentration. Grafting could be increased significantly by the use of benzophenone as photo-initiator. The maximum graft yield was of the order of 2 % without BP, and 20 % with the addition of 1 % BP. The graft yield showed a saturation behavior with regard to all parameters. In addition to grafting, the tertiary amino groups of the grafted PDMAPMA were quaternized with alkyl bromides of different chain lengths (C_6, C_8, C_{12} and C_{16}). The quaternization reaction had a high yield when bromides with shorter alkyl chain were employed. This is related to the steric effect, which prevents the approach of the reactive molecules to the tertiary groups on the fiber surfaces. The yield of quaternization was also proportional to the amount of grafted groups on the surface. Chemical and morphological changes for the modified PET fabrics were confirmed by ATP-FTIR, XPS and

SEM. The data of XPS summarized that after UV grafting of DMAPMA, the amount of C-O and C-N bonds is increased. On the other hand, the number of C-C and C-H of bonds is reduced. This is an indication for the complete coverage of the PET fibers with PDMAPMA. After quaternization of PDMAPMA with alkylbromides of different chain lengths, the amount of C-C and C-H increases again, and the amount of C-O and C-N decreases. This is an indication for the successful reaction between the tertiary amino group of PDMAPMA and the alkylbromide and therefore for covering the PDMAPMA with the alkyl chains of the alkylation reagent. It could be shown that the dyeability of PET with acid dye was significantly improved due to the established amino groups. These groups improve the affinity of the acidic dye due to ionic and polar interactions between positive charges on the grafted and quaternized fiber surfaces and the negative charge of the acidic dye. The amount of cationic charges of the PET-g-PDMAPMA and quaternized PET-g-PDMAPMA were increased with increasing nitrogen content

The antibacterial activity of the samples was characterized by evaluating the inhibition of the growth of *E. coli* bacteria. Visual inspection after incubation gave no evidence of an ‘inhibition zone around the fabric samples, this indicates that no diffusion or transfer of quaternary ammonium compounds (QACs) took place. A Visual inspection of the agar plate, after removal of the fabric samples, shows a lighter shade of the agar where the circular samples were removed indicating a reduction of bacteria density at theses places. Quantitative values of the antimicrobial activity against *E. coli* for the original PET, grafted PET-g-PDMAPMA and quaternized PET-g-PDMAPMA were measured by using o ASTM E2149-01 method. The ASTM E2149-01 test shows the highest effect for the samples quaternized with 1-bromohexane (C_6) and 1-bromooctane (C_8). An increase in the alkyl chain lengths of the quaternary ammonium groups of the PET-g-PDMAPMA appears to reduce the antibacterial effect again. This data is in agreement with previous results published. These observations prove the antimicrobial effect of the grafted and quaternized PET, but also based on the lack of inhibition zone the effective fixation of the QACs on the fiber surfaces. A

reason for this behavior might be seen in the effect of the alkyl chain lengths of the quaternary ammonium groups on the wetting properties of the PET fabrics. As could be established by contact angle measurements as well as drop penetration measurements, the originally hydrophobic PET fabric becomes increasingly hydrophilic following grafting and quaternization with 1-bromohexane (C_6) and 1-bromooctane (C_8). In contrast, quaternization with bromides with long alkyl chain, i.e. 1- bromododecane (C_{12}) and 1-bromohexadecane (C_{16}) increased the hydrophobicity of the fabrics.

Ag NPs have been found to exhibit interesting antibacterial activities. Due to high antibacterial properties of Ag NPs, they have been applied for various medical applications such as surgical products and wound dressings. The reduction of Ag^+ ions with low molecular weight of sodium salt of poly (methacrylic acid) (PMAA) as stabilizing agent were carried out by irradiation with UV light. This method of preparing stable silver nanoparticles is nontoxic, low-cost and easily applicable. The maximum absorption of Ag NPs was found to increase with irradiation time as the particle concentration and size grew. The results show that a size distribution of the Ag NPs has diameters ranging from 3 nm to 35 nm. More than 70% of the Ag NPs have a size smaller than 15 nm and no particles larger than about 35 nm. Ag NPs colloid is stable at pH values more than 6. The isoelectric point (IEP) has been observed at pH values of 3.5-4. Ag NPs solution showed good antibacterial activity with inhibition zone test. The minimum inhibitory concentration of silver nanoparticle (MIC) was $7x\ 10^{-7}$ mol/l

Ag NPs could be deposited on a textile fabric by applying the colloid in a simple finishing process. SEM images showed the Ag NPs to be well distributed on the surface of PET fibers finished with the silver colloid, and energy-dispersive X–ray spectroscopy (EDX) proved the chemical identity and gave some indication of the quantity of Ag NPs. Inductively coupled plasma optical emission spectrometry (ICP-OES) was used for quantitative assessment of the amount of deposited silver on finished PET fabrics. It was found that the amount of silver increased with UV exposure of the original $AgNO_3$ and PMAA solution and also with Ag^+ concentration. However, a saturation behavior was found. Laundering

durability of the silver nanoparticles on the PET fabric was evaluated by determination of the deposited amount of silver over five washing cycles in a laboratory dyeing machine. The data was shown that most of the silver nanoparticles were removed from the fabric after five times laundering, due to the adhesion of the silver nanoparticles is weak.

As we expected, the PET and PA 6 fabrics showed antibacterial activity after deposition of Ag NPs. The antibacterial activity was high when the amount of silver on the surface was approximately 3-5 mg/kg and higher.

A pre-treatment of synthetic fabrics by atmospheric air plasma was found to increase the wettability of the fabrics, the carboxyl content on PET fiber surface, determined by methylene blue method, increased linearly with the plasma dose. The plasma treatment did not increase significantly the adhesion of the particles and the laundering stability of the finish. The textile fabrics showed antibacterial activity after deposition of Ag NPs. The antibacterial activity was high after pre-treatment of synthetic fabrics by atmospheric air plasma when the amount of silver on the surface was approximately 3-5 mg/kg and higher.

From above mentioned we could conclude that the antibacterial properties of the modified PET were observed by qualitative and quantitative methods. The antimicrobial effect of the grafted and quaternized PET was found highest for the samples quaternized with 1-bromohexane (C_6) and 1-bromooctane (C_8). In general, it is not strong like Ag NPs antibacterial efficiency. An increase in the alkyl chain lengths of the quaternary ammonium groups of the PET-g-PDMAPMA reduced the antibacterial effect again. The lack of inhibition zone around the fabric samples indicates the effective fixation of the QAGs on the fiber surfaces (as chemically bound antibacterial agents). While the textile (PET and PA 6) fabrics showed higher antibacterial efficiency after deposition of Ag NPs than quaternized PET fabrics with QAGs. Ag NPs were removed by laundering, which indicates weak adhesion on the surfaces PET and Pa 6 (as leaching antibacterial agents) even after pretreated with plasma to improve the wettability of the fabrics. The antibacterial activity was high when the amount of silver on the surface was approximately 5-3 mg/kg and higher.

6.2 Recommendations for future work

In this work, surface modification of synthetic fibers for antibacterial activity, have been studied. Through this studies, a great deal was gained into understanding photochemical reaction of DMAPMA on the surface of PET, Which gives promise to introduce this treatment or this photochemical reaction in the finishing processes for synthetic fibers. Future working may include photochemical reaction of DMAPMA on the surface of polyamide-6 to achieve antibacterial properties on the PA 6 surface. Also future working may include a series of active monomers on various synthetic fibers to achieve desirable properties on the surface.

Ag NPs were prepared by a simple, inexpensive and single step synthesis based on UV activation of a solution of silver nitrate and poly (methacrylic acid). This method of preparing silver nanoparticles is nontoxic, low-cost and easily applicable, which give promise to produce Ag NPs in large scale. Further study may be understanding mechanism of Ag nanoparticles formation and physical properties. Future working may include various stabilizer agents to get Ag NPs stable and combine with other metal oxides such as zinc oxide (ZnO) or titanium dioxide (TiO_2).

A pre-treatment of synthetic fabrics by atmospheric air plasma was found to increase the wettability of the fabrics. The plasma treatment did not increase significantly the adhesion of the particles and the laundering stability of the finishing with Ag NPs colloid. Future working may include using various cross-linkers to increase stability and adhesion of Ag NPs on the surface substances.

Also further studying may be the effect of the grafting of DMAPMA and quaternization reaction with alkyl groups via photochemical reaction, on the adsorption of Ag NPs synthesized by photochemical reduction on the synthetic fibers such as PET and PA 6.

7. Chapter 7: References

1. Cloete, T. E. “Resistance mechanisms of bacteria to antimicrobial compounds”, *International Biodeterioration and Biodegradation*, **2003,** 51, 277-282.
2. http://www.typesofbacteria.co.uk/what-are-bacteria.html
3. http://www.usifi.com/pdf/AKC_Outlook_**2011**.pdf
4. Neely, A. N; Orloff, M. M. Survival of Some Medically Important Fungi on Hospital Fabrics and Plastics. *Journal of Clinical Microbiol.* **2001**, 39,3360.
5. Schindler, W. D; Hauser, P. J. *“Chemical Finishing of Textiles”,* Woodhead Publishing Ltd, Cambridge, 2004.
6. Vigo, T. L. *Protection of Textiles from Biological Attack, In “Functional* Finishes, Part A, Chemical Processing of Fibres and Fabrics, Handbook of Fiber Science and Technology, Volume II”, Sello, S. B. (Ed.), Marcel Dekker, Inc., New York,**1983**, 367–426.
7. Bahners, T; Milster, M; Opwis, K; Wego A; Schollmeyer, E. Photo-chemical Surface modification for the control of cell growth on textile substrates. Polymer surface Modification: Relevance to Adhesion Vol 5, K.L. Mittal (Ed.), **2009**, 107-124, Brill, Leiden.
8. Gao, S. L; Häßler, R; Mäder, E; Bahners, T; Opwis, K; Schollmeyer, E. Photochemical surface modification of PET by excimer UV lamp irradiation, *Appl. Phys. B,* **2005**, 81, 681-690.
9. Spadaro D.; Barletta E.; Barreca F.; Curro` G.; Neri F. PMA capped silver nanoparticles produced by UV-enhanced chemical process ; *Appl. Surf. Sci.*, **2009,** 255, 8403–8408.
10. Falletta E., Bonini M., Fratini E., Nostro A. L., Pesavento G., Becheri A., Nostro P. L.; Canton P.; Baglioni P. Clusters of Poly(acrylates) and Silver Nanoparticles: Structure and Applications for Antimicrobial Fabrics; *J. Phys. Chem. C*, **2008***,* 112, 11758–11766.

11. Henglein A. Colloidal Silver Nanoparticles: Photochemical Preparation and Interaction with O_2, CCl_4, and Some Metal Ions; *Chem. Mater.* , **1998***,* 10, 444-450.
12. Zhang J. G.; Xu S. Q.; Kumacheva E. Photogeneration of Fluorescent Silver Nanoclusters in Polymer Microgels. *Adv. Mater.* , **2005***,* 17, 2336.
13. Maja, R.; Vesna, I.; Vesna, V.; Suzana, D.; Petar, J.; Zoran, S.; Jovan, M. N. Antibacterial effect of silver nanoparticles deposited on corona-treated polyester and polyamide fabrics. *Polym. Adv. Technol*., **2008**, 19, 1816–1821.
14. McDonnell, G; Russell, A.D. Antiseptics and disinfectants: activity, action and resistance. *Clinical Microbiology Reviews*, **1999***,* 12, 147–179.
15. Chen, J. C.; Yeh, J. T.; Chen, C. C. Crosslinking of cotton cellulose in the presence of alkyl diallyl ammonium salts. I. Physical properties and agent distribution. *J. Appl. Polym. Sci*., **2003**, 90, 1662-1669.
16. Seong, H.-S.; Whang, H.-S.; Ko, S.-W. Synthesis of a quaternary ammonium derivative of chito-oligosaccharide as antimicrobial agent for cellulosic fibers. *J. Appl. Polym. Sci.*, **2000***,* 76, 2009-2015.
17. Kenawy, E. R.; Abdel-Hay, F. I.; El-Shanshoury, A.; El-Newehy, M. H. Biologically active polymers. V. Synthesis and antimicrobial activity of modified poly(glycidyl methacrylate-*co*-2-hydroxyethyl methacrylate) derivatives with quaternary ammonium and phosphonium salts. *J. Polym. Sci. Part A: Polym. Chem.*, **2002***,* 40, 2384-2393.
18. Kim, J. Y.; Lee, J. K.; Lee, T.S.; Park, W. H. Synthesis of chitooligosaccharide derivative with quaternary ammonium group and its antimicrobial activity against Streptococcus mutans. *Int. J. Biol. Macromol.* , **2003,** 32, 23-7.
19. Thorsteinsson, T., Masson, M., Kristinsson, K. G., Hjalmarsdottir, M. A., Hilmarsson, H. and Loftsson, T. “Soft Antimicrobial Agents: Synthesis and Activity of Labile Environmentally Friendly Long Chain Quaternary Ammonium Compounds” *J. Med. Chem.*, **2003***,* 46*,* 4173-4181.

20. Sauvet, G.; Dupond, S.; Kazmierski, K.; Chojnowski, J. Biocidal polymers active by contact. V. Synthesis of polysiloxanes with biocidal activity. *J. Appl. Polym. Sci.*, **2000**, 75, 1005– 1012.
21. Goodson, B.; Ehrhardt, A.; Ng, S.; Nuss, J.; Johnson, K.; Giedlin, M.; Yamamoto, R.; Moos, W. H.; Krebber, A.; Ladner, M.; Giacona, M. B.; Vitt, C.; Winter, J. Characterization of Novel Antimicrobial Peptoids. *Antimicrob. Agents Chemother,* **1999***,* 43, 1429–1434.
22. Franklin, T. J.; Snow, G. A. *Biochemistry of Antimicrobial Action; Chapman and Hall: London,* **1981**.
23. Gilbert, P.; and Moore, L. E. Cationic Antiseptics: Diversity of Action under a Common Epithet, *J. Appl. Microbiol.* , **2005**, 99, 703–715.
24. Purwar, R.; Joshi, M. Recent Developments in Antimicrobial Finishing of Textiles – A review, *AATCC Rev.* , **2004**, **4**, 22–26.
25. Murguia, M. C.; Machuca, L. M.; Lura, M. C.; Cabrera M. I.; Grau, R. J. Synthesis and Properties of Novel AntifungalGemini Compounds Derived from N-Acetyl Diethanolamines, *J. Surfactants Deterg*., **2008**, **11**, 223–230.
26. Son, Y. ; Sun, G. “Durable Antimicrobial Nylon 66 Fabric: Ionic Interactions with Quaternary Ammonium Salts”, *J. Appl. Polym. Sci.*, **2003,** 90, 2194-2199.
27. Lu, G.; Wu, D.; Fu, R. Studies on the Synthesis and Antibacterial Activities of Polymeric Quaternary Ammonium Salts from Dimethylaminoethyl Methacrylate, *React. Funct. Polym.* , **2007***,* 67, 355–366.
28. Owusu, K.; Guymon, C. A. Photopolymerization Kinetics of Poly(acrylate)–clay Composites Using Polymerizable Surfactants, *Polymer*, **2008,** 49, 2636–2643.

29. Roy, D.; Knapp J. S.; Guthrie, J. T.; Sébastien Perrier, S.; Antibacterial Cellulose Fiber via RAFT Surface Graft Polymerization. *Biomacromolecules*, **2008***,* 9*,* 91–99.

30. Marini, M.; Bondi, M.; Iseppi, R.; Toselli, M.; Pilati, F. Preparation and Antibacterial Activity of Hybrid Materials Containing Quaternary Ammonium Salts via Sol-Gel Process, *Eur. Polym. J.*, **2007***,* 43, 3621–3628.

31. Nalwa H. S. (ed.), "Handbook of Organic–Inorganic Hybrid Materials and Nanocomposites", American Scientific Publisher, Stevenson Ranch, **2003**.

32. Tomši, B.; Simoni, B. Antimicrobial Activity of 3-(trimethoxysilyl)-propyldimethylalkilamonium Chloride, *Tekstilec*, **2005**, **48**, 79–87.

33. Li, Z.; Lee, D.; Sheng, X.; Cohen, R. E.; Rubner, M. F. Two-Level Antibacterial Coating with Both Release-Killing and Contact Killing Capabilities, *Langmuir*, **2006**, **22**, 9820–9823.

34. Ma, M.; Sun, Y.; Sun, G. Antimicrobial Cationic Dyes. Part 1: Synthesis and Characterization, *Dyes Pigm.* , **2003***,* **58**, 27–35.

35. Liu, S.; Ma, J.; Zhao, D. Synthesis and Characterization of Cationic Monoazo Dyes Incorporating Quaternary Ammonium Salts, *Dyes Pigm.* , **2007**, **75**, 255–262.

36. Liu, J.; Sun, G. The Synthesis of Novel Cationic Anthraquinone Dyes with High Potent Antimicrobial Activity, *Dyes Pigm.* , **2008***,* **77**, 380–386.

37. Kim, Y. H.; G. Sun, G. "Durable Antimicrobial Finishing of Nylon Fabrics with Acid Dyes and a Quaternary Ammonium Salt", *Textile Research Journal*, **2001**, 71: 4, 318-323.

38. Kim Y. H.; Sun, G. "Dye Molecules as Bridges for Functional Modifications of Nylon: Antimicrobial Functions" *Textile Research Journal*, **2000**, 70: 8, 728-733.

39. Ionpure Report, Why Inorganic? http://marubenisunnyvala.com/anti_bacterial)additives_ionpure.html.

40. Lee, H. J.; Jeong, S. H. Bacteriostasis of Nanosized Colloidal Silver on Polyester Nonwovens *Textile Research Journal*, **2004***,* 74, 5.

41. Morones, J. R.; Elechiguerra, J. L.; Camacho, A.; Holt K.; Kouri, J. B.; Ramirez J. T.; Yacaman, M. J. The Bactericidal Effect of Silver Nanoparticles, *Nanotechnology*, **2005**, 16, 2346–2353.

42. Lok, C. N.; Ho, C. M.; Chen, R.; He, Q. Y.; Yu, W. Y.; Sun, H. Z.; Tam, P. K. H.; Chiu, J. F.; Che, C. M. Proteomic Analysis of the Mode of Antibacterial Action of Silver Nanoparticles *J. Proteome Res*., **2006**, 5, 916–924.

43. Dastjerdi, R.; Montazer, M. A review on the application of inorganic nanostructured materials in the modification of textiles: Focus on antimicrobial properties Colloids and Surfaces B: Biointerfaces*, **2010***, *79 5–18.*

44. Aruoja, V.; Dubourguier, H. C.; Kasemets, K.; Kahru, A. Toxicity of Nanoplarticles of CuO, ZnO and TiO2 to Microalgae *Pseudokirchneriella subcapitata*, *Sci. Total Environ*. , **2009**, 407, 1461–1468.

45. Dahl, J. A.; Maddux, B. L. S.; Hutchison, J. E. Toward Greener Nanosynthesis, *Chem. Rev*., **2007**, 107, 2228–2269.

46. Hu, B.; Wang, S. B.; Zhang, M.; Yu, S. H. Microwave- Assisted Rapid Facile “Green” Synthesis of Uniform Silver Nanoparticles: Self-Assembly Into Multilayered Films and Their Optical Properties, *J. Phys. Chem. C*, **2008**., 112, 11169–11174.

47. Sharma, V. K.; Yngard, R. A.; Lin, Y. Silver Nanoparticles: Green Synthesis and Their Antimicrobial Activities, *Adv. Colloid Interface Sci*. , **2009**, 145, 83 96.

48. Ramirez, M. I.; Bashir, S.; Luo, Z.; Liu, J.L. Green Synthesis and Characterization of Polymer-Stabilized Silver Nanoparticles, *Colloids Surf. B*, **2009**, 73, 185–191.

49. Balantrapu, K; Goia, D. V. Silver nanoparticles for printable electronics and biological applications *Journal of Materials Research*, **2009**, 24, 9, 2828-2836

50. Tripathi, R. M; Saxena, A; Gupta, N; Kapoor, H; Singh, R.P. *Digest journal of nanomaterials and Biostrucutres* **2010**, 5, 2.

51. Lee, P. C.; Meisel, D. Adsorption and Surface-Enhanced Raman of Dyes on Silver and Gold Sols. *J. Phys. Chem.* **1982**, 86, 339.

52. Wu, X.; Redmond, P.L.; Liu, H.; Chen, Y.; Steigerwald, M.; Brus, L. Photovoltage mechanism for Room Light Conversion of Citrate Stabilized Silver Nanocrystal Seeds to Large Nanoprisms. *J. Am. Chem. Soc*. **2008**, 130, 9500–9506

53. Xia, Y; Xiong, Y; Lim, B; Skrabalak, S.E. Shape-controlled synthesis of metal nanocrystals: simple chemistry meets complex physics? *Angew. Chem. Int. Ed. Engl.* **2009**, 48, 1, 60-103.

54. Brust, M; Walker, M; Bethell, D; Schiffrin, D. J; Whyman, R. Synthesis of thiolderivatizedgold nanoparticlesin a 2-phase liquid-liquid system. *J. Chem. Soc. Chem. Commun.* **1994**, 801–802.

55. Balan, L; Burget, D. synthesis of metal / polymer nanocomposite by uv radiation curing. *Eur. Polym. J.* **2006**, 42, 3180-3189.

56. Yuranova, T.; Rincon, A. G.; Bozzi, A.; Parra, S.; Pulgarin, C.; Albers P.; Kiwi, J. "Antibacterial Textiles Prepared by RF-Plasma and Vacuum-UV Mediated Deposition of Silver", *Journal of Photochemistry and Photobiology, A: Chemistry*, **2003**, 161: 1, 27-34.

57. Maja, R.; Vesna, I.; Vesna, V.; Suzana, D.; Petar, J.; Zoran, S.; Jovan, M. N. Antibacterial effect of silver nanoparticles deposited on corona-treated polyester and polyamide fabrics, *Polym. Adv. Technol.*, **2008***,* 19 1816–1821.

58. Ilić, V.; Šaponjić, Z.; Vodnik, V.; Molina, R.; Dimitrijević, S.; Jovančić, P.; Nedeljković, J. M.; Radetić, M. Antifungal efficiency of corona pretreated polyester and polyamide fabrics loaded with Ag nanoparticles *J. Mater. Sci.*, **2009***.* 44, 3983–3990.

59. Ilić, V.; Šaponjić, Z.; Vodnik, V.; Lazović, S.; Dimitrijević, S.; Jovančić, P.; Nedeljković J.M.; Radetić, M.Bactericidal Efficiency of Silver Nanoparticles Deposited onto Radio Frequency Plasma Pretreated Polyester Fabrics. *Ind. Eng. Chem. Res.*, **2010***, 49,* 7287–7293.

60. Gorensek, M.; Gorjanc, M.; Bukosek, V.; Kovac, J.; Jovancic, P.; Mihailovic, D. Functionalization of PET Fabrics by Corona and Nano Silver *Textile Research Journal*, **2010***,* 80: 253.

61. Zhao, G. J; Stevens S. E. Multiple parameters for the comprehensive evaluation of the susceptibility of Escherichia coli to the silver ion. *Biometals* **1998**, 11, 27–32

62. Rai, M; Yadav, A; Gade, A. Silver nanoparticles as a new generation of microbials. *Biotechnol. Adv.* **2009**, 27, 76–83

63. Ahearn, D. G; May, L. L; Gabriel, M. M. Adherence of organisms to silver-coated surfaces. *J. Ind. Microbiol*. **1995**, 15, 372–376

64. Lok, C.N; Ho, C.M; Chen, R; He, Q. Y; Yu, W. Y; Sun, H; Tam, P.K; Chiu, J.F; Chen, C. M. (2006) Proteomic analysis of the mode of antibacterial action of silver nanoparticles. *J. Proteome. Res.* **2006**, 5, 916–924

65. Mastsumure, Y.; Yoshikata, K; Kunisaki, S. I; Tsuchido. T.. Mode of bactericidal action of silver zeolite and its comparison with that of silver nitrate. *Appl. Environ. Microbiol*. **2003**, 169, 4278–4281.

66. Aysin D. E.; Gulay O.; Mikael S. Antibacterial activity of PA6/ZnO nanocomposite fibers *Textile Research Journal*, **2011,** 81, 1638.

67. Matsumura, Y.; Yoshikata, K.; Kunisaki, S.; Tsuchido, T. Made of Bactericidal Action of Silver Zeolite and Its Comparison with that of Silver Nitrate, *Appl. Environ. Microb*. , **2003**, 69, 4278–4281.

68. Thomas, V.; Yallapu, M. M.; Sreedhar, B.; Bajpai, S. K. A Versatile Strategy to Fabricate Hydrogel-Silver Nanocomposites and Investigation of Their Antimicrobial Activity, *J. Coll. Interfac. Sci.*, **2007**, 315, 389–395.

69. Vimala, K.; Samba, S. K.; Murali, M. Y.; Sreedhar, B.; Mohana R. K. Controlled Silver Nanoparticles Synthesis in Semi-Hydrogel Networks of Poly(acrylamide) and Carbohydrates: A Rational Methodology for Antibacterial Application, *Carbohydr. Polym*. , **2009**, 75, 463–471.

70. Jeon, H. J.; Yi, S. C.; Oh, S. G. Preparation and Antibacterial Effects of Ag-SiO2 Thin Films by Sol–Gel Method, *Biomaterials*, **2003**, 24, 4921–4928.

71. Kim, Y. H.; Lee, D. K.; Cha, H. G.; Kim, C. W.; Kang, Y. S., Synthesis and Characterization of Antibacterial Ag-SiO2 Nanocomposite, *J. Phys. Chem. C*, **2007**, 111, 3629–3635.

72. Mahltig, B.; Gutmann, E.; Meyer, D. C.; Reibold, M.; Bund A.; Böttcher, H. Thermal Preparation and Stabilization of Crystalline Silver Particles in SiO2-based Coating Solutions, *J. Sol–Gel Sci. Technol*., **2009,** 49, 202–208.

73. Tomši, B; Orel, B; Jovanovski, V; Jerman, I; Simoni,. B. Bacterial Growth Reduction on Cotton Fabrics Treated by Titanium Isopropoxide/ Aminopropyltriethoxy Silane, in: “Magic World of Textiles: Book of Proceedings”, Dragčević, Z. (Ed.), Faculty of Textile Technology, University of Zagreb, Zagreb, **2008**, pp. 465–470.

74. Li, Z., Lee, D., Sheng, X., Cohen, R. E., and Rubner, M. F., Two-Level Antibacterial Coating with Both Release-Killing and Contact Killing Capabilities, *Langmuir*, **2006**, 22, 9820–9823.

75. Dastjerdi, R.; Mojtahedi, M.R.M.; Shoshtari, A.M. Investigating the effect of various blend ratios of prepared masterbatch containing Ag/TiO2 nanocomposite on the properties of bioactive continuous filament yarns, *Fibers and Polymers*, **2008**, 9, 6, 727–734.

76. Mihailović, D.; Šaponjić, Z.; Vodnik, V.; Potkonjak, B.; Jovančić, P.; Jovan M.; Nedeljković, M. R. Multifunctional PES fabrics modified with colloidal Ag and TiO2 nanoparticles Polymers for Advanced Technologies, **2011**, 22: 12, 2244–2249.

77. Sun, G.; Chen, T. Y.; Wheatley, W. B.; Worley, S. D. Preparation of Novel Biocidal N-Halamine Polymers, *J. Bioact. Compat. Polym*., **1995**, 10, 135–144.

78. Sun, G.; Xu, X. "Durable and Regenerable Antibacterial Finishing of Fabrics: Biocidal Properties", *Text. Chem. Colorist*, **1998**, 30, 26-30.

79. Williams, D. E.; Swango, L. J.; Wilt G. R.; Worley, S. D. "Effect of Organic *N*-halamines on Selected Membrane Functions in Intact Staphylococcus Aureus Cells", *Appl. Environ. Microbiol.* , **1991,** 54, 1121-1127.

80. Barnes, K.; Liang, J.; Wu, R.; Worley, S. D.; Lee, J.; Broughton, R. M.; Huang, T. S. Synthesis and Antimicrobial Applications of 5,50-ethylenebis[5-methyl-3-(3-triethoxysilylpropyl) hydantoin], *Biomaterials*, **2006**, 27, 4825–4830.

81. Lin, J.; Cammarata, V.; Worley, S. D. Infrared Characterization of Biocidal Nylon, *Polymer*, **2001,** 42, 7903–7906.

82. Ren, X.; Kocer, H. B.; Kou, L.; Worley, S. D.; Broughton, R. M.; Tzou, Y. M.; Huang, T. S. Antimicrobial Polyester, *J. Appl. Polym. Sci*., **2008**, 109, 2756–2761.

83. Lin, J.; Winkelmann, C.; Worley S. D.; Kim, J.; Wei, C-I.; Cho, U.; Broughton, R. M.; Santiago J. I.; Williams, J. F. "Biocidal polyester", *Journal of Applied Polymer Science*, **2002***,* 85: 1, 177-182.

84. Sun Y.; Sun, G. "Novel Regenerable *N*-halamine Polymeric Biocides. III. Grafting Hydantoin-Containing Monomers onto Synthetic Fabrics", *Journal of Applied Polymer Science*, **2001**, 81: 6, 1517-1525.

85. Lin, J.; Winkelman, C.; Worley, S. D.; Broughton R. M.; Williams, J. F. "Antimicrobial Treatment of Nylon", *Journal of Applied Polymer Science*, **2001**, 81: 4, 943-947.

86. Lim, S. H.; Hudson, S. M., Review of Chitosan and its Derivatives as Antimicrobial Agents and Their Uses as Textile Chemicals. *J. Macromol. Sci., Polym. Rev.*, C, **2003,** 43, 223–269.

87. Chang, Y.-B.; Tu, P.-T.; Wu, M.-W.; Hsueh, T.-H.; Hsu, S.-H. A Study on Chitosan Modification of Polyester Fabrics by Atmospheric Pressure Plasma and Its Antibacterial Effects *Fibers and Polymers*, **2008,** 9: 3, 307-311.

88. Lim, S. H.; Hudson, S. M. Synthesis and Antimicrobial Activity of a Water-Soluble Chitosan Derivative with a Fiber- Reactive Group, *Carbohydr. Res*, **2004***,* 339, 313–319.

89. Krebs, F. C.; Miller, S. R.; Ferguson, M. L.; Labib, M.; Rando, R. F.; Wigdahl, B. Polybiguanides, Particularly Polyethylene Hexamethylene Biguanide, Have Activity Against Human Immunodeficiency Virus Type 1, *Biomed. Pharmacother.* , **2005,** 59, 438–445.

90. Moore, K.; Gray, D. Using PHMB Antimicrobial to Prevent Wound Infection, Wounds UK, **2007**, 3, 96–102.

91. Orhan, M.; Kut, D.; Gunesoglu, C. Improving the Antibacterial Property of Polyethylene Terephthalate by Cold Plasma Treatment Plasma Chem *Plasma Process*, **2012,** 32, 293–304.

92. Abo El-Ola, S. M. Recent Developments in Finishing of Synthetic Fibers for Medical Applications- *Review Designed Monomers and Polymers, **2008,** 11, 483–533.*

93. Abo El-Ola, S M. New Approach for Imparting Antimicrobial Properties for Polyamide and Wool Containing Fabrics, *Polymer-Plastics Technology and Engineering*, **2007***,* 46: 9, 831-839.

94. Aggarwal, P.; Phaneuf, M. D.; Bide, M.; Sousa K. A.; LoGerfo, F. W. Development of an infection-resistant bifunctionalized Dacron biomaterial. *J. Biomed. Mater. Res.* A, **2005,** 75, 224.

95. Parekh, N.; Maheria, K. Studies on Antimicrobial Activity for Multidrug Resistance Strain by Using Phenyl Pyrazolones Substituted 3-(4-Aminophenyl)-2-phenylquinazolin-4(3h)- one Derivatives in vitro Condition and their Dyeing Performance *Fibers and Polymers* , **2012,**13: 2, 162-168.

96. Bide, M.; Choi, H.; Phaneuf, M.; Quist W.; LoGerfo, F. in: *Medical Textile and Biomaterials for Healthcare*, S. C. Anand, J. F. Kennedy, M. Miraftab and S. Rajendroon (Eds) , **2006**, p. 136. Woodhead, Cambridge.

97. Cowan, M. M. Plant Products as Antimicrobial Agents, *Clin. Microbiol. Rev.*, **1999**, 12, 564–582.

98. Holme, I. Finishes for Protective and Military Textiles, *International Dyer*, **2005**, 190, 9–11.

99. Son, Y. A.; Kim, B. S.; Ravikumar, K.; Kim, T. K. Berberine Finishing for Developing Antimicrobial Nylon 66 Fibers: Exhaustion, Colorimetric Analysis, Antimicrobial Study, and Empirical Modeling, *J. Appl. Polym. Sci.*, **2007**, 103, 1175 1182.

100. Gupta, D.; Khare, S. K.; and Laha, A. Antimicrobial Properties of Natural Dyes Against Gram-Negative Bacteria. *Color. Technol*., **2004**, 120, 167–171.

101. Joshi, M.; Ali, S. W.; Rajendran, S. Antibacterial Finishing of Polyester/Cotton Blend Fabrics Using Neem (*Azadirachta indica*): A Natural Bioactive Agent. *J. Appl. Polym. Sci.*, **2007**, 106, 793–800.

102. Haufe, H.; Muschter, K.; Siegert, J.; Böttcher, H. Bioactive Textiles by Sol–Gel Immobilized Natural Active Agents, *J Sol–Gel Sci Technol*, **2008**, 45, 97–101.

103. Boh, B.; and Knez, E. Microencapsulation of Essential Oils and Phase Change Materials for Applications in Textile Products. *Indian J. Fibre Text. Res.*, **2006**, 31, 72–82.

104. Thilagavathi, G.; Bala, S. K.; Kannaian, T. Microencapsulation of Herbal Extracts for Microbial Resistance in Healthcare Textiles. *Indian J. Fibre Text. Res.*, **2007**, 32, 351–354.

105. Simons, C.; Walsh, S. E.; Maillard J.-Y. "A note: Ortho-phthalaldehyde: proposed mechanism of action of a new antimicrobial agent. *Letters in Applied Microbiology*, **2000***,* 31, 299-302.

106. Block, S. S. *Disinfection, Sterilization and Preservation* (3th ed.), Philadelphia: Lea & Febiger, **1983**, 225-239.

107. Weavers L. K.; Wickramanayake, G. B. Disinfection and sterilization using ozone. In *Disinfection, Sterilization and Preservation,* 5th edn (S. S. Block., Ed.) **2001**, pp. 205-214. Lippincott Williams & Wilkins, Philadelphia, USA.

108. Griebe, T.; Chen, C.-I.; Srinivasan, R.; Geesy G. G.; Stewart, P. S. *Analysis of biofilm disinfection by monochloramine and free chlorine*, **1994**, pp. 151-161. In Proceedings of the Center for Biofilm Engineering, Montana State University, Bozeman.

109. Green, D. E.; Stumpf, P. K. "The mode of action of chlorine", *J. Am. Water Works Assoc*., **1946**, 38, 1301-1305.

110. Bellar, T. A.; Lichtenberg, J. J.; Kroner, R. C. "Occurrence of organohalides in chlorinated drinking waters", *J. Am. Water Works Assoc*., **1974**, 66: 12, 703-706.

111. Retrieved from: http://www.science.uwaterloo.ca/~cchieh/cact/c120/bondel.html, February 2, **2009**.

112. Bahners, T; Textor T; Schollmeyer, E. in: Polymer Surface Modification: Relevance to Adhesion, K. L. Mittal (Ed.) **2004**, 3, 97–124. VSP, Utrecht.

113. Bahners, T; Klingelhöller, K; Ulbricht, M; Wego, A; Schollmeyer, E. "Photo-chemical surface modification for the control of protein adsorption on textile substrates*", J. Adhes. Sci. Technol*, **2011***.* 25, 2219–2238.

114. Rånby, B. photochemical modification of polymer photovrosslinking, surface photografting and lamination. *Polymer Engineering and Science*, **1998***,* 38: 8, 1229.

115. Huang, W; Jang J. Hydrophilic modification of PET fabric via continuous photografting of acrylic acid (AA) and hydroxyehtyl methacrylate (HEMA). Fibers and Polymers **2009**, 10, 1, 27-33.

116. Gupta, D; Siddhan, P; Banerjee, A. Basic dyeable polyester: a new approach using a VUV excimer lamp Source. *Coloration Technology,* **2007**, 123, 4, 248-251.

117. Opwis, K; Wego, A; Bahners, T; Schollmeyer, E. Permanent flameretardantfinishing of textile materials by a photochemical immobilization of vinyl phosphonic acid. *Polymer Degradation and Stability.* 2011, 96, 3, 393–395.

118. Praschak, D; Bahners, T; Schollmeyer, E. PET surface modifications by treatment with monochromatic excimer UV lamps, *Appl. Phys. A: Mater. Sci. Process.* **1998**, 66, 69–75.

119. K. Opwis, T. Bahners, E. Schollmeyer, A. Geschewski, H. Thomas, H. Höcker,Tiefenwirkung physikalischer Verfahren zur Modifizierung textiler Substrate. *Technische Textilien* **2002**, 45, 215-217.

120. Praschak, D; Bahners, T; Schollmeyer, E. Excimer UV lamp irradiation induced grafting on synthetic polymers. *Appl. Phys.* ***2000****, A* 71, 577-581.

121. K. Opwis, T. Bahners, E. Schollmeyer, Improvement of the alkali-restistance of poly(ethylene terephthalate) by a photochemical modification using excimer-UV-lamps. *Chemical Fibers*. **2004**, 54, 116-119.

122. Zhengmao, Z.; Kelley, M. Poly(ethylene terephthalate) surface modification by deep UV (172 nm) irradiation. *Appl. Surf. Sci.* **2004**, 236, 416.

123. Chan, C.-M. Polymer Surface Modification and Characterization. Hanser Publishers, Munich. 4quantum mechanics equation and reference, **1994**.

124. Uchida E, Ikada Y. Introduction of Quaternary Amines Onto a Film Surface by Graft-Polymerization. *Journal of Applied Polymer Science*, **1996**, 61: 8, 1365-1373.

125. Wirsén, A; Sun, H: Albertsson, A.C. Solvent-free vapor-phase photografting of acrylamide onto poly(ethylene terephthalate). *Biomacromolecules*, **2005***,* 6, 2697 -2702.

126. Kim, E.M; Min, B.G; Jang, J. Reactive dyeing of meta-aramid fabrics photografted with dimethylaminopropyl methacrylamide . *Fibers and Polymers*, **2011,** *1*2, 580–586.

127. Dong, Y; Lyoo, W.S; Jang, J. Union dyeing of the photografted PET/wool blend fabrics with dimethylaminopropyl methacrylamide . *Fibers and Polymers*, **2010,** 11, 213–217.

128. Roth, J.R. Industrial Plasma Engineering, Principles, Vol. 1, (Bristol: Institute of Physics Publishing), Philadelphia, **1995**, ISBN 0-7503-0318-2.

129. Thorsen, W.; Landwehr; R. A Corona Discharge Method of Producing Shrink- Resistant Wool and Mohair, Part III: A Pilot-Scale Top Treatment Reactor. *Textile Research Journal*, **1970**, 40: 8, 688-695.

130. Roth; J. Industrial Plasma Engineering, Volume II, Applications to Nonthermal Plasma Processing, (Bristol: Institute of Physics Publishing), Philadelphia, **2001**, ISBN 0- 7503-0545-2.

131. Inagaki, N.; Tasaka, S.; Narushima K.; Teranishi. K. Surface Modification of Poly (tetrafluoroethylene) with Pulsed Hydrogen Plasma. *Journal of Applied Polymer Science*, **2002**, 83, 340-348.

132. Inagaki, N. Plasma Surface Modification and Plasma Polymerization. Lancaster, Pennsylvania: **1996,** Pub. Co., Inc.

133. Zubaidi, Hirotsu, T. Graft Polymerization of Hydrophilic Monomers onto Textile Fibers Treated by Glow Discharge Plasma. *Journal of Applied Polymer Science*, **1996**, 61, 1579-1584.

134. Wilken, R.; Hollander A.; Behnisch. J. Surface Radical Analysis on Plasma-treated Polymers. *Surface and Coatings Technology*, **1999**, 116-119, 991-995.

135. Friedrich, J.; Loeschcke, I.; Frommelt, H.; Reiner, H.; Zimmermann H.; Lutgen. P. Ageing and Degradation of Poly (ethylene terephthalate) in an Oxygen Plasma. *Polymer Degradation and Stability*, **1991**, 31, 97-114.

136. Hollander, A.; Wilken R.; Behnisch. J. Subsurface Chemistry in the Plasma Treatment of Polymers. *Surface and Coatings Technology*, **1999,** 116-119, 788-791.

137. Öteyaka, M. Ö.; Chevallier, P. ; Turgeon, S. ; Robitaille , L.; Laroche G. Low Pressure Radio Frequency Ammonia Plasma Surface Modification on Poly (ethylene terephthalate) Films and Fibers: Effect of the Polymer Forming Process. *Plasma Chem. Plasma Process*, **2012**, 32, 17–33.

138. Ferrante, D.; Iannace S.; Monetta. T. Mechanical Strength of Cold Plasma Treated PET Fibers. *Journal of Materials Science*, **1999**, 34, 175-179.

139. Gupta, B.; Hilborn, J.; Hollenstein, C.; Plummer, J.; Houriet, R.; Xanthopoulos, N. Surface Modification of Polyester Films by RF Plasma. *Journal of Applied Polymer Science*, **2000**, 78, 1083-1091.

140. Gouveia, I. C.; Antunes, L. C.; Gomes, A. P. Low - pressure plasma treatment for hydrophilization of poly (ethylene terephthalate) fabrics. *Journal of the Textile Institute*, **2011**, 102: 3, 203-213.

141. Cireli, A.; Kutlu, B.; Mutlu, M. Surface modification of polyester and polyamide fabrics by low frequency plasma polymerization of acrylic acid. *Journal of Applied Polymer Science, **2007**, 104: 4, 2318–2322.*

142. Inagaki, N.; Yasukawa, Y. Improvement of Wicking Property of PET Fabrics by Plasma Polymerization of Nitro Compounds. *Sen'i Gakkaishi*, **1988**, 44, 333-338.

143. Gawish, S. M.; Ramadan, A. M.; Matthews S. R.; Bourham, M. A. Modification of PA6,6 by Atmospheric Plasma and Grafting 2-hydroxy ethyl methacrylate (HEMA) to Improve Fabric Properties. *Polymer-Plastics Technology and Engineering, **2008**, 47:5, 473-478.*

144. Bhat, J. N.; Benjamin, Y. Surface Resistivity Behavior of Plasma Treated and Plasma Grafted Cotton and Polyester Fabrics. *Textile Research Journal*, **1999**, 69, 38-42.

145. Kamel, M.M.; El Zawahry, M.M.; Helmy H.; Eid M.A. Improvements in the dyeability of polyester fabrics by atmospheric pressure oxygen plasma treatment, *Journal of The Textile Institute*, **2011***,* 102:3, 220-231.

146. Wakida, T.; Cho, S.; Choi, S.; Tokino, S.; Lee, M. Effect of Low Temperature Plasma Treatment on Color of Wool and Nylon 6 Fabrics Dyed with Natural Dyes. *Textile Research Journal*, **1998**, 68, 848-853.

147. Byrne, G.; Brown, K. Modifications of Textiles by Glow-Discharge Reactions. *Journal of the Society Dyers and Colourist*, **1972**, 88, 113-117.

148. Park, J.; Kim, J.; Song, S. Surface Modification of Polyester Fabric by Plasma Polymerization of Acrylic Acid in the Presence of Oxygen. *Journal of Korean Fiber Society*, **1996**, 33, 790-797.

149. Oktem, T.; Ayhan, H.; Seventekin, N.; Piskin, E. Modification of Polyester Fabrics by in situ Plasma or Post-plasma Polymerisation of Acrylic Acid, *Journal of the Society Dyers and Colourist*, **1999**, 115, 274-279.

150. Seto, F.; Muraoka, Y.; Sakamoto, N.; Kishida, A.; Akashi. M. Surface Modification of Synthetic Fiber Nonwoven Fabrics with

Poly(acrylic acid) Chains Prepared by Corona Discharge Induced Grafting. *Angewandte Makromolekulare Chemie*, **1999**, 266, 56- 62.

151. Ilić, V.; Šaponjić, Z.; Vodnik, V.; Mihailović, D.; Jovančić, P.; Nedeljković, J.; Maja Radetić, M. The Study of Coloration and Antibacterial Efficiency of Corona Activated Dyed Polyamide and Polyester Fabrics Loaded with Ag Nanoparticles *Fibers and Polymers*, **2009**, 10:5, 650-656.

152. Mihailović, D.; Šaponjić, Z.; Molina, R.; Puač, N.; Jovančić, P.; Nedeljković, J.; Radetić, M. Improved Properties of Oxygen and Argon RF Plasma-Activated Polyester Fabrics Loaded with TiO2 Nanoparticles *Appl. Mater. Interfaces*, **2010**, 2*:* 6, 1700–1706**.**

153. Huh, M. W.; Kang, I.-K. ; Lee, D. H.; Kim, W. S.; Lee, D. H.; Park, L. S.; Min K. E.; Seo, K. H. Surface characterization and antibacterial activity of chitosan-grafted poly(ethylene terephthalate) prepared by plasma glow discharge. *J. Appl. Polym. Sci.*, **2001**. 81, 2769.

154. Yang, M. R.; Chen, K. S.; Tsai, J. C.; Tseng, C. C.; Lin, S. F. The antibacterial activities of hydrophilic-modified nonwoven PET. *Mater. Sci. Eng. C*, **2002,** 20, 167.

155. Yuranova, T.; Rincon, A. G.; Bozzi, A.; Parra, S.; Pulgaien, C. ; Albers P.; Kiwi, J. Antibacterial textiles prepared by RF-plasma and vacuum-UV mediated deposition of silver. *J. Photochem. Photobiol. A: Chem.* , **2003,** 161, 27.

156. Malshe, P; Mazloumpour, M; El-Shafei, A; Hauser, P. Functional Military Textile: Plasma-Induced Graft Polymerization of DADMAC for Antimicrobial Treatment on Nylon-Cotton Blend Fabric. *Plasma Chemistry and Plasma Processing*, **2012,** 32: 4, 833-843.

157. Orhan, M.; Kut, D.; Gunesoglu, C. Improving the Antibacterial Property of Polyethylene Terephthalate by Cold Plasma Treatment Plasma *Chem. Plasma Process* , **2012,** 32: 293–304*.*

158. Hyun, S.-H.; Kim, M.-W.; Oh, D.-H.; Kang, I.-K.; Kim, W.-S. Surface Characterization of 8-Quinolinyl Acrylate-Grafted Poly(ethylene terephthalate) Prepared by Plasma Glow Discharge and It's Antibacterial Activity *Journal of Applied Polymer Science*, **2006***,* 101, 863–868.

159. Ramadan, A.M; Mosleh, S; Gawish, S.M. Grafting and quaternization of 2-(dimethylamino) ethyl methacrylate onto polyamide-6 fabric pretreated with acetone. *Journal of Applied Polymer Science*, **2001***,* 81, 2318–2323.

160. klemm, D.; Philipp, B.; Heinze, T.; Heinze, U.; Wgaenknecht, W. *Comprehensive Cellulose Chemistry Volume I, Fundamentals and Analytical Methods.* Wiley-VCH: Weinheim, **1998**.

161. Vogel A.I. Elemental practical inorganic chemistry, part 3, Quantitative inorganic analysis. Longman, **1975**.

162. Desai, S; Singh. R.P. Surface modification of polyethylene. In: Albertsson AC, editor. Long-term properties of polyolefins. *New York: Springer;* **2004**, 231–93.

163. http://www.cryst.bbk.ac.uk/PPS2/projects/schirra/html/2dnmr.htm

164. Ernst, R. R; Bodenhausen, G; Wokaun. A. Principles of nuclear magnetic resonance in one and two dimensions. *Claredon Press, Oxford,* **1987**.

165. Sabbatini, L; Zambonin, P .G. Surface characterization of advanced polymers. *New York: VCH Publishers, Inc.;* **1993**.

166. Arbeitsgruppe "Textile Vorbehandlung" Melliand Textilber. , **1987**, 8, 581-583.

167. Fouda, M.; Knittel, D.; Zimehl, R.; Hipler, C.; Schollmeyer, E. Functionalization of Fibre Surfaces by thin Layers of Chitosan and The Antimicrobial Activity . *Adv. Chitin Sci*., **2005**, 8, 418.

168. AATCC Technical Manual, **2002**, 77, 341-343.

169. Seidler, E. The tetrazolium-formazan system: design and histochemistry, Gustav Fischer Verlag, New York, **1991**.

170. Goldblatt, R.D; Park, J.M; White, R.C; Matienzo, L.J. Photochemical surface modification of poly (ethylene terephthalate) *Journal of Applied Polymer Science*, **1989***,* 37, 335–347.

171. Dizman, B; Elasri, M.O; Mathias, L.J. Synthesis and antibacterial activities of water-soluble methacrylate polymers containing quaternary ammonium compounds *Journal of Polymer Science Part A: Polymer Chemistry*, **2006***,* 44: 5965–5973.

172. Deng, J.P; Wang, L.F; Liu, L.Y; Yang, W.T. Developments and new applications of UV-induced surface graft polymerizations. *Progress in Polymer Science*, **2009***,* 34, 156–193.

173. Wilkinson; L. J; White, R.J; Chipman, J.K. Silver and nanoparticles of silver in wound dressings: a review of efficacy and safety. *J. Wound Care.* **2011**, 20, 11, 543-9.

174. Shahverdi, A.R; Fakhimi, A. Synthesis and effect of silver nanoparticles of the anti-bacterial activity of 2. different antibiotic against Staphylococcus aureus and Escherichia coli. *Nonomedicine*, **2007**, 3, 168-171.

175. Liz-Marzan, L. M; Lado-Tourino, I, Reduction and Stabilization of Silver Nanoparticles in Ethanol by Nonionic Surfactants. *Langmuir*, **1996**, 12, 3585-3589.

176. Sun, Y.P; Atorngitjawat, P; Meziani, M. J. Preparation of Silver Nanoparticles Via Rapid Expansion of Water in Carbon Dioxide Microemulsion into Reductant Solution. *Langmuir*. **2001**, 17, 5707-5710.

177. Henglein, A. Colloidal Silver Nanoparticles: Photochemical Preparation and Interaction with O_2, CCl_4, and Some Metal Ions. *J. Chem. Mater.***1998**, 10, 444-446.

178. Haes, A. J; VanDuyne, R. P. A unified view of propagating and localized surface plasmon resonance biosensors. *Anal. Bioanal.Chem*. **2004**, 379, 920.

179. Mulvaney, P. Surface Plasmon Spectroscopy of Nanosized Metal Particles. *Langmuir*. 1996, 12, 788.

180. Kreibig, U; Vollmer, M. Optical Properties of Metal Clusters. *Berlin :Springer.* **1995** .

181. Huber, K; Witte, T; Hollmann, J; Baumann, K. S. Controlled Formation of Ag Nanoparticles by Means of Long-Chain Sodium Polyacrylates in Dilute Solution *J. Am. Chem.. Soc.* **2007**, 129, 1089-1094

182. Lee, J. Synthesis and application of novel antimicrobial polymeric materials, *Doctor of Philosophy Thesis, Graduate Faculty of Auburn University,* **2006**.

Appendix A

List of papers, conferences and additional training during doctoral study

Paper in journal:

1. Nasser H. Mohamed, Andreas Wego, Thomas Bahners, Jochen S. Gutmann and Mathias Ulbricht. Surface Modification of Poly (ethylene terephthalate) Fabric via Photo-chemical Reaction of Dimethylaminopropyl methacrylamide" *Applied Surface Science* 259 (**2012**) 261– 269.

Paper in proceedings:

2. Nasser H. Mohamed, Thomas Bahners, Jochen S. Gutmann and Mathias Ulbricht. Antibacterial properties of poly (ethylene terephthalate) impregnated with photochemically synthesized silver nanoparticles. Aachen-Dresden International Textile 5th Conference Aachen, November 24-25, **2011**.
3. Nasser H. Mohamed, Thomas Bahners, Jochen S. Gutmann and Mathias Ulbricht Antibacterial properties of plasma Pre-treated Polyester fabric impregnated with photochemically synthesized silver nanoparticles, 14th Romanian Textiles and Leather Conference – CORTEP 2012**,** Sinaia, 6 - 8 September **2012**

Conferences:

1. Participation in 1st Junges Chemie Symposium Ruhr (1st JCS)-Ruhr on September 9th, **2010**, in Bochum. **Poster** presentation, **title**: Surface Modification of Poly (ethylene terephthalate) PET fabric via photochemical Reaction of Dimethylaminopropyl methacrylamide).
2. Participation in 2nd Junges Chemie Symposium Ruhr (2nd JCS)-Ruhr on September 22nd, **2011**, Essen. **Poster** presentation, **title**: Synthesis of

Silver Nanoparticles by Photochemical Reduction using Poly (methacrylic acid) and their Application as Antimicrobial agent.

3. Participation in the international conferences the world's most established textile and garment machinery technology exhibition. ITMA, Barcelona, Spain from 22 to 29 September **2011**.
4. Participation in the international conferences in Aachen-Dresden International Textile 5-th Conference Aachen, November 24-25, **2011**. **Poster** presentation, **title**: (Antibacterial properties of poly (ethylene terephthalate) impregnated with photochemically synthesized silver nanoparticles).
5. Participation in the 14-th Romanian Textiles and Leather Conference, CORTEP' **2012**, Sinaia, Romania, 6-8 September 2012. **Oral** presentation, **title**: (Antibacterial properties of plasma Pre-treated Polyester fabric impregnated with photochemically synthesized silver nanoparticles).
6. Participation in 3rd Junges Chemie Symposium (3rd JCS)-Ruhr on September 27th, **2012**, in Dortmund. **Poster** presentation, **title**: Antibacterial properties of plasma pre-treated polyamide fabric impregnated with photo-chemically synthesized silver nanoparticles

Trainings:

1. Training course "Nanosized particles as building blocks for creation of nanostructures" Erasmus Intensive Program held at Adam Mickiewicz University. 9th-22nd May **2010**, Poznan, Poland
2. Training Seminar "nano analytics" (Fortbildungsseminar " nanoanalytik") 02nd-03rd. Mai **2011**, Duisburg, Germany.
3. Professional Training "Approaches to regulating nanotechnology and workshop on nanoparticle synthesis" 07th- 08th. Mai **2012**, Duisburg, Germany.

Appendix B

Curriculum Vitae

Personal Data

Name:	Nasser Hassan Abdella Mohamed
Date of Birth:	04.02.1974
Marital Status:	Married
Nationality:	Egyptian
Place of birth:	Cairo, Egypt
E-mail	nasserha74@yahoo.com
Address	National Research Centre- Textile Research Division El Buhouth St., Dokki, 12311, Cairo, Egypt

Education

1992-1996	**Bachelor of Science (BSc in Chemistry),** (Very good with Honour degree), Chemistry Department, Faculty of Science, Ain shams University, Egypt.
2000-2001	**Preliminary Master Study courses** in Organic Chemistry Department, Ain shams University, Egypt
2002-2005	**Master of Science (MSc in Organic Chemistry**, Chemistry Department, Faculty of Science, Ain shams University, Egypt.
2008-2012	**Studied for Ph.D degree**, at German Textile Research Institute, University of Duisburg-Essen, Germany.

Scholarships

1998-2002	**Academy of Scientific Research and Technology (ASRT), Egypt, scholarship** for Master study at National Research Center, Egypt
2008-2012	**Egyptian Government Scholarship** for Doctoral study at Deutsches Textilforschungszentrum Nord-West e.V.(DTNW), Institut an der Universität Duisburg-Essen.

Employment and Responsibilities

1996-1997	**Chemist** in Egyptian- German Co. for textile – Egypt
1997-1998	**Chemist** in al sherif for plastic factories - Egypt
2002-2005	**Researcher Assistant**, Textile Research Division, National Research Center, Cairo, Egypt
2005-2006	**Assistant Researchers**, Textile Research Division, National Research Center, Cairo, Egypt.
2008-2012	**Studies for PhD degree** at German Textile Research Institute, University of Duisburg-Essen; Krefeld, Germany.